Université Lille Nord de France
Pôle de Recherche et d'Enseignement Supérieur

Université Lille1
Sciences et Technologies

Order number: 41420

University of Lille 1 - Sciences and Technology
Lille Mechanics Laboratory (UMR CNRS 8107)
Doctoral School of Engineering Sciences - University of Lille Northern France

A dissertation
Submitted to Lille Mechanics Laboratory
University of Lille 1 – France
In Fulfillment of the Requirements for the
Degree of Doctor of Philosophy in Mechanics, Energy, Materials

by

Younis Khalid KHDIR

May 23 2014

Non-linear numerical homogenization: Application to elasto-plastic materials

Jury

R. ESTEVEZ	Professor	University of Grenoble	President
S. AHZI	Professor	University of Strasbourg	Reviewer
I. DOGHRI	Professor	University of Louvain	Reviewer
T. KANIT	Associate professor	University of Lille 1	Ph.D. co-director
F. ZAIRI	Professor	University of Lille 1	Ph.D. co-director
M. NAIT-ABDELAZIZ	Professor	University of Lille 1	Ph.D. director

EDSPI Ecole Doctorale des Sciences pour l'Ingénieur - Lille

LABORATOIRE de MECANIQUE de LILLE UMR CNRS 8107

E.C. LILLE E.N.S.A.M. U.S.T.L.

Numéro d'ordre : 41420

Université des Sciences et Technologies de Lille
Laboratoire de Mécanique de Lille (UMR CNRS 8107)
Ecole Doctorale Sciences Pour l'Ingénieur - Université Lille Nord de France

THESE

Pour obtenir le grade de

Docteur de l'Université Lille 1 Sciences et Technologies

Discipline : Mécanique, Energétique, Matériaux

Présentée et soutenue publiquement

par

Younis Khalid KHDIR

23 Mai 2014

Homogénéisation numérique non-linéaire : Application aux matériaux élasto-plastiques

Non-linear numerical homogenization: Application to elasto-plastic materials

Jury

R. ESTEVEZ	Professeur	Université de Grenoble	Président
S. AHZI	Professeur	Université de Strasbourg	Rapporteur
I. DOGHRI	Professeur	Université de Louvain	Rapporteur
T. KANIT	Maître de Conférences	Université Lille 1	Codirecteur de thèse
F. ZAIRI	Professeur	Université Lille 1	Codirecteur de thèse
M. NAIT-ABDELAZIZ	Professeur	Université Lille 1	Directeur de thèse

Boulevard Paul Langevin, Cité Scientifique, 59655 VILLENEUVE D'ASCQ CEDEX

Dedication

To my
PARENTS, FAMILY
To all my
FRIENDS

Younis

Acknowledgments

At the end of the PhD process, I can take sometime to reflect upon and I can hardly begin to enumerate in the space of a few paragraphs all the people whose influence has shaped this work. Undoubtedly I will miss a few people and to them I apologize in advance. I would like to express my special appreciation and thanks to my advisor Professor Moussa Naït-Abdelaziz. You have been a tremendous mentor for me. I would like to thank you for encouraging my research and for allowing me to grow as a research scientist. Your advice on both research as well as on my career have been invaluable.

The good advices, supports and friendship of my second supervisors, Professor Fahmi Zaïri have been invaluable on an academic and a personal level, for which I am extremely grateful and Dr. Toufik Kanit. I would also like to thank my committee members, Professors Saïd Ahzi, Issam Doghri and Raphael Estevez for serving as my committee members even at hardship, and for their helpful career advice and suggestions in general. I also want to thank you for letting my defense be an enjoyable moment, and for your brilliant comments and suggestions, thanks to you. I would especially like to thank all members at University of Lille 1. All of you have been there to support me when I started my PhD dissertation. A special thanks to my family. Words can not express how grateful I am to my father and mother for all of the sacrifices that you have made on my behalf. Your prayer for me was what sustained me thus far. It would not have been possible to write this doctoral dissertation without the help and support of the kind people around me, to only some of whom it is possible to give particular mention here. Above all, I would like to thank my

brothers and sisters have given me their unequivocal support throughout, as always, for which my mere expression of thanks likewise does not suffice.

I would like to acknowledge the financial, academic and technical support of the Regional Government of Kurdistan – Iraq and Government of France and University of Lille 1. These past four years have not been an easy ride, both academically and personally. I truly thank my friends for sticking by my side, even when I was irritable and depressed. I feel that what we all learned a lot about life and strengthened our commitment and determination to each other and to live life to the fullest.

I would also like to thank some of my friends, who provided support leading up to and during my post graduate studies. I will never forget their kindness. In addition to these, must thank my parents who selflessly supported me during my graduate education and my entire life. Their assistance by taking care of a number of mundane, domestic chores freed up time for my pursuits outside of academics. Most comforting was that I always knew with absolute certainty that I had their help, I have had needed it. Finally I would like to recognize every one of my relatives who helped me and with my best respects.

Younis

Résumé

Ce travail de thèse se veut une contribution à l'homogénéisation numérique des milieux élasto-plastiques hétérogènes aléatoires via des calculs sur des grands volumes. Le travail comporte deux parties principales. La première est dédiée à la réponse élasto-plastique macroscopique des composites à distribution aléatoire de la seconde phase sollicités en traction uniaxiale. La deuxième est focalisée sur la réponse macroscopique à la limite d'écoulement des milieux poreux aléatoires sur une large gamme de triaxialités.

Dans la première partie, nous décrivons une méthode d'homogénéisation numérique pour estimer la réponse élasto-plastique macroscopique de milieux composites aléatoires à deux phases. La méthode est basée sur des simulations éléments finis utilisant des cellules cubiques tridimensionnelles de différentes tailles mais plus petites que le volume élémentaire représentatif de la microstructure. Nous proposons d'étendre l'approche développée dans le cas des milieux hétérogènes élastiques par Drugan et Willis (1996) et Kanit et al. (2003) aux composites élasto-plastiques. Un mélange de polymères particulier, constitués de deux phases aux propriétés mécaniques très différentes, est sélectionné pour illustrer cette approche ; il consiste en une dispersion aléatoire de sphères d'élastomère élastiques dans une matrice de polymère thermoplastique élasto-plastique.

Dans une seconde partie, nous décrivons une étude d'homogénéisation numérique sur des cellules cubiques tridimensionnelles afin de prédire la surface d'écoulement macroscopique de milieux poreux aléatoires contenant une ou deux populations de vides. La représentativité des résultats est examinée en utilisant des cellules cubiques contenant des vides répartis et orientés aléatoirement. Des vides sphériques et sphéroïdales (oblongs/allongés) sont considérés dans les calculs numériques. Les résultats sont comparés à des critères d'écoulement existants de type Gurson.

Mots-clefs : Homogénéisation numérique; Représentativité; Milieux composites aléatoires; Milieux poreux aléatoires; Modèles de type Gurson.

Abstract

This PhD dissertation deals with the numerical homogenization of heterogeneous elastic-plastic random media via large volume computations. The dissertation is presented in two main parts. The first part is dedicated to the effective elastic-plastic response of random two-phase composites stretched under uniaxial loading. The second part is focused on the effective yield response of random porous media over a wide range of stress triaxialities.

In the first part, we describe a computational homogenization methodology to estimate the effective elastic-plastic response of random two-phase composite media. The method is based on finite element simulations using three-dimensional cubic cells of different size but smaller than the deterministic representative volume element of the microstructure. We propose to extend the approach developed in the case of elastic heterogeneous media by Drugan and Willis (1996) and Kanit et al. (2003) to elastic-plastic composites. A specific polymer blend, made of two phases with highly contrasted mechanical properties, is selected to illustrate this approach; it consists in a random dispersion of elastic rubber spheres embedded in an elastic-plastic thermoplastic polymer matrix.

In the second part, we describe a computational homogenization study of three-dimensional cubic cells in order to estimate the effective yield surface of random porous media containing one or two populations of voids. The representativity of the overall yield surface estimates is examined using cubic cells containing randomly distributed and oriented voids. Spherical and (oblate/prolate) spheroidal voids are considered in the computations. The computational results are compared with some existing Gurson-type yield criteria.

Keywords: Computational homogenization; Representativity; Two-phase composite media; Random porous media; Gurson-type models.

Contents

GENERAL INTRODUCTION

General introduction

The present PhD dissertation deals with the effective mechanical response prediction of elastic-plastic heterogeneous media. The mechanical behavior of any heterogeneous medium depends on its heterogeneous microstructure. Analyzing large structures on a microstructural level, however, is clearly an intractable problem, especially in the case of a random microstructure. Methods have therefore been developed to approximate heterogeneous materials by analyzing a representative section of the heterogeneous microstructure, which is universally called representative volume element (RVE). For many cases, especially for random microstructures, continuum-based micromechanical analytical modeling remains complex. As a powerful alternative method, computational homogenization, performed directly on the whole microstructure, may be used to estimate the effective material response of random heterogeneous media. Indeed, unit cell generally, invoked in order to check the validity of analytical models, can only represent a periodic microstructure. Another important example of random media is porous materials. Even this subject has been widely investigated; there are still some interesting issues that need to be clarified, such as the effect of void shapes on the overall yield surface, and the effect of a multiple population of voids.

This work is divided into two main parts. The first part (Chapters I and II) is dedicated to the effective elastic-plastic response of random two-phase composites stretched under uniaxial loading. The second part (Chapters III and IV) is focused on the effective yield response of random porous media over a wide range of stress triaxialities.

In the Chapter I, a brief review of some fundamental approaches about the micromechanical homogenization of heterogeneous media is given in order to cover the necessary information that are required to understand the next chapter.

In the Chapter II, we describe a computational homogenization methodology to estimate the effective elastic-plastic response of random two-phase composite media. It is based on finite element simulations using three-dimensional cubic cells of different size but smaller than the deterministic RVE of the microstructure. We propose to extend the approach developed in the case of elastic heterogeneous media by Drugan and Willis (1996) and Kanit et al. (2003) to elastic-plastic composites. A specific polymer blend, made of two phases with highly contrasted properties, is selected to illustrate this approach; it consists of a random dispersion of elastic rubber spheres in an elastic-plastic glassy polymer matrix. The goal is to compare the effective elastic-plastic response of this particulate composite with the apparent response determined by computing a sufficient number of small subvolumes of fixed size extracted from the deterministic RVE and containing different realizations of the random microstructure. The necessary realization number to reach acceptable precision is examined for two examples of particle volume fractions.

The Chapter III begins with a concise review of some existing yield criteria for plastic porous media. Then, we present the results of a computational homogenization study of three-dimensional cubic cells in order to estimate the overall yield surface for different stress triaxialities of random porous media in relation to the issue of representativity of the volume element. The representativity of the overall yield surface is

examined using cubic cells containing randomly distributed and oriented non-overlapping identical voids with different void volume fractions and void shapes. Spherical and (oblate/prolate) spheroidal voids are considered in the computations. The computational results are compared with some existing Gurson-type yield criteria.

Finally, in the Chapter IV, the macroscopic yield response of random porous media containing two populations of spherical voids is investigated via large volume computations. The computed yield surface is compared to analytical criteria recently developed for above-mentioned porous media. To overcome the observed discrepancies, the analytical models are modified by introducing additional parameters which are numerically derived.

General conclusion and future studies are given at the end of the document.

This PhD work led to the following publications:

- Younis-Khalid Khdir, Toufik Kanit, Fahmi Zaïri, Moussa Naït-Abdelaziz, 2013. Computational homogenization of elastic-plastic composites. International Journal of Solids and Structures 50, 2829-2835.

- Younis-Khalid Khdir, Toufik Kanit, Fahmi Zaïri, Moussa Naït-Abdelaziz, 2014. A computational homogenization of random porous media: effect of void shape and void content on the overall yield surface. Submitted for publication.

- Younis-Khalid Khdir, Toufik Kanit, Fahmi Zaïri, Moussa Naït-Abdelaziz, 2014. Computational homogenization of plastic porous media with two populations of voids. Materials Science and Engineering A 597, 324-330.

PART I

COMPUTATIONAL HOMOGENIZATION OF ELASTO-PLASTIC COMPOSITES

CHAPTER I

A BRIEF FOCUS ON HOMOGENIZATION METHODS

1.1. Introduction

Heterogeneous materials are widely used in different products and structures, from agriculture equipments to aerospace vehicles and electrical products. Composites that are composed of spatially distributed particles became popular in a wide range of different industrial productions. This is because using spatially distributed spherical particles or other shapes of particles as reinforcing elements in a controlled manner can improve their mechanical properties.

The real microstructures of heterogeneous media are generally simplified in the models, both materially and geometrically, the degree of simplification of the model depending on the desired engineering accuracy. In this way, the theory of homogenization is a useful tool to estimate the composite properties (e.g. Nemat-Nasser and Hori, 1993).

Predictions of the mechanical properties of heterogeneous materials containing randomly distributed particles or voids have been an active research area during the last few decades. Several analytical models have been proposed to predict the composite properties from those of the constituents. To account for the complexity of the microstructure which could not be reached by the analytical models, finite element simulations on sufficiently representative volume element have been developed this last decade. In this chapter, a brief review of the homogenization techniques is presented.

1.2. The concept of homogenization

In the present section, we introduce the concept of homogenization theories for linear and non-linear heterogeneous materials. The fundamental elements that are required for homogenization are detailed here.

The homogenization technique is generally used to get the effective mechanical properties of an equivalent homogeneous medium representing the heterogeneous medium at a macro-scale (Fig. 1.1).

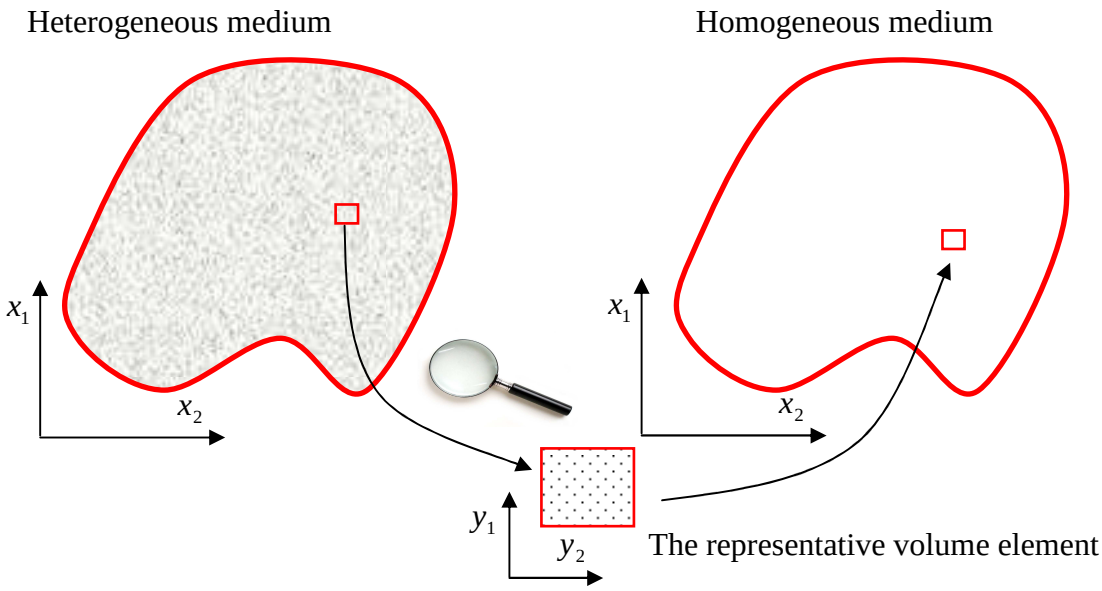

Fig. 1.1. The equivalent homogenous material.

Analysis methods have therefore sought to approximate composite structural mechanics by analyzing a representative section of the microstructure, which is universally called representative volume element (RVE) (e.g. Sun and Vaidya, 1996; Kanit et al., 2003; Sab and Nedjar 2005; Khisaeva and Ostoja-Starzewski, 2006; Galli, et al., 2008).

The term RVE has been explained by Hill (1963) and then it has also been detailed extensively by Hashin (1962; 1964; 1983). Determine the effective elastic properties of the microstructure in details is achieved by means of the local level analysis; then it is possible to calculate the relationship between the effective or average RVE strain and the local strain (Hollister and Kikucki, 1992).

The composite structure can be then replaced by an equivalent homogeneous medium that has the same congruent calculated effective properties. Calculating the average or effective stress and strain within the equivalent homogeneous structure is the global level analysis. The term "homogenization" is the process of calculating effective properties (Suquet, 1987). Another term used is "localization" for determining the local stress and strain; they can be computed by using the relationship between the average and local strain obtained from the local analysis (Suquet, 1987; Hollister and Kikucki, 1992).

The overall property of a heterogeneous medium is governed by the properties of its constituents and the effective properties are obtained by ensemble-volume averaged homogenization procedure. The average stress on the RVE can be defined by the following equation:

$$\left\langle \sigma_{ij} \right\rangle = \frac{1}{V} \int_V \sigma_{ij}(x) dv \tag{1.1}$$

and the average strain can be determined according to:

$$\left\langle \varepsilon_{ij} \right\rangle = \frac{1}{V} \int_V \varepsilon_{ij}(x) dv \tag{1.2}$$

in which *V* represents the volume of the RVE.

To derive the effective properties and overall stress-strain relations, several methods have been proposed in the past.

1.3. Homogenization methods

The researchers who worked on this field considered that the medium is periodic at the micro-scale and it can reach a high degree of sophistication, considering that the homogenization problem as a two-scale problem, which drives the behavior of the heterogeneous medium at the macro-scale. The term of homogenization can be defined as the process where the heterogeneous medium can be replaced by a homogeneous medium that has the same mechanical behavior. Normally, the micro-scale is characterized stress-strain fields which present fluctuations and oscillations that are related to the size of the specimen. However, the oscillations can be seen only in the micro-scale. Some phenomena that affects in the macro-scale can be seen such as crack propagation, damage and fracture.

According to the literature presented above, this method can be divided into two main groups; asymptotic method and mean method. The asymptotic method was presented by for example (Yu and Tang, 2007; Kalamkarov et al., 2009; Ji-wei and Miao-lin, 2010; Orlik, 2010; Neto et al., 2010; Willoughby, 2012; Yang et al., 2013), and some equations have been proposed which depend on the constitutive relation at the micro-scale and inelastic strain of the problem between the matrix and the inclusion or during the damage case. The spatial average approach (Pierard et al., 2004;

Doghri et al., 2010; Wu et al., 2012) uses the mean method to obtain the mean values of stresses and strains of the microscopically scales.

The fundamental key points in the theory of homogenization are:

- RVE
- Statistical homogeneity
- Material symmetry
- Homogenization and localization
- Mean field homogenization
- Micromechanical modeling approaches

1.3.1. RVE

The term of “representative” was for the first time indicated by Hill (1963). He defined that the RVE as: i) Structurally entirely typical of the composite material on average and ii) Containing sufficient number of inclusions such that the apparent moduli are independent of the RVE boundary displacement or tractions. The accuracy of the RVE approximation depends on how well the assumed boundary conditions reflect each of the myriad boundary conditions to which the RVE is subjected in-situ. Thus, RVE analysis under applied displacements gives an upper bound on apparent stiffness while applied tractions give a lower bound (Hollister and Kikuchi, 1992).

There are a number of RVE approaches or methods to analyze heterogeneous media, of which each of the method may give different approximate results depending upon the different ranges of assumptions made and ratio between RVE size to the size of global region of interest

(Hollister and Kikucki, 1992). It is important to know how the RVE size and the choice of analysis method will affect the accuracy of the analysis. One of the important points is to obtain the maximum accuracy of analysis for the smallest RVE size.

The more common descriptions of the RVE are explained below.

1- The RVE can be defined as a sample that i) is structurally entirely typical of the whole mixture on average, and ii) contains a sufficient number of inclusions for the apparent overall moduli to be effectively independent of the surface values of traction and displacements, as long as these values are macroscopically uniform (Hill, 1963).

2- The RVE is a model of the material to be used to determine the corresponding effective properties for the homogenized macroscopic model. The RVE should be large enough to contain sufficient information about the microstructure in order to be representative. However, it should be much smaller than the macroscopic body. This is known as the micro-meso-macro principle (Hashin, 1983).

3- The RVE must be chosen sufficiently large compared to the microstructural size for the approach to be valid, and it is the smallest material volume element of the composite for which the usual spatially constant overall modulus macroscopic constitutive representation is a sufficiently accurate model to represent the mean constitutive response as defined by Drugan and Willis (1996).

4- The size of the RVE should be large enough with respect to the individual grain size in order to define overall quantities such as stress

and strain, but this size should also be small enough in order not to hide macroscopic heterogeneity (Evesque, 2000).

Also, the RVE can graphically be expressed as in Fig. 1.2. According to the all above definitions, the RVE should be sufficiently smaller than the microstructure dimensions and contain the same microstructure information as explained by Gitman et al. (2007). The concept of RVE can clearly be defined in two situations; first it is a unit cell in a periodic microstructure, and second, it is a small volume containing a very large (mathematically infinite) set of micro-scale elements, possessing statistically homogeneous and ergodic properties[1]. So in order to indicate a RVE for a material, it is essential to have, i)- Statistical homogeneity and ergodicity of the material; which these properties assure the RVE to be statistically representative of the macro response, ii)- Length scale of the RVE sufficiently large relative to the micro-scale diameter of the inclusions so as ensure the independence of the boundary conditions (Ostoja-Starzewski, 2002).

---

[1] In fact, all epistemological value of the theory of probability is based on this: Large-scale random phenomena in their collective action create strict, nonrandom regularity. Now, this is how Gnedenko and Kolmogorov introduced their classic study of the limit laws for independent random variables, but most of the random phenomena we encounter around us are not independent. Ergodic theory is a study of how large-scale dependent random phenomena nonetheless create non-random regularity. The classical limit laws for IID variables $X_1, X_2, \ldots$ assert that, under the right conditions, sample averages converge on expectations:

$$\frac{1}{n}\sum_{i=1}^{n} X_i \to \mathrm{E}\left[X_i\right]$$

where the sense of convergence can be "almost sure" (strong law of large numbers), "L_p" (p^{th} mean), "in probability" (weak law), etc., depending on the hypotheses we put on the Xi. One meaning of this convergence is that sufficiently large random samples are representative of the entire population; that the sample mean makes a good estimate of E[X]. The ergodic theorems, likewise, assert that for dependent sequences $X_1, X_2, \ldots$, time averages converge on expectations:

$$\frac{1}{t}\sum_{i=1}^{t} X_i \to \mathrm{E}\left[X_\infty \middle| Z\right]$$

where X_∞ is some limiting random variable, or in the most useful cases a non-random variable, and Z is a σ-field representing some sort of asymptotic information. Once again, the mode of convergence will depend on the kind of hypotheses we make about the random sequence X. Once again, the interpretation is that a single sample path is representative of an entire distribution over sample paths, if it goes on long enough. The IID laws of large numbers are, in fact, special cases of the corresponding ***ergodic*** theorems.

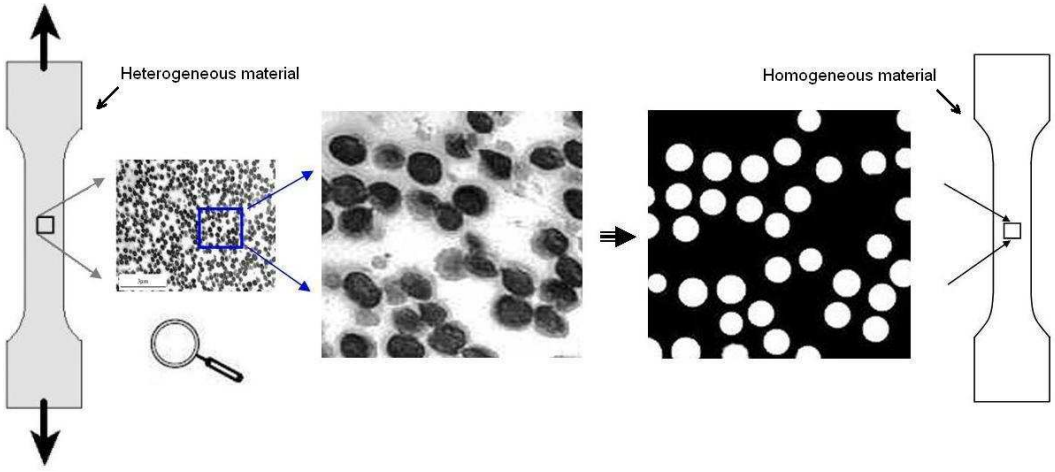

Fig. 1.2. Micro to macro-scales of a polymer blend constituted by rubber nodules embedded in a glassy polymer matrix.

1.3.2. Statistical homogeneity

In a heterogeneous medium, containing particles or voids, the mechanical and physical properties may be varying from point to point. Generally heterogeneous media possess randomly distribution of the properties. In this case for a complete description of the properties, all the different probabilities should be known and considered.

An average sample selected from the volume of the body should be independent of the location of the whole volume. Thus in a statistically sense a sample is necessary to represent the total heterogeneous medium. The heterogeneous medium may be transformed to a homogeneous one using the statistical homogeneity. Henceforth the average properties are termed as effective properties (Hashin, 1962; Hashin and Shtrikman, 1963; Hill, 1965; Mori and Tanaka, 1973; Hashin, 1983; Torquato, 1997; Kanit et al., 2003; Mortazavi et al., 2012).

1.3.3. Material symmetry

One of the other assumptions in the statistical homogenization is material symmetry. For the heterogeneous media, containing particles or voids, the symmetry is considered according to the particle packing patterns or array of the particles or voids. For examples, if the particles or voids array is rectangular, orthotropic would be assumed, and for hexagonal array and completely random distribution of particles it assumed to be isotropic microstructure. Additionally, for square array of particles it assumed square symmetry (Hashin, et al., 1963; Hill, 1965; Sun and Vaidya, 1996; Yuan, et al., 1997; Hassani and Hinton, 1998; Wongsto and Li, 2005).

1.3.4. Homogenization and localization

The aim of continuum-based micromechanics framework is to make the bridge of scales and to describe the structure-property relationships of heterogeneous materials. The bridge of length scale involves two main issues. The behavior of macro-scale must be estimated or bounded depending on the information from the micro-scale, and homogenization that must be solved. The second point is the local response at the micro-scale that may be deduced from the loading conditions on the macro-scale. The corresponding to the local fields in a heterogeneous material is referred to as localization or downscaling. The localizations may be more demanding than homogenization, because the local fields tend to show a marked dependence on details of the local geometry of the constituents (Böhm, 2013).

1.3.5. Mean field homogenization

The mean-field approach is an efficient semi-analytical method for modeling heterogeneous materials, which is based on the extension from the single inclusion results (established by Eshelby (1957)) to multiple inclusions interacting in an average way. The mean-field method is developed for composite materials but it may be extended to porous materials, considering that one of the constituents could be as voids without stiffness. Among those different methods, the mean-field homogenization approach provides predictions for the macroscopic behavior of the heterogeneous materials at a reasonable computational cost. To account for the interactions between inclusions in an average way, additional assumptions are applied as shown in the Mori-Tanaka scheme (Mori and Tanaka, 1973) or in the self-consistent scheme (Budiansky, 1965). Multi-scale homogenization methods, particularly the mean-field homogenization schemes can predict accurately the macroscopic behavior of heterogeneous materials exhibiting non-linear irreversible behaviors at the microscopic components scale (Pierard et al., 2004; 2006; Friebel et al., 2006; Doghri et al., 2010; Tsukamoto, 2010; Wu et al., 2012).

1.3.6. Micromechanical modeling approaches

Through the determination of the constitutive relations and setting up some hypotheses at the micro-scale on the stress and strain fields, the elasticity problems are solved analytically. The first attempt is the rule of mixtures and more sophisticated micromechanical methods were developed since the earlier Eshelby theory (Mori and Tanaka, 1973; Morais, 2000; Yan, 2003; Kiris and Inan, 2006; Doghri and Tinel, 2006; Zou et al., 2010; Brassart et al., 2012; Böhm, 2013).

It requires sophisticated modeling programs to predict the overall effective mechanical behaviors of heterogeneous materials. Micromechanical models are used in a wide variety to explain the local mechanisms and mechanics which governs the macroscopic elastic-plastic deformation of heterogeneous solid media. The important point is to provide overall behavior from known properties of the individual constituents and their detailed interaction. Additionally, when a computational model uses, the heterogeneous structure behavior should be known to predict the aggregate behavior. Micromechanical modeling provides some opportunities to analyze the heterogeneous materials on a microstructural scale, in a manner to calculate later the results on the macroscopic scale (Nicoletto, 2004; Alabbasi, 2004). Some common features where used in most of the micromechanical modeling approaches:

1. Geometric definition of the RVE which possesses the fundamental characteristics of the microstructure.
2. Description of the overall mechanical behavior of each phase of the composite and interaction between the phases.
3. Homogenization procedure based on the RVE to obtain the overall macroscopic material behavior.

For non-linear plastic composites precise methods have not been available until fairly last decade. Several efforts have been going on especially about ductile polycrystals (e.g. Hill, 1965a; 1965b; Hutchinson, 1976). Hill (1965a; 1965b) presented an incremental extension of the self-consistent procedure, in the context of flow theory of plasticity, making use of the tangent modulus tensors of the constituent phases. Then, Hutchinson (1976) determined a simple form of Hill procedure for power-law viscous

materials. Later, Berveiller and Zaoui (1979) presented an alternative form for more general types of composites, which resulted in the use of the phase secant modulus tensors. For elasto-plastic two-phase composites, a good deal of the literature on homogenization revolves from the method that is proposed by Tandon and Weng (1988) in which a Mori-Tanaka (1973) is classified to elasto-plasticity with a secant deformation formulation. Talbot and Willis (1992) provided a simultaneous generalization of the variational principles of Talbot and Willis (1985) and linear comparison composite method of Ponte Castañeda (1991), which has the potential to give improved estimates for certain special, non-standard situations. Suquet (1995) showed that these variational estimates make use of the secant moduli of the phases that is evaluated at the second-moments of the fields in the phases. Ponte Castañeda (1996) presented an alternative approach that helps use of more sophisticated linear comparison composites, incorporating the tangent moduli of the phases, evaluated self-consistently. It was early recognized that in the incremental approaches, based on the tangent stiffness tensors of the phases, the flow stress of the material are overestimated, and the origin of this error was traced to the anisotropic nature of the tangent stiffness tensor during plastic deformation (Pierard et al., 2007). The development of the secant methods is required because of this limitation, which deals with the elasto-plastic. Particularly, in composite materials containing one elastic phase, there is another source of error, when the plastic strain in the matrix is determined from a reference equivalent stress computed from the volumetric average of the matrix stress tensor. This equivalent stress is lower than the average phase of the equivalent stress because of the large stress gradients which develops during plastic deformation, hence the composite yield and flow stresses are overestimated (Pierard et al., 2007). Then, several attempts were made to determine the equivalent stress from energy considerations or statistically-

based theories (Tandon and Weng, 1988; Qiu and Weng, 1992). Later, modified secant approximation was proposed by Suquet (1995), where the reference equivalent stress in the matrix is determined from the volumetric average of second-order moment of the stress tensor in this phase instead of the usual first-order moment. The classical secant formulation is presented by Ponte Castañeda and Suquet (1998). Ponte Castañeda (1991) proposed a more general approach consisting in the use of optimally chosen linear comparison composites. Later, Suquet (1993) proposed power-law approach which may be used for delivering bounds for non-linear composites and can be used for generating bounds and estimates of other types, such as self-consistent estimates and three-point bounds. Talbot and Willis (1997) presented a generalization of these methods to be workable for two-sided bounds for non-linear composites, whereas the previous procedures were given to one-sided bounds which depends on the type of constitutive non-linearity present. The second-order estimates had given a more accurate variational explanation by Ponte Castañeda and Willis (1999). A further alternative technique, using of path integral and other methods from statistical mechanics, was proposed by Pellegrini et al. (2000) to produce estimates that are also accurate to second-order in the compare. The second-order estimates, presented by Ponte Castañeda and Suquet (2002), can be quite correct even at high values of the heterogeneities. Leroy and Ponte Castañeda (2001) have recently found that the second-order estimates can violate rigorous bounds near the percolation limit. The third-order variational bound was explicitly derived for non-linear composites subject to hydrostatic deformation by Xu (2011) and Xu and Jie (2014). Using the formulation of the stochastic extreme principle for non-linear boundary value problems, they derived the third-order upper bound of the potential for non-linear two-phase composites, which is further explicitly specialized to porous media. While this method

does not yield bounds, it appears to give more accurate results. In particular, this method was the first to yield general homogenization estimates capable of reproducing exactly to second-order in the contrast to the asymptotic expansions of Suquet and Ponte Castañeda (1993). Improved estimates of the Hashin-Shtrikman-Willis type was generated by Ponte Castañeda (2012) for the class of non-linear composites consisting of two well-ordered, isotropic phases distributed randomly with prescribed two-point correlations. The second-order theory was presented by Ponte Castañeda (1996) for rigidly reinforced composites for stationary isotropic microstructures or isotropic distributions of spherical particles. For example, the approximate second-order homogenization provides estimates for non-linear composites incorporating field fluctuations (Ponte Castañeda, and Tiberio, 2000; Ponte Castañeda 2002a; 2002b). Recently, Xu and Jie (2014) presented a third-order bound for non-linear composites and porous media subjected to hydrostatic deformation, by formulating the stochastic extreme principle for non-linear boundary value problems. The found third-order upper bound for composite media is explicitly specialized to porous media by these authors.

1.4. Computational approaches

For some cases, such as random microstructures, obtaining analytical solution is a challenging task. Indeed, for the analysis of the stress concentration and inclusion clustering it will be very difficult to use the analytical techniques. The computational approach is emerging as a powerful tool which has the ability to directly compute the mechanical fields on the heterogeneous medium by representing explicitly the microstructure features (Alzebdeh et al., 1996; Ostoja-Starzewski and Alzebdeh, 1996; Ostoja-Starzewski et al., 1997; Borberly et al., 2001;

Graham and Baxter, 2001; Kanit et al., 2003; Buryachenko et al., 2003; Bystrom, 2003; Knight et al., 2003; Bilger et al., 2005; Kari et al., 2007, Brassart et al., 2009; 2010; Khdir et al., 2013; 2014).

The important point in the computational approach is the RVE size which should be small from the computational reasons but big enough from the mechanics view. Also, it should be satisfy to represent a certain media and hold all the properties of the heterogeneous media. The convergence of the effective properties is based on the definition of the RVE presented by Hill (1965). Other researchers studied the convergence of the effective properties according to the RVE size (Gusev, 1997; Kanit et al., 2003; Trias et al., 2006; Gitman et al., 2007) while in other studies, researchers determined the RVE size based on the statistical calculation (Terada et al., 2000; Graham and Yang, 2003; Stroeven et al., 2004; Grufman and Ellyin, 2007; Pelissou et al., 2009; Galli et al., 2012; Zangenberg and Brondsted, 2013). They performed convergence calculations to show that the homogenization theory is valid for non-periodic heterogeneous materials too.

Monte Carlo simulations are used to predict the effective properties of heterogeneous materials. The method is based on the repetition of some experiments which depend on some random variables. Using the average values of the results for several realizations cut in the RVE can give the same accuracy (Kanit et al., 2003; Khdir et al., 2013). Kanit et al. (2003) applied a solid composed by polycristals and grains. They found the mean and variance of the thermal and elastic properties using three-dimensional Voronoi cells by Monte Carlo simulation method. They presented the analyses of the convergence of the elastic and thermal properties and discussed the variance of the obtained results using different sizes of RVE.

The chosen number of realizations is based on the size of the RVE. Whenever the RVE size is smaller the required number of realizations increase and vice versa, more examples can be seen in (Kaminski and Kleiber, 2000; Ma et al., 2011; Kaminski and Lauke, 2012).

The concept of Hill (1963) about the relations between volume average strain and stress should be the same regardless for both kinematic or stress boundary conditions that are used. This means that both interpretations of the Hooke law are equivalent (Ostoja-Starzewski, 1993; 1998). The concept is that the large volume of the material needs to be considered to render the influence of the boundary conditions to vanish. The essential (Dirichlet, or displacement controlled) as pointed out by Ostoja-Starzewski (1998) can be presented by the following equation:

$$u = \bar{\varepsilon}_i x_i \tag{1.3}$$

where u is the displacement, $\bar{\varepsilon}$ is the volume (area) average strain and **x** is the position vector.

The other type of boundary condition is natural (Neumann, or stress-controlled) which can be expressed as follows:

$$\sigma = \bar{\sigma}_i m_i \tag{1.4}$$

where σ is the stress traction, $\bar{\sigma}$ is the volume (area) average stress and **m** is the outer unit normal to the window boundary.

An important practice in structural mechanics when dealing with heterogeneous structure is to replace their inhomogeneous constituents with simplified (homogenized) one. In practice, it is possible to determine their overall properties experimentally, but for many of them remains difficult to determine. In the past three decades, many methods in the area of solid mechanics were developed theoretically to predict the effective properties of composite materials directly from the properties of their individual phases and their morphological. As discussed in the previous sections considerable progress has been made about the linear elastic problems. Non-linear problems did not reach the same degree of knowledge. There are increasing needs for incorporating more information about small scale mechanisms of deformation into phenomenological models of plasticity which are commonly called homogeneous. Local stresses, ductile rupture, stress concentration, cavitations, all at small scale are not understandable from a simple point of view of average stress and strain (classical models). Accurate estimation of non-linear overall properties required computational efforts. Numerical simulations using finite element method play a central role in the area of composite homogenizations (Michel et al., 1999).

1.4.1. Periodic heterogeneous media

A periodic medium is defined by a unit cell and three vectors of translation invariance. The choice of unit cell is motivated by differences in geometrical symmetries which can be used by the numerical calculation of the local problems. There are a lot of examples, such as hexagonal array (approximated by an axisymmetric unit cell) which is considered as the simplest unit cell. The periodicity conditions on this type of unit cell are difficult to handle with standard numerical codes and it may be easier to

consider unit cells. An example is illustrated in Fig. 1.3 in the case of an axisymmetric unit cell.

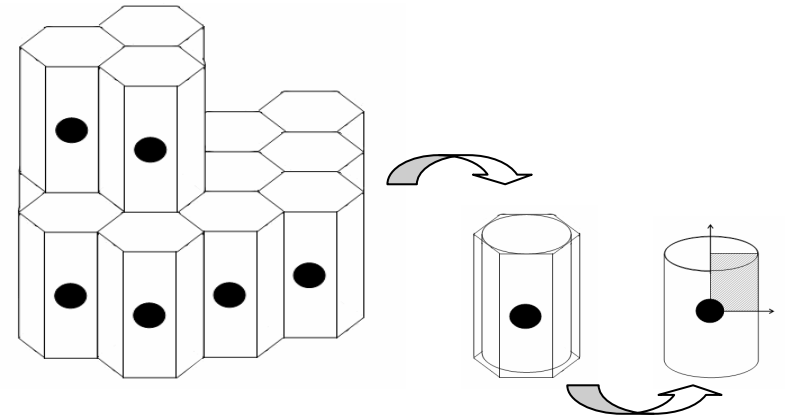

Fig. 1.3. Hexagonal array approximated to an axisymmetric unit cell.

The unit cell representation of periodic microstructure is widely discussed in the literature, either using two-dimensional or three-dimensional calculations (Doghri and Leckie, 1994; Doghri and Ouaar, 2003; Ristinmaa, 1997; Ma and Kishimoto, 1998; Ostoja-Starzewski, 1998; Lee and Ghosh, 1999; Michel et al., 1999; Berger et al., 2005; Selmi et al., 2007; Charles et al., 2010; Miled et al., 2011; 2013). Some different possibilities of unit cell are illustrated in Fig. 1.4.

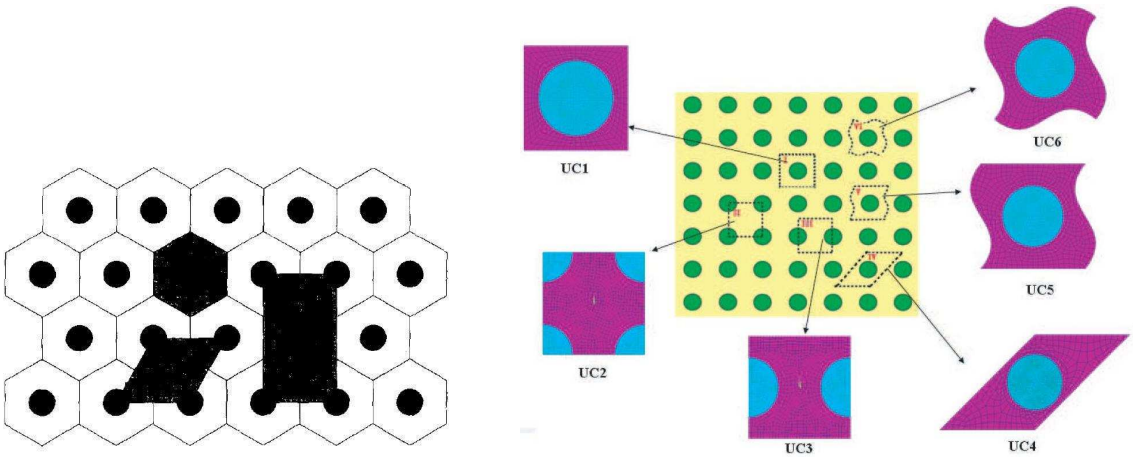

(a) (b)

Fig. 1.4. Different possibilities of unit cells used by (a) Michel et al. (1999) and (b) Ye (2013).

1.4.2. Random heterogeneous media

Periodic microstructure may rarely exist in reality. Heterogeneous microstructures consist in randomly distributed phases. Several authors worked on random microstructures (Brockenbrough et al., 1991; Nakamura and Suresh, 1993; Ghosh et al., 1996; Ostoja-Starzewski et al., 1997; Moulinec and Suquet, 1994; 1998; Moraleda et al., 2007; Delannay et al., 2007; Pierard et al., 2007a; 2007b; Brassart et al., 2009; 2010; Mortazavi et al., 2013a; 2013b; 2013c; El Ghezal et al., 2013; Miled et al., 2013). They have performed comparison of overall properties of the composites resulting from the modeling of regular and random microstructures. They explained that there is a significant difference, especially in the plastic regime. Most of these considerations have been performed for small deformations. Later, the influence of the spatial distribution of heterogeneities on overall macroscopic behavior was discussed in Kouznetsova et al. (2001) by comparing the results of micro-macro modeling for regular and random structures. Different random possibilities and regular unit cells that used by Kouznetsova et al. (2001) are shown in Fig. 1.5.

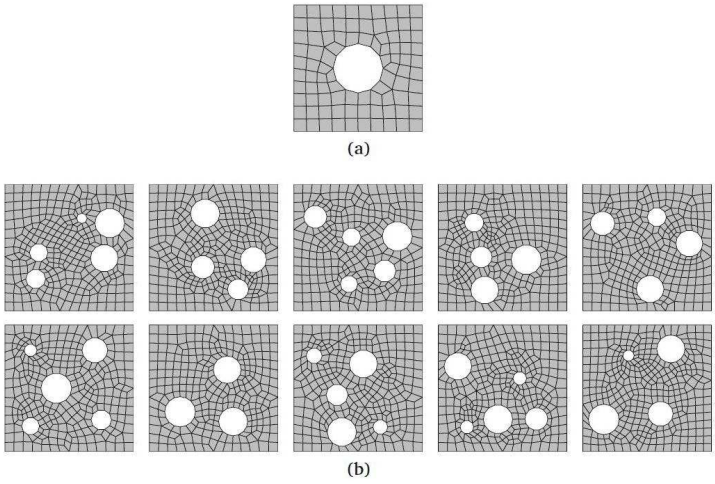

Fig. 1.5. Different possibilities of random porous microstructures compared with a regular unit cell (Kouznetsova et al., 2001).

Recently, three dimensional RVEs with random microstructure were studies by some authors such as Bilger et al. (2005) which showed the effect of non-uniform distribution of voids on the plastic response of porous materials, using numerical simulations with Fast Fourier Transform. They proposed an image analysis tool for the statistical characterization of the porosity distribution and they made assumptions for implementation of the voids to obtain different types of microstructures. The two-dimensional microstructures that presented by Bilger et al. (2005) are shown in Fig 1.6. In the classical Boolean model, the centers are randomly implanted according to standard Poisson process, with no limitation on their relative positions. Therefore, the voids can overlap (Fig. 1.6a). Constraint on the minimal distance between voids can be imposed to prevent void overlapping. This distance is zero for hard sphere model (Fig. 1.6b) and is strictly positive for cherry pit model (Fig. 1.6c) in which voids can neither overlap nor come into contact.

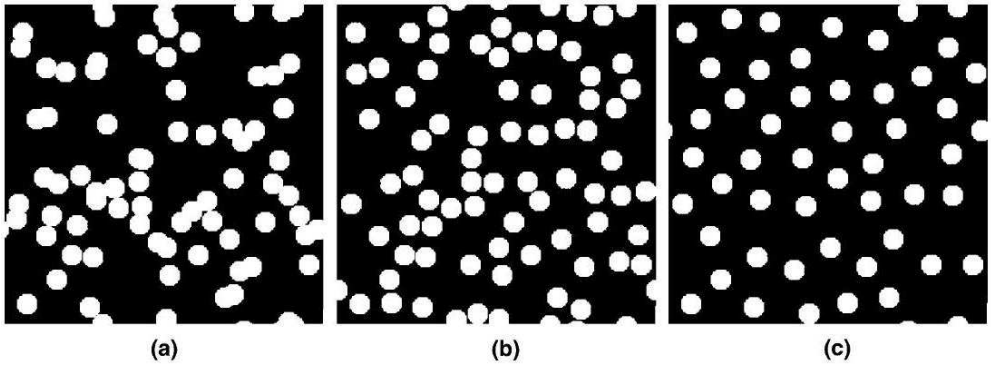

Fig. 1.6. Two-dimensional microstructures with identical size: (a) classical Boolean model, (b) hard sphere model and (c) cherry pit model.

Lee and Ghosh (1999) and Ghosh et al. (2001) proposed an elastic-plastic constitutive model that incorporates the details of microstructures for modeling porous and composite materials. They used two-scale analysis with asymptotic homogenization method and the Voronoi cell finite

element model for detailed microstructure analysis. Microstructures with different shapes, sizes, orientations, and spatial distributions for porous and composite materials are used, as shown in Fig. 1.7. Indicating that: square edge pattern with a circular inclusion (C1), square edge pattern with an elliptical inclusion (C2), random pattern with 25 identical circular inclusions (C3), horizontally aligned random pattern with 25 identical elliptical inclusions (C4), randomly oriented random pattern with 25 identical elliptical inclusions (C5), and random pattern with 17 random shape and size inclusions (C6).

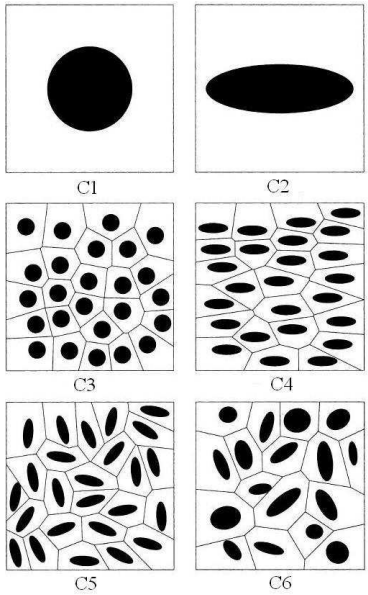

Fig. 1.7. Microstructures with different shapes, sizes, orientations and spatial distributions for composite materials (Lee and Ghosh, 1999; Ghosh et al., 2001).

As an example, Fig. 1.8 shows different three-dimensional microstructures with multiple inclusions used in the literature by different authors.

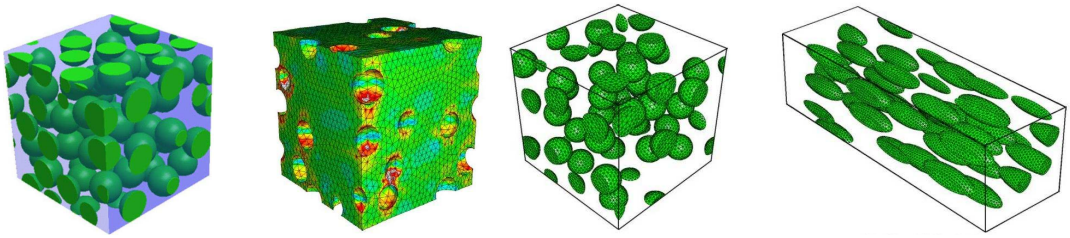

(a) (b) (c)

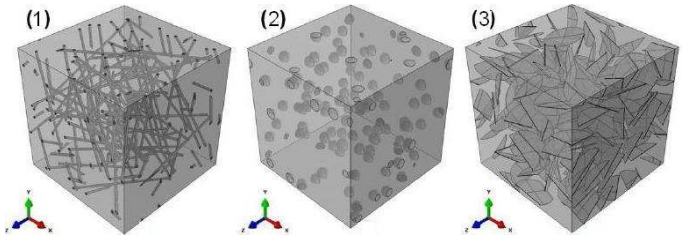

(d)

Fig. 1.8. Three-dimensional microstructures with multiple inclusions: (a) Fritzen et al. (2012), (b) Delannay et al. (2007), (c) Brassart et al. (2010), (d) Mortazavi et al. (2013b; 2013c).

1.5. Concluding remarks

Although the continuum-based micromechanical theory has reached a high degree of sophistication, it considers as material volume element a unit cell in which the microstructural representation is oversimplified. As an alternative, the computational homogenization appears to be a powerful tool to bring a better understanding of inclusion distribution effects and interaction phenomena on the overall properties.

In the next chapter, computational homogenization strategy is described in order to estimate the effective elastic-plastic response of particulate composites.

CHAPTER II

COMPUTATIONAL HOMOGENIZATION OF ELASTO-PLASTIC COMPOSITES[2]

[2] This chapter is based on the following paper: Y.K. Khdir, T. Kanit, F. Zaïri, M. Naït-Abdelaziz, 2013. Computational homogenization of elastic-plastic composites. International Journal of Solids and Structures 50, 2829-2835. Email: younis.khalid@hotmail.com

2.1. Introduction

Over the past five decades, the prediction of the effective mechanical response of random composite media has been an active research area. Because of the wide use of composite materials in high performance structures, the macroscopic mechanical analysis of the heterogeneous materials becomes very important. It is not easy to predict the non-linear macroscopic mechanical behavior of the structures with a large number of heterogeneities. Even it is possible to determine the equivalent material properties, it is in practice very costly and unrealistic to carry out such experiments for all possible microstructures. Composite materials comprise a matrix which could be polymeric, metallic or ceramic, and reinforcements (particles or fibers). Composite materials may be defined as heterogeneous materials with dissimilar constituents occupying different regions with distinct interfaces between them (Kalamkarov and Savi, 2012).

Many analytical works using homogenization methods have been achieved to bound or estimate effective material properties of composite materials (e.g. Nemat-Nasser and Hori, 1993). These methods which assume that the effective material properties can be defined via relationship between the volume averages of stress and strain fields were initially developed within the linear elastic framework. The well-known Voigt-Reuss and Hashin-Shtrikman (Hashin and Shtrikman, 1963) bounds are often used to give a useful bound of the effective properties, but they are too far apart for highly contrasted properties of constituents. The direct estimation of the effective properties can be achieved using approaches based on the Eshelby equivalent inclusion theory such as the Mori-Tanaka model (Mori and Tanaka, 1973) or the self-consistent scheme (Hill, 1965).

The Mori-Tanaka model considers the heterogeneities diluted in the matrix whereas in the self-consistent scheme the physical approximation is enhanced by incorporating the interaction effects between heterogeneities, see e.g. the papers of Anoukou et al. (2011a; 2011b) for a comparison of these theories. Although these analytical approaches have reached a high degree of sophistication and efficiency, and are nowadays well-established, it remains quite complex to transpose them to the plastic regime for which tangent and secant formulations were developed. In tangent formulations, the effective elastic-plastic response is computed incrementally by integrating along the loading path the effective stiffness tensor obtained from the tangent stiffness tensor of each phase (e.g. Hutchinson, 1970; Ju and Sun, 2001; Doghri and Friebel, 2005; Zaïri et al., 2011a). In secant formulations, the effective elastic-plastic response is computed from the secant stiffness tensor of each phase within the non-linear elastic framework (Berveiller and Zaoui, 1979; Tandon and Weng, 1988, Ponte Castañeda and Suquet, 1998). Numerical methods to estimate composite properties usually involve analysis of a RVE. The important points that need to be carefully considered when carrying out such analysis:

- The correct RVE corresponding to the assumed reinforced particle distribution must be isolated.
- Correct boundary conditions have to be applied to the chosen RVE, in order to model any type of loading.

This has been correctly modeled and simulated by many researchers. Zheng et al. (2001) indicated that the main requirements on homogenization methods for predicting the effective properties are:

- A simple structure which can be solved explicitly.

- A valid structure for multiphase heterogeneous with various inclusion geometries.
- An accurate model for the influence of various inclusion distributions and interactions between their immediately surrounding matrix.

Alternatively to these analytical approaches, the numerical simulations directly performed on the microstructure can be of a great help to solve non-trivial homogenization problems such as plasticity in random composite media. The material volume used to represent the microstructure, namely the RVE, is therefore of prime importance. Conventionally, the RVE must be chosen sufficiently large compared to heterogeneities to contain sufficient information about the microstructure in order to be representative, but it must remain small enough, much smaller than the macroscopic body, in order to be considered as a material volume element. Drugan and Willis (1996) proposed to define this notion as follows: "*It is the smallest material volume element of the composite for which the usual spatially constant (overall modulus) macroscopic constitutive representation is a sufficiently accurate model to represent the mean constitutive response*". This definition of the "deterministic" representative volume element (DRVE) ought to be verified in the context of elastic-plastic composites. The effective stress-strain response, defined from spatial averages of stress and strain fields over the volume element, must be obtained with a given accuracy. For large-scale computations the computational cost is a paramount issue and it is appealing to work on volumes smaller than the DRVE. The use of smaller volumes induces fluctuations of the estimated responses which must be compensated by averaging over several realizations of the microstructure in order to get the same estimation as that obtained for the whole volume. This strategy was proposed by Huet (1990), Hazanov and Huet (1994), Drugan and Willis

(1996) and Kanit et al. (2003; 2006) to estimate the linear elastic response of heterogeneous materials and it is extended in the present work to elastic-plastic composites.

The purpose of the present chapter is to describe a computational homogenization strategy to estimate the effective elastic-plastic response of particulate composites. The methodology is applied to a specific composite, namely a rubber-toughened thermoplastic polymer. The numerical estimates of the stress-strain response, and their scatters, obtained on volumes of fixed size but containing different realizations of a given volume of the microstructure are investigated.

The present chapter is organized as follows. In Section 2.2, we present the investigated microstructure and the computational method. The results are presented and discussed in Section 2.3. Some concluding remarks are given in Section 2.4.

2.2. Computational homogenization

2.2.1. Microstructure and mechanical properties of the studied polymer blend

The example of microstructure chosen in the present investigation to illustrate the methodology is a rubber-toughened poly(methyl methacrylate). It is constituted by a disordered distribution of soft rubbery inclusions in a stiff polymer matrix. The mechanical properties are known for the two individual constituents and were thoroughly investigated by Zaïri et al. (2011b) under uniaxial tensile loading. The rubbery inclusions are assumed linear elastic while the matrix is elastic-plastic. A very large

contrast exists in the mechanical properties of the constituents. The Young's moduli are 1550 MPa and 1 MPa for the matrix and the inclusions, respectively. The Poisson's ratios are 0.4 and 0.49, respectively.

The inelastic properties of the matrix were taken from the experimental data employed by Zaïri et al. (2011b). The choice of a microstructure with such a contrast in properties allows enhancing the variability of apparent mechanical responses obtained from small material volume elements. The elastic-plastic response of rubber-toughened thermoplastic polymers have been investigated in the past by several authors (Steenbrink et al., 1997; Socrate and Boyce, 2000; Riku et al., 2008) via numerical simulations of either a unit cell or a representative microstructure but never related to the issue of representativity of the volume element. By contrast, the representativity of the elastic-plastic responses obtained from limited domains of the random composite material is investigated in this work.

2.2.2. Mesh generation

One of the methods that help to get a deeper insight into the composite microstructure is serial sectioning. According to this method the three-dimensional (3D) microstructure is cut into several two-dimensional (2D) sections. However, some authors have directly evaluated the two-dimensional sections. We can put back them together to a simulated 3D microstructure. This procedure can be performed using a computer program. The method of sectioning has been investigated for some years ago (Chawla and Chawla, 2006; Chawla et al., 2006; Holm and Duxbury, 2006; Lieberman et al., 2006; Michailidis et al., 2010; Schmidt et al., 2011).

From a real microstructure, we can conclude that non-equally sized two-dimensional circles, which appear in the sections, could have the same 3D size. In order to explain in more detail about this method, we can look at the sectioning of an elementary volume element that contains one sphere. Fig. 2.1 shows some sections through the sphere in a unit cell that contains only one inclusion. It can be observed that the inclusion size first increase with increasing distance, reaches a maximum, and then decreases again until it finally disappears. This procedure gives the section through a sphere inside the elementary volume that always yields a circle, only with different radii, which depends on the distance of the sectioning. The forms, the sections of the inclusion, depend on the distance and orientation of the sectioning (Annapragada et al., 2007).

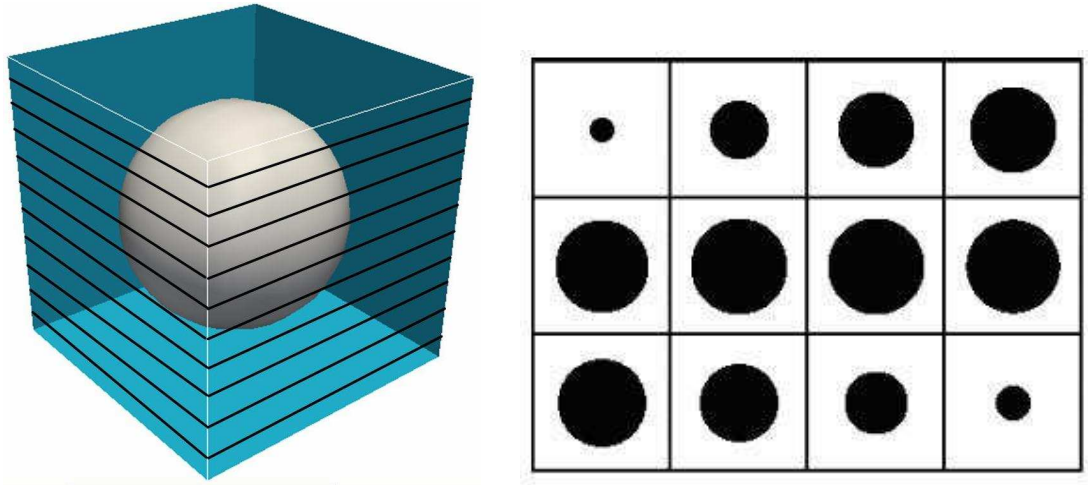

(a) (b)

Fig. 2.1. Equally distanced sections through a sphere for a unit cell containing one inclusion: (a) three-dimensional simulation, (b) equal distance sections of image.

The geometrical description of a 3D microstructure is much more difficult than in the planner case. Experimental techniques to 3D images from the actual macrostructure are very complex and expensive. The

homogenized macroscopic non-linear behaviors of the composites were obtained by finite element (FE) analysis of a random cubic which consists of randomly distributed non-overlapping spherical particles. The 3D microstructure is reconstructed from two-dimensional images by means of a serial sectioning process, which gives more accurate results. To generate the RVE a numerical procedure is used to generate the two-dimensional images and these images are used to generate 3D cubic cells. The procedure of generating two-phase cubic RVE from multiple 2D images and the simulation with the real microstructure of the application sample are illustrated in Fig. 2.2.

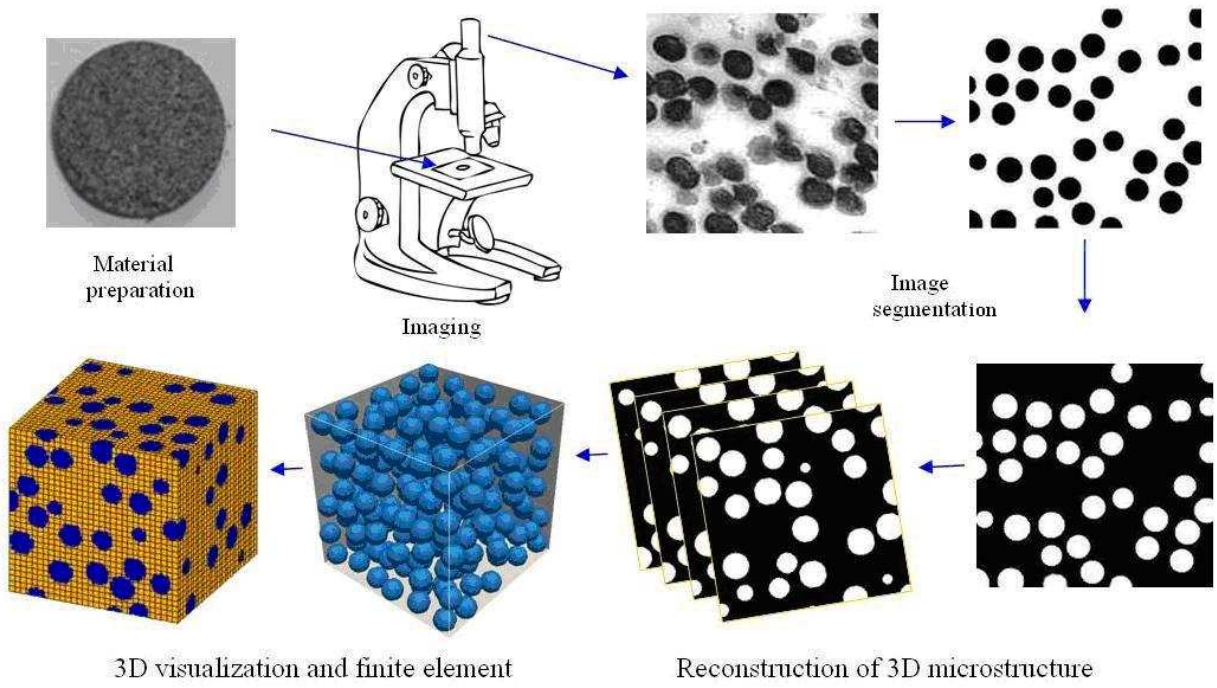

Fig. 2.2. Flow chart of serial sectioning and 3D virtual microstructure generation process.

The mesh density used in this study is fine enough to accurately represent the geometry of two phases (inclusions and matrix). In general, with the identical spherical particles, it is possible to generate all the

different ratios of volume fractions, that they can be used for designing purpose in the future. The layers of 2D images are created from a group of inclusions in a cubic zone which is generated by using MATLAB codes (Fig. 2.2).

In the numerical homogenization procedure, the important approach to model the macroscopic behavior of multiphase composites is to generate a RVE, which should capture the main features of the microstructure. The FE models of RVE for the randomly spherical particles reinforced composites are shown in Fig. 2.2.

The FE calculations were carried out with Zebulon FE software. The 3D microstructure was reconstructed from 2D images by means of a serial sectioning process. A numerical procedure was used to randomly generate the 2D microstructure section by section. These images have being assembled to generate the wanted 3D cubic microstructure. The procedure is illustrated in Fig. 2.3. The obtained microstructure consists in randomly distributed non-overlapping identical spherical particles embedded in the matrix. The volume is considered large enough to represent the investigated microstructure. A FE mesh was then superimposed on the 3D image using quadratic brick elements.

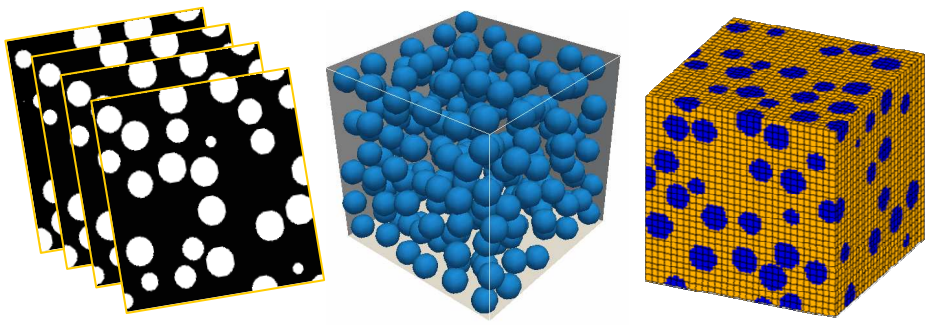

Fig. 2.3. 3D image reconstruction from 2D images and finite element mesh.

The inclusion volume fraction f is defined as the ratio between the volume of n inclusions in the RVE and the entire volume V of the RVE:

$$f = \frac{4\pi r^3 n}{3V} \tag{2.1}$$

where r is the inclusion radius.

In what follows, the term “effective” will be reserved for the overall response of the RVE, and when working on smaller volume than the RVE, the term of “apparent” will be used.

2.2.3. Boundary conditions

The second important issue for the numerical tests after generating microstructures concerns the boundary conditions (see e.g. Kanit et al., 2003; Li and Ostoja-Starzewski, 2006) which for a uniaxial tensile loading in the x-direction for example, as depicted in Fig 2.4, are prescribed as follows:

$$\begin{aligned} &u\{\text{plane}\,(x=0,y,z)\}=0 \qquad && v\{\text{point}\,O(0,0,0)\}=0 \\ &u\{\text{plane}\,(x=l,y,z)\}=\delta \qquad && w\{\text{point}\,O(0,0,0)\}=0 \\ &v\{\text{point}\,A(0,0,l)\}=0 \qquad && w\{\text{point}\,B(0,l,0)\}=0 \end{aligned} \tag{2.2}$$

in which u, v and w are the applied displacements in the x, y and z-directions, l is the RVE length and δ is the prescribed displacement.

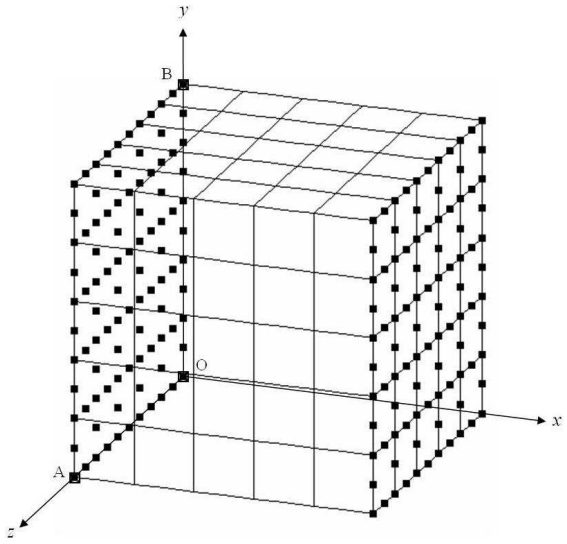

Fig. 2.4. Description of the boundary conditions.

2.2.4. Number of realizations and RVE sizes

FE computations on subvolumes of different sizes extracted from the entire volume *V* were performed. The main advantage of this strategy is that it allows us to work on a sufficiently large volume for a low computational cost. Fig. 2.5 presents an example of DRVE containing 200 inclusions and a subdivision of this whole microstructure into 27 and 8 subvolumes. The term *n* corresponds to the number of soft rubbery inclusions in each volume and *p* denotes the number of realizations.

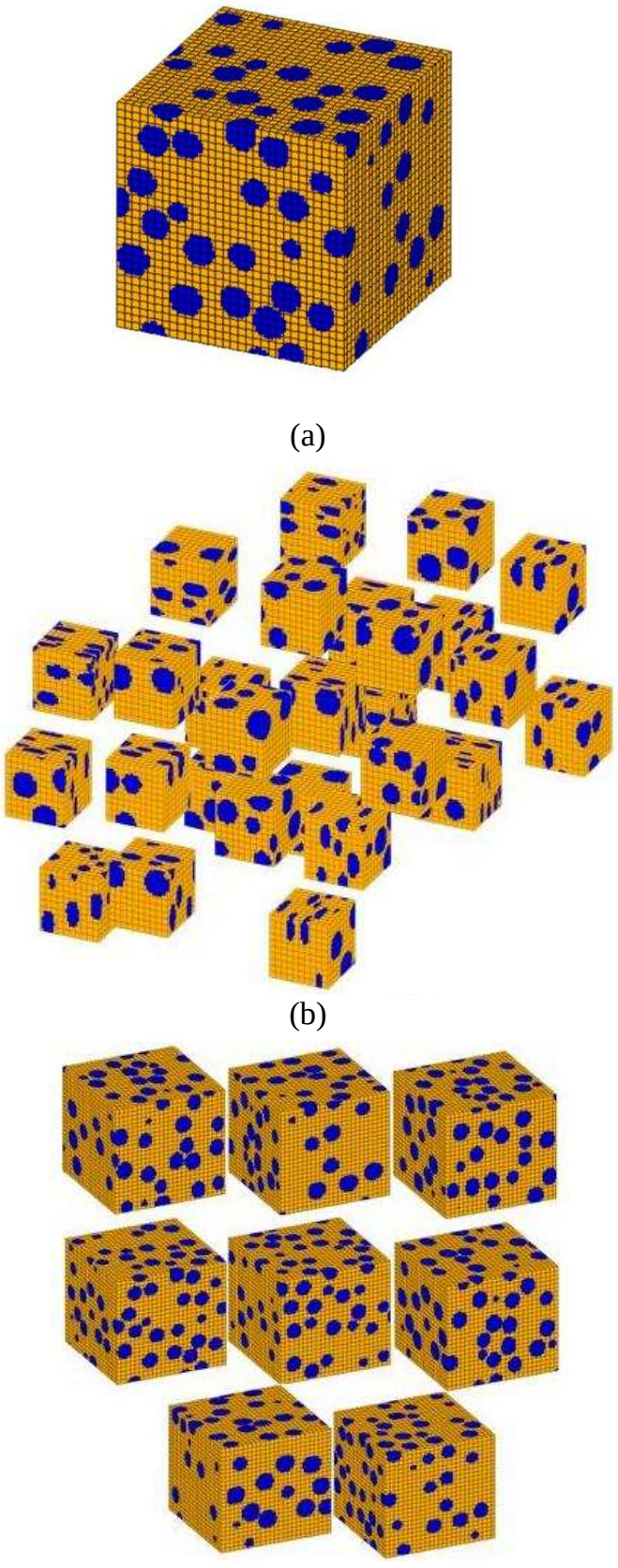

(a)

(b)

(c)

Fig. 2.5. Examples of microstructures with the superimposed FE mesh with f = 0.23: (a) n = 200, p = 1, (b) n = 8, p = 27, (c) n = 116, p = 8.

The different configurations with increasing sizes are summarized in Table 2.1. Note that decreasing *p* means an increasing number of soft rubbery inclusions *n* in a subvolume. That leads to a total of 268 different arrangements which were divided into six configurations including the entire volume *V*.

P	*N*
216	1
27	8
8	25
8	60
8	116
1	200

Table 2.1. Characteristics of all considered configurations.

Three configurations in which the entire volume *V* was decomposed into *p* subvolumes containing 1, 8 and 25 inclusions lead to non overlapping subvolumes. Two other configurations (*n* = 60 and 116) exhibit the same number of overlapping subvolumes *p*. Note that the realizations in the same configuration have the same number of inclusions. The *p* apparent strains and stresses computed for each subvolume are used to calculate the average strain $\overline{E}^{app}$ and the average stress $\overline{\Sigma}^{app}$ at each increment as follows:

$$\begin{aligned} \overline{E}^{app} &= \frac{1}{p}\sum_{i=1}^{p} E_i^{app} \\ \overline{\Sigma}^{app} &= \frac{1}{p}\sum_{i=1}^{p} \Sigma_i^{app} \end{aligned} \tag{2.3}$$

in which Σ_i^{app} is the stress for a given strain E_i^{app} of the realization i.

In the computations, the same boundary conditions were applied to the whole volume and to all individual subvolumes. The average stress-strain response of subvolumes is compared to the effective one found for the whole volume.

2.3. Results and discussion

2.3.1. Apparent and effective mechanical responses

Particle volume fractions of $f = 0.13$ and $f = 0.23$ are considered in the simulations. As shown in Fig. 2.6a identical effective stress-strain responses in the three orthogonal directions were obtained for the whole microstructure ($p = 1$, $n = 200$). It is worth noticing that identical stress-strain responses in the three orthogonal directions are a necessary, but not a sufficient condition for isotropy. It was also ensured that the shear stress-strain behavior is identical in two perpendicular planes[3]. Consider now the case of averaging on subvolumes.

[3] The found isotropy proves that the considered volume is representative enough of the examined microstructure and that its apparent response can be assimilated to the effective one.

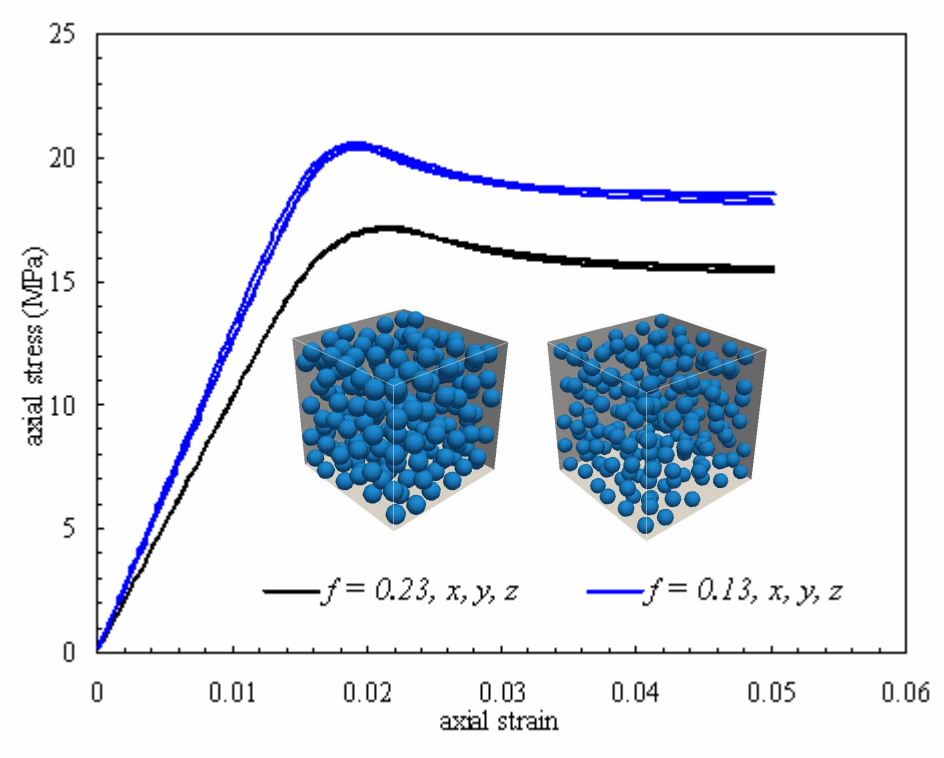

(a)

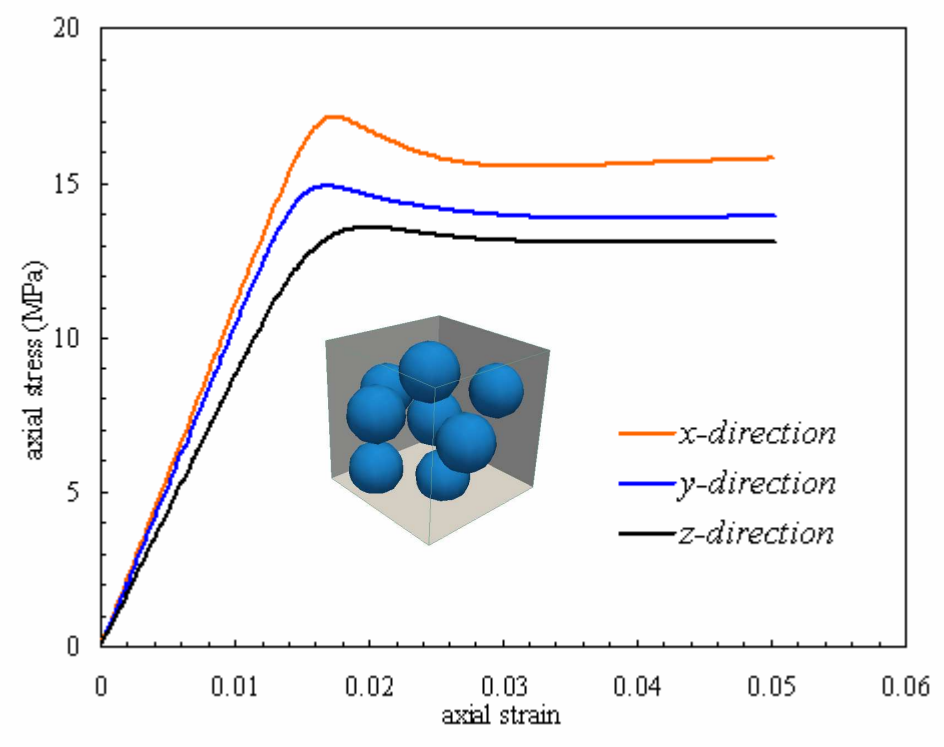

(b)

Fig. 2.6. Apparent stress-strain curves: (a) for the whole microstructure (p = 1, n = 200) with f = 0.13 and 0.23, (b) for only one subvolume (p = 27, n = 8) in the three directions.

Numerical predictions of the apparent stress-strain response of subdomains cut inside the entire volume element show substantial differences in the three directions. If we consider only one subvolume, the mechanical response is clearly anisotropic as shown in Fig. 2.6b. However, if the average process is undertaken for all subvolumes in each direction (Figs. 2.7a, b and c), we can note that the averages of apparent responses are identical in the three directions (Fig. 2.7d). Less than 0.5% error was noticed for all the realizations.

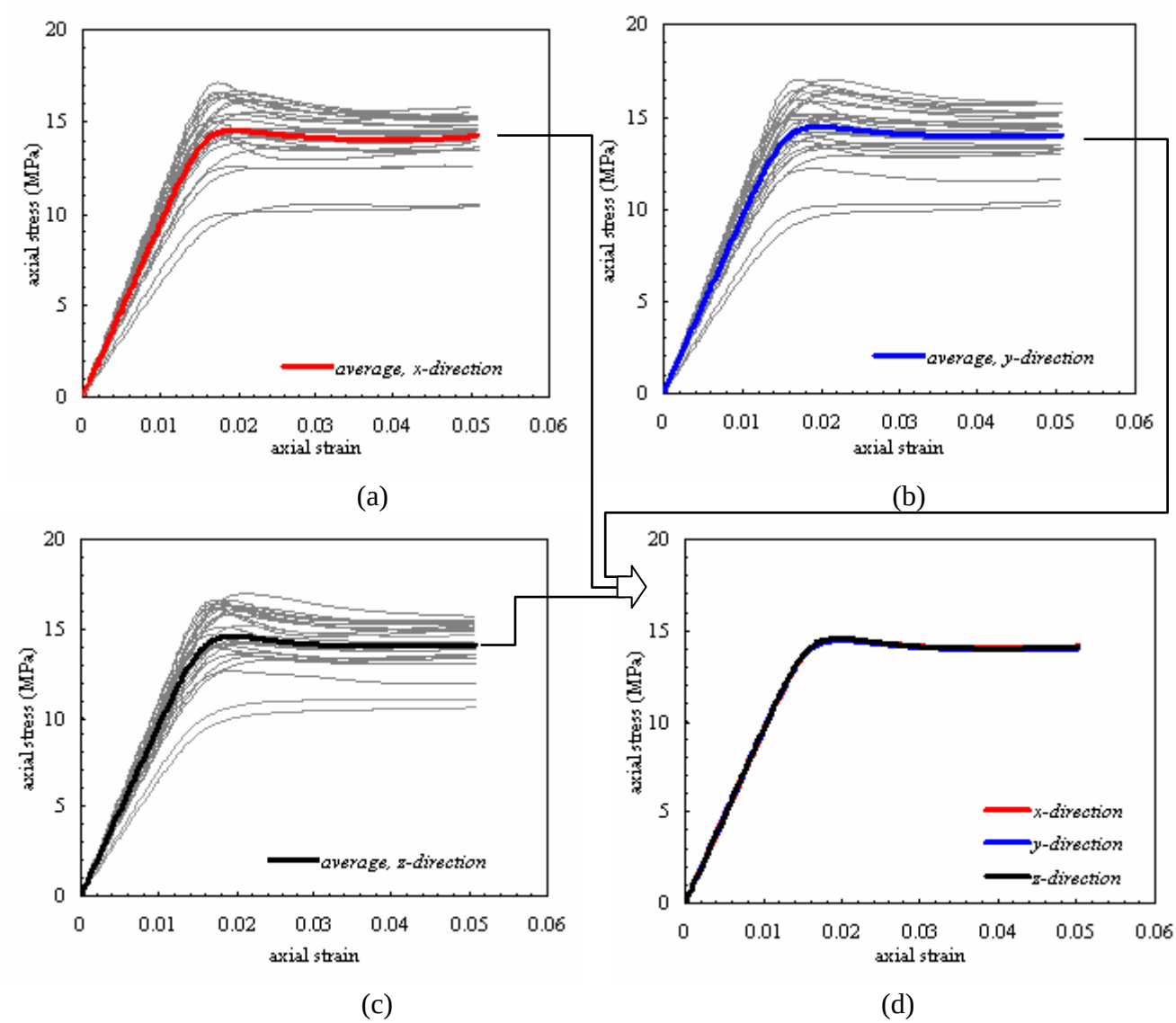

Fig. 2.7. Apparent stress-strain curves: for a collection of 27 subvolumes (p = 27, n = 8) stretched in the (a) x, (b) y and (c) z-directions, and (d) comparison of average curves in the three directions (f = 0.23).

Even this recovered isotropy is shown for a particular case, the same trends were observed for all configurations. One may conclude that only one subvolume could not be used as RVE to describe the mechanical response since the observed anisotropy is not in agreement with the isotropic character of the random microstructure at the macroscopic scale.

The mechanical responses obtained for other configurations are shown in Figs. 2.8, 2.9 and 2.10. As expected, for a given subdivision, the scattering from one subvolume to another decreases when the size of subvolumes increases. It turns out that a sufficiently large subvolume must be selected inside the whole volume to avoid fluctuations and to reach a good estimation of the average. The 216 and 27 subvolumes provide, respectively, 216 and 27 apparent stress-strain curves (Figs. 2.8a and 2.8b) with a significant dispersion. This significant scattering can be interpreted as a measure of the loss of representativity due to a high variability of properties over limited domains. For the same number of subvolumes the scattering induced by the regular non-overlapping subvolumes, forming a uniform partition of the whole volume, is larger than for the overlapping ones. It can be noticed that the error decreases with the domain size. The mathematical parameter characterizing the dispersion in the apparent stress-strain response is the quadratic error χ_l defined as:

$$\chi_l = \frac{1}{m}\sum_{j=1}^{m}\left(\frac{\Sigma_j^{app}}{\overline{\Sigma}_j^{app}} - 1\right)^2, \; 1 \le l \le p \tag{2.4}$$

in which Σ_j^{app} is the axial stress value for a given axial strain E_j^{app} $1 \le j \le m$ (m is the total number of increments) and $\overline{\Sigma}_j^{app}$ is the corresponding average axial stress computed on the p curves.

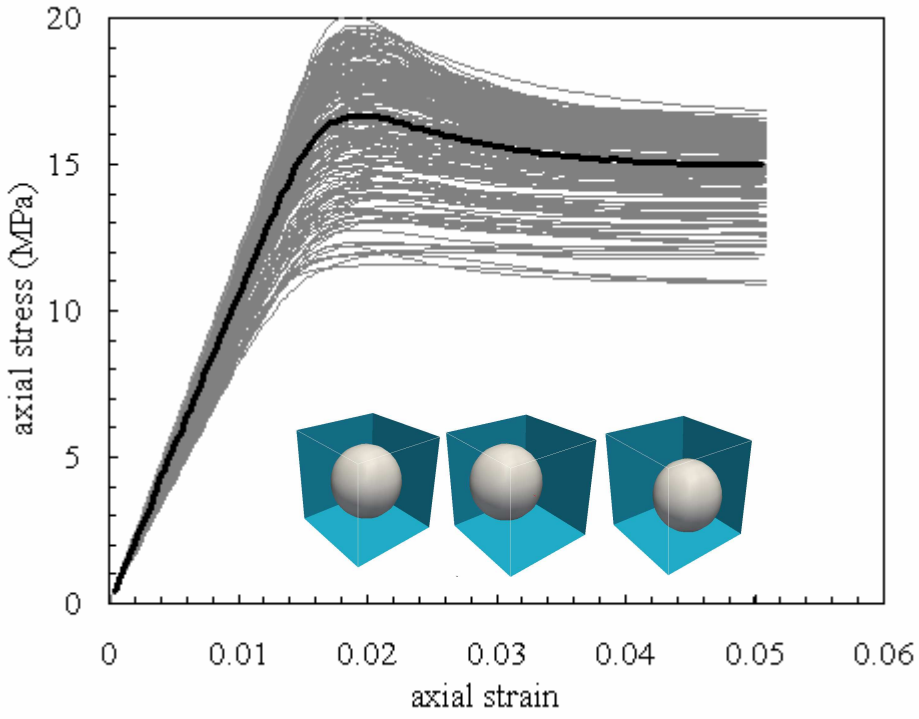

(a)

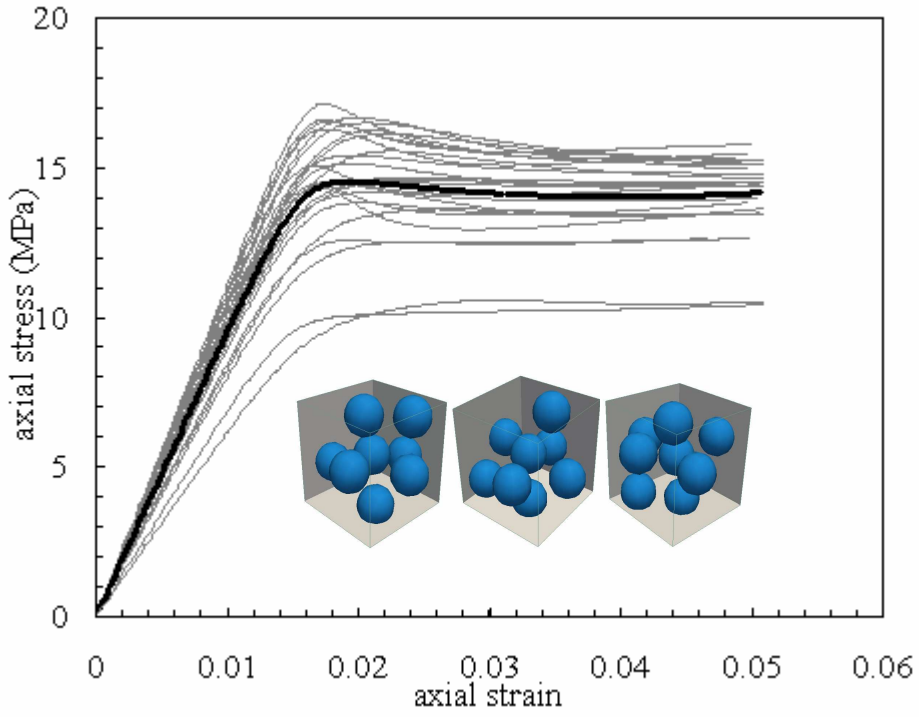

(b)

Fig. 2.8. Examples of apparent stress-strain curves (thin lines) and comparison with the average curve (thick line) for different configurations with f = 0.23: (a) n = 1, p = 216, (b) n = 8, p = 27.

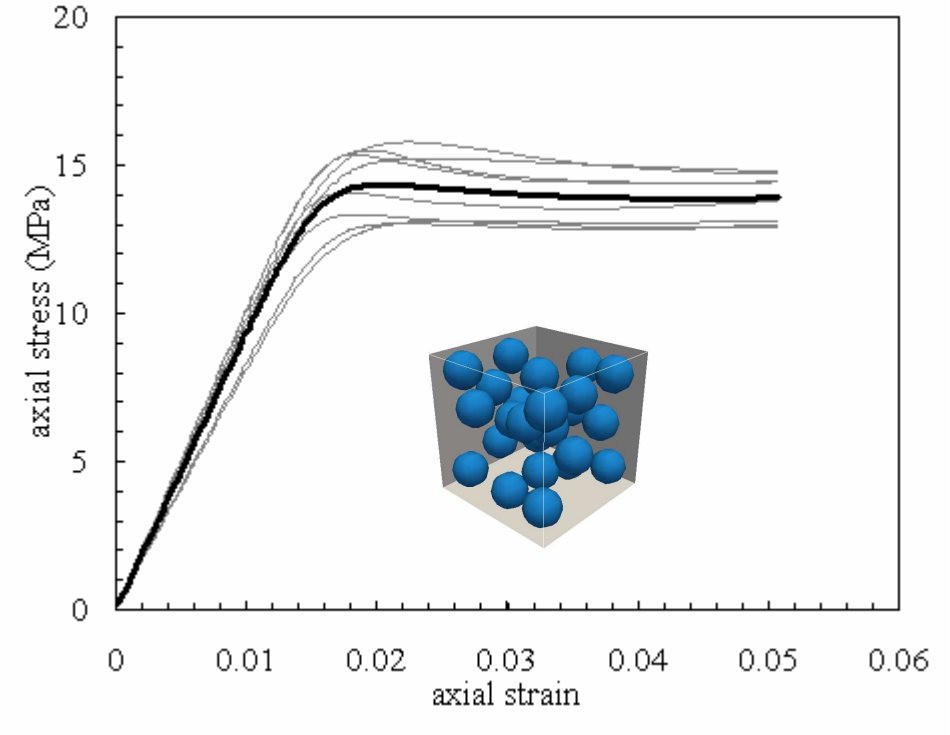

(a)

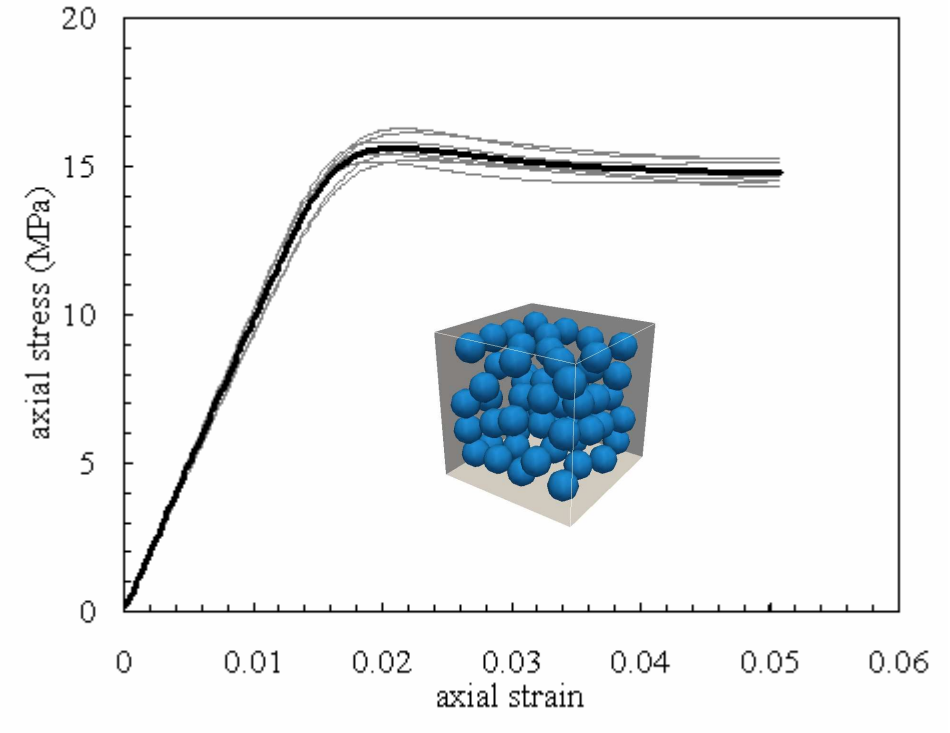

(b)

Fig. 2.9. Examples of apparent stress-strain curves (thin lines) and comparison with the average curve (thick line) for different configurations with f = 0.23: (a) n = 25, p = 8, (b) n = 60, p = 8.

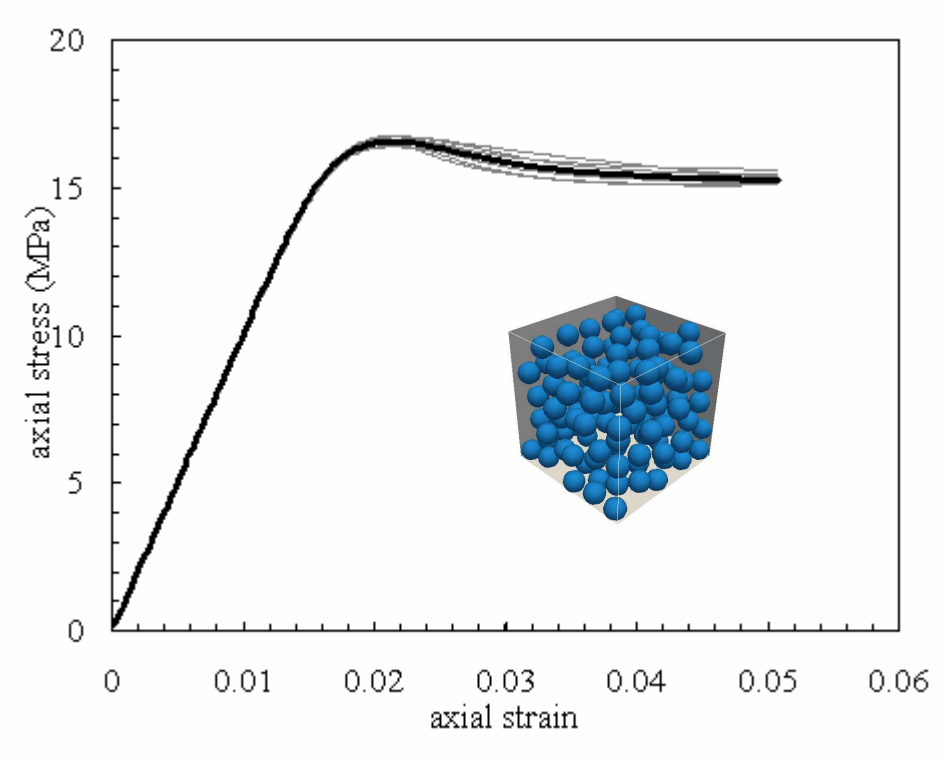

(a)

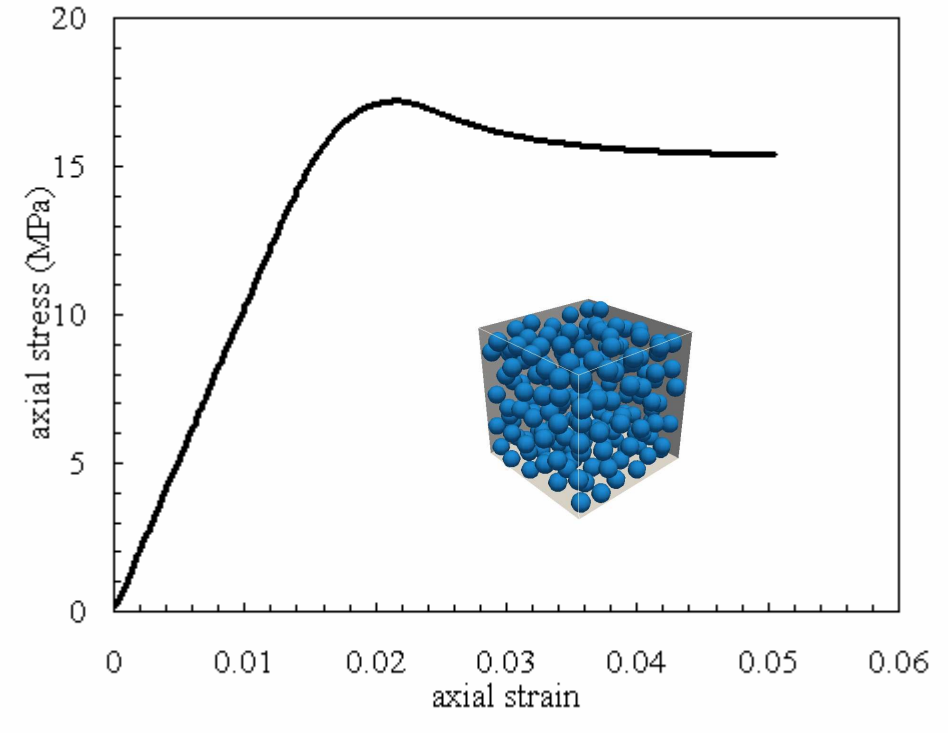

(b)

Fig. 2.10. Examples of apparent stress-strain curves (thin lines) and comparison with the average curve (thick line) for different configurations with f = 0.23: (a) n = 116, p = 8, (b) n = 200, p = 1.

The average quadratic error $\bar{\chi}$ of p realizations is given by:

$$\bar{\chi} = \frac{1}{p}\sum_{l=1}^{p} \chi_l \tag{2.5}$$

The average quadratic error is reported for each group of realizations in Table 2.2 for two volume fractions. The results show that the average quadratic error decreases with the number of inclusions.

n	$\bar{\chi}$ Error $f = 0.23$	$\bar{\chi}$ Error $f = 0.13$
1	1.52	1.48
8	1.29	0.73
25	0.49	0.25
60	0.07	0.08
116	0.01	0.02
200	0	0

Table 2.2. Errors for each group of realizations.

The average apparent stress-strain curves obtained for each subdivision are presented in Fig. 2.11 for two volume fractions. One can clearly notice that the computed average responses within the elastic regime do not vary significantly with the volume size and therefore represent a fair estimate of the effective elastic modulus. Drugan and Willis (1996) also showed that the RVE size of particulate composites is unexpectedly small in the statistical sense within the elastic regime. This means that the average value generated from the simulations of different RVE is reasonably close to the exact solution. Even the elementary volume element containing one centered inclusion gives satisfactory results in the elastic regime. By contrast, the average curves computed with a set of smaller volume elements underestimate the effective response beyond the yield stress. For

sufficiently large volumes the average elastic-plastic curves converge towards the effective one. The fact that the apparent curve obtained with the couple $n = 1$ and $p = 216$ is closer to the effective curve than for other configurations with higher sizes can be due to some edge effects generated by the boundary conditions. It is also due to the fact that in this case, the average is not significant because of a high degree of scattering. One may note that the response of the elementary volume element containing one centered inclusion ($p = 1$, $n = 1$) clearly underestimates the real response. For such boundary conditions, although this kind of modeling is widely used in the literature, it has to be taken as a minor bound of the real response.

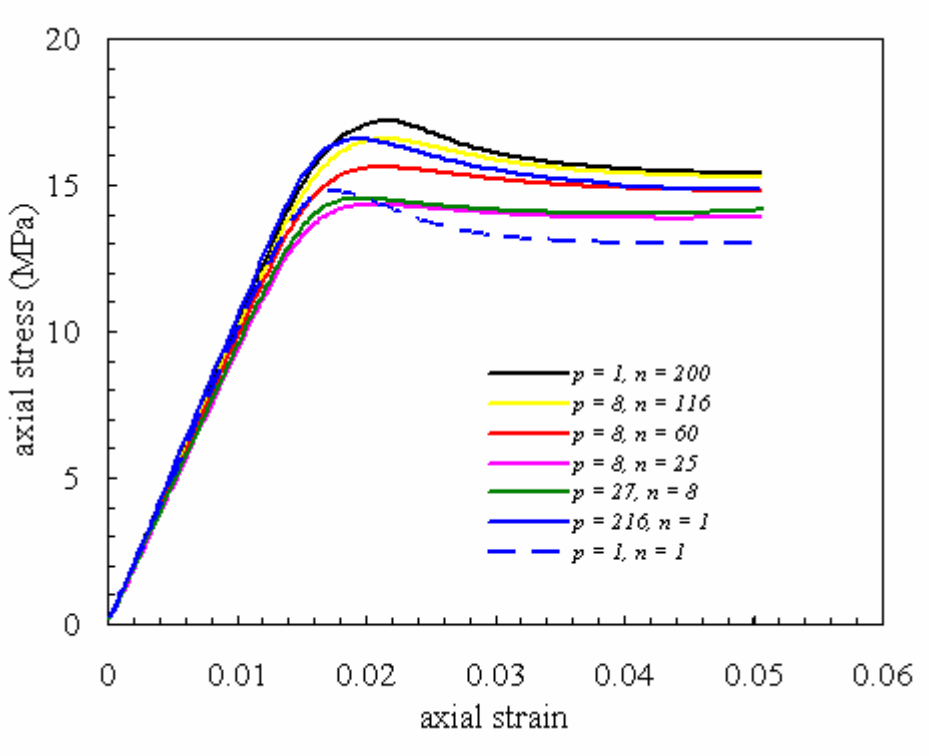

(a)

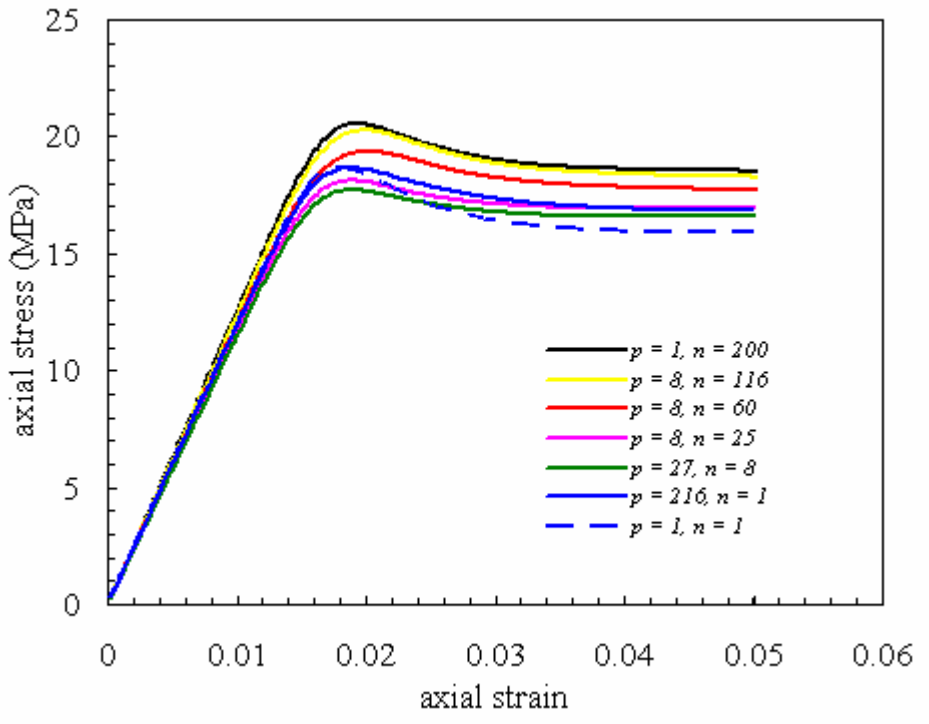

(b)

Fig. 2.11. Examples of average stress-strain curves of different configurations for: (a) f = 0.23, (b) f = 0.13.

2.3.2. Time and memory consumption

Using such numerical calculations on RVE require very large memory and time spending. Fig. 2.12 shows the evolution of the required memory and time as a function of the number of inclusions involved in the calculations. They exhibit the same evolution. The worst configuration corresponding to the higher values in time and memory is clearly pointed out (p = 8, n = 116). Another configuration must be avoided too (p = 8, n = 60), because time and memory required are larger than that involved by the calculation on the whole microstructure.

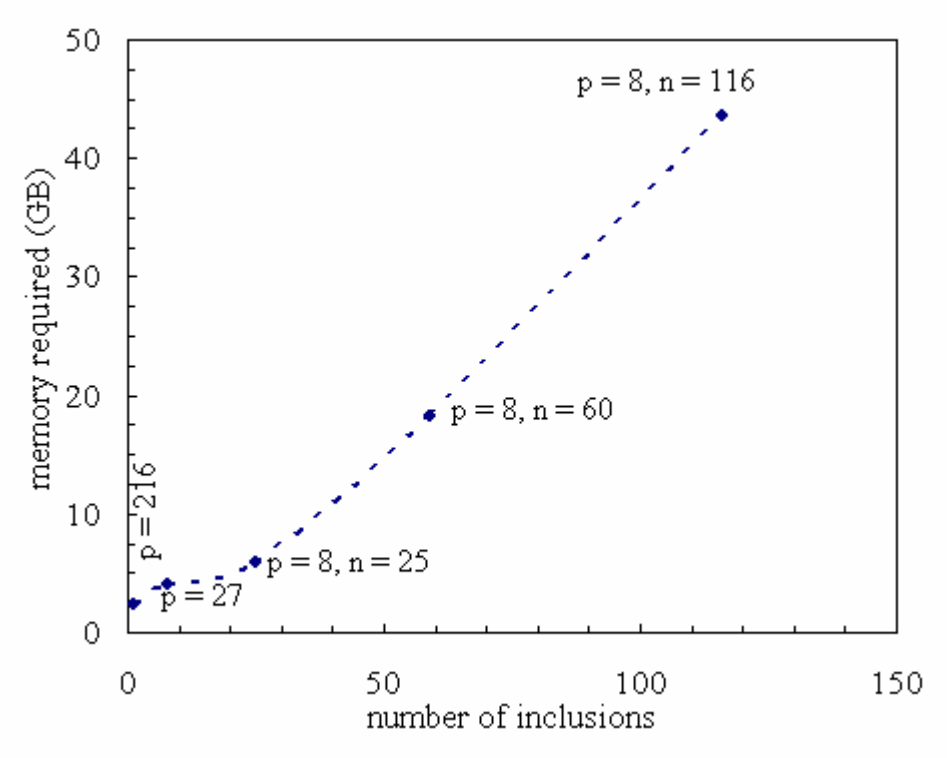

(a)

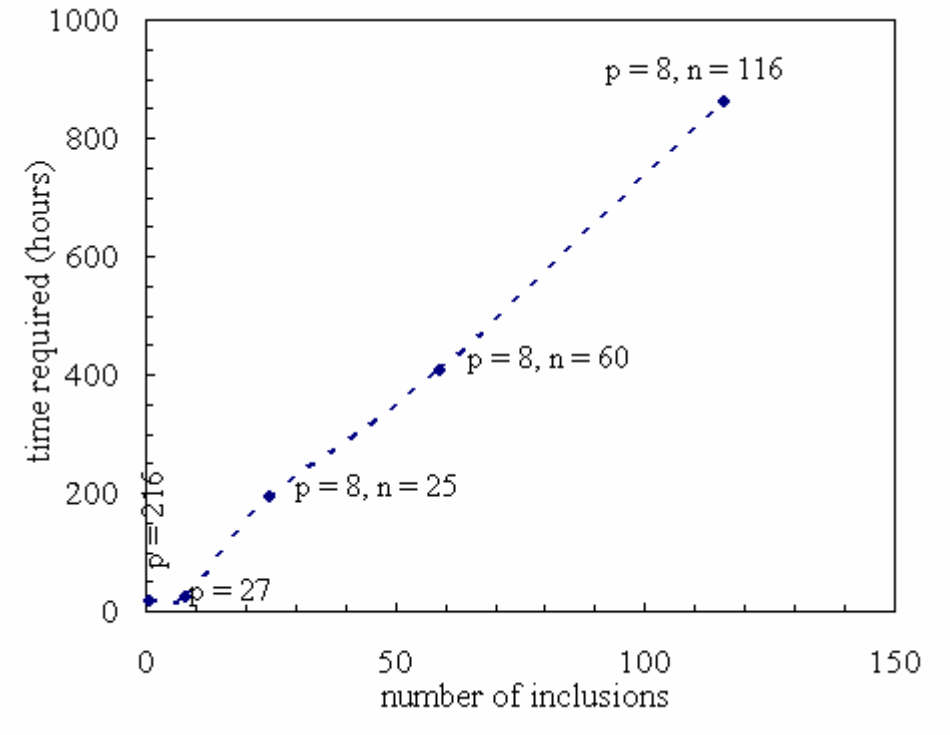

(b)

Fig. 2.12. Memory required in GB (a) and time required in hours (b) as a function of the number of inclusions (f = 0.23).

2.4. Concluding remarks

A computational homogenization method was used to estimate the effective elastic-plastic response of particulate composites. The method is based on the computations of small limited volumes of fixed size extracted from a larger one and containing different realizations of the random microstructure. Both non-overlapping and overlapping partitions of the larger volume element into subvolumes were considered. If a small subvolume did not necessary exhibit an isotropic response (even if the microstructure is expected to be macroscopically isotropic) we showed that the average response of a sufficient number of different realizations is isotropic. A significant scatter in the plastic regime of the apparent stress-strain curves was observed for too small subvolumes. It was shown that the dispersion of the results decreases when the domain size increases. It was also found that for a given number of realizations the overlapping of subvolumes significantly decreases the dispersion. Finally, it was also shown that the elementary volume element containing one centered inclusion, even widely used in the literature, represents a minor bound of the real mechanical response.

The second part of this work is focused on the computational homogenization of random porous media using the DRVE.

PART II

COMPUTATIONAL HOMOGENIZATION OF RANDOM POROUS MEDIA

CHAPTER III

COMPUTATIONAL HOMOGENIZATION OF RANDOM POROUS MEDIA: EFFECT OF VOID SHAPE AND VOID CONTENT ON THE OVERALL YIELD SURFACE[4]

[4] This chapter is based on the following paper: Younis-Khalid Khdir, Toufik Kanit, Fahmi Zaïri, Moussa Naït-Abdelaziz, 2014. A computational homogenization of random porous media: effect of void shape and void content on the overall yield surface. Submitted. Email: younis.khalid@hotmail.com

3.1. Introduction

Over the last four decades, the mathematical development of yield criteria for the plastic porous solids has been widely investigated (Rice and Tracey, 1969; Gurson, 1977; Tvergaard, 1982; Koplik and Needleman, 1988; Sun and Wang, 1989; Ponte Castaneda, 1991; Gologanu et al., 1993; 1994; 1997; 2001; Zuo et al., 1996; Gărăjeu and Suquet, 1997; Faleskog et al., 1998; Ma and Kishimoto, 1998; Corigliano et al., 2000; Pardoen and Hutchinson, 2000; Zhang et al., 2000; Negre et al., 2003; Kim et al., 2004; Wen et al., 2005; McElwain et al., 2006; Monchiet et al., 2008; Zaïri et al., 2005; 2008; Besson, 2009; Laiarinandrasana et al., 2009; Li and Karr, 2009; Nielsen and Tvergaard, 2009; Vadillo and Fernandez-Saez, 2009; Zadpoor et al., 2009; Dunand and Mohr, 2011; Li et al., 2011; Mroginski et al., 2011; Fei et al., 2012; Shen et al., 2012; Yan et al., 2013) essentially because of the role of porosities regarding the ductile fracture process, these voids being the consequence of manufacturing processes. The mathematical derivations of these criteria are generally based upon the continuum-based micromechanical framework, for which the starting point is the microstructural representation of the porous medium. The non-triviality of the theoretical problem leads to define a basic unit cell containing one centered void for the material volume used to represent the microstructure. The unit cell is an elementary volume element consisting in a hollow sphere or cylinder subjected to a uniform macroscopic strain rate at its external boundary. Gurson (1977) proposed the most widely used micromechanics-based yield criterion to analyze plastic porous solids containing spherical voids.

The Gurson model is based upon the following assumptions: isotropy, incompressibility and rigid-plasticity for the local yielding of the surrounding matrix material which obeys to the von Mises criterion. The resulting macroscopic yield criterion of Gurson (1977) for the porous medium is hydrostatic pressure-dependent, integrates the volume fraction of porosities as a model parameter and accounts for a possible void growth driven by the local plastic deformation of the surrounding matrix material. As pointed out by Tvergaard (1982), the Gurson model gives an upper bound of the macroscopic yield stress as a function of the mean stress for a periodic arrangement of voids. In order to improve its agreement with two-dimensional finite element simulation results on a periodic unit cell, Tvergaard (1982) proposed to introduce heuristic parameters in the Gurson yield criterion. These adjustable parameters have no direct physical meaning but may be correlated to interaction effects between voids. The extension of the Gurson model by Tvergaard (1981), known as the Gurson-Tvergaard (GT) model, was thenceforth widely used by many researchers to check its capability to capture the poroplastic behavior of many engineering porous materials. In very useful background papers, Benzerga and Leblond (2010) and Besson (2010) reviewed the various extensions of the Gurson model based upon enhanced micromechanical approaches or upon phenomenological generalizations to take into consideration the void shape or the matrix material features such as isotropic/kinematic hardening, viscoplasticity, compressibility and anisotropy. Using micromechanical approaches, Ponte Castaneda (1991) and Sun and Wang (1995) proposed, respectively, upper and lower bounds for the overall yield surface of porous media. Using the variational technique introduced by Ponte Castaneda (1991), Gărăjeu and Suquet (1997) proposed another upper bound which overcomes the well known basic drawbacks of the Gurson criterion at low stress triaxiality values. The effect of void shape on the macroscopic yield

response of porous materials was investigated by several authors (Gologanu et al., 1993; 1994; 1997; 2001; Yee and Mear, 1996 ; Son and Kim, 2003; Siruguet and Leblond, 2004; Flandi and Leblond, 2005a; 2005b; Li and Huang, 2005; Li and Steinmann, 2006; Monchiet et al., 2006; 2008; Gao et al., 2009; Keralavarma and Benzerga, 2010; Lin et al., 2010; Lecarme et al., 2011; Scheyvaerts et al., 2011; Zaïri et al., 2011; Danas and Aravas, 2012; Madou and Leblond, 2012; Monchiet and Kondo, 2013).

Although the mathematical developments have reached a high degree of sophistication, the resulting yield criteria generally involve a certain number of parameters with no physical significance. That may be explained by the fact that these micromechanics-based models consider as material volume element an elementary volume element containing a single void. Because the voids are diluted in the matrix material, the interactions between voids are neglected. Moreover, this microstructural representation of the porous material implies periodicity. However, to be statistically representative, the material volume element should contain sufficient information about the porous microstructure, in particular the void distribution. This last decade, the material response of porous media was also investigated using computational homogenization. This approach is emerging as a powerful tool to bring a better understanding of void distribution effects and interaction phenomena on the mechanical behavior of random porous media. The main advantage of the computational homogenization is its ability to directly compute the mechanical fields on the random porous media by representing explicitly the microstructure features such as shape, orientation and distribution of voids. Although many studies were dedicated to the development of yield criteria for plastic

porous media, it seems that only few works have been devoted to three-dimensional computational homogenization involving multiple voids. To our knowledge, only Bilger et al. (2005; 2007), Fritzen et al. (2012; 2013) and Khdir et al. (2014) used this approach to estimate the overall yield surface of porous materials. Their computations were limited to spherical voids. The calculations of Bilger et al. (2005; 2007) were performed on the basis of three-dimensional Fast Fourier Transform. The pore clustering effect on the overall material response was the key point of their investigation. Fritzen et al. (2012; 2013) assumed the random porous media as a volume of porous material which is periodically arranged. The results highlighted by Fritzen et al. (2012) led them to extend the GT yield criterion in order to overcome the analytical/numerical discrepancies. Khdir et al. (2014) focused their investigations on the porous materials containing two populations of voids. Their results showed that, for an identical fraction of porosities, there is no significant difference between a double and a single population of voids.

In this contribution, a computational homogenization of random porous media, including spherical and oblate/prolate spheroidal voids, is presented in order to determine their overall yield surface while still studying the representativity of the computational results. Notably, the computational investigations performed in this study can account for the complex coupling existing between void distribution, void shape and external loading mode. The first aim is to compare the simulation results with some Gurson-type yield criteria. The second aim is to verify the extension of the GT yield criterion provided by Fritzen et al. (2012) in the case of random porous media containing non-spherical voids.

The present chapter is organized as follows. We first review some existing analytical models for porous materials in Section 3.2. We present in Section 3.3 the investigated microstructures and the computational homogenization method. Section 3.4 is devoted to results and discussions. Concluding remarks are finally given in Section 3.5.

3.2. A brief survey of existing analytical models

3.2.1. Rice-Tracey (1969)

Many constitutive models with evolving damage have been estimated over the past years. Some of these models are based on the scheme that the degradation of the stress holding capacity of the material is caused by void initiation, void growth and coalescence. Simultaneous plastic deformation and hydrostatic tension in the material lead to the void growth.

The criterion of Rice and Tracey (1969) does not include any coupling between the material damage and the constitutive behavior. This model states that the material damage evolves according to the following equation:

$$\ln\left(\frac{R}{R_o}\right)_c = \int_1^2 \kappa \exp\left(\frac{3}{2}T\right) dE_{eq}^p \tag{3.1}$$

where $\kappa = 0.283$ and $T = \Sigma_m / \Sigma_{eq}$ is the triaxiality ratio (Σ_m being the hydrostatic stress and Σ_{eq} the von Mises equivalent stress), E_{eq}^p is the equivalent plastic deformation, R_o and R are the mean initial and actual void radius as indicated in Fig. 3.1.

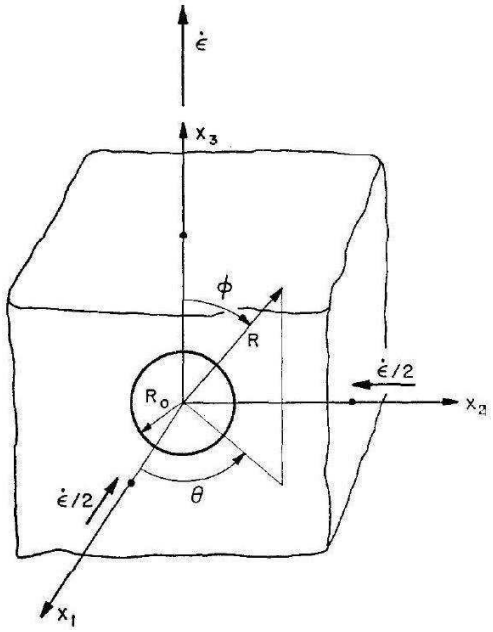

Fig. 3.1. Spherical void in a remote simple tension strain rate field; taken from (Rice and Tracey, 1969).

3.2.2. Gurson (1977)

Using homogenization techniques, Gurson (1977) proposed a macroscopic behavior model for the plastic deformation of porous materials. The Gurson analyze is based upon a porous hollow sphere or a cylinder, and assumes that the matrix is rigid perfectly plastic obeying to the von Mises criterion. The porous sphere is subjected to an axisymmetric loading analysis that leads to the macroscopic criterion expressed as follows:

$$\Phi(\Sigma, f) = \frac{\Sigma_{eq}^2}{\sigma_o^2} + 2f\cosh\left\{\frac{3}{2}\frac{\Sigma_m}{\sigma_o}\right\} - 1 - f^2 = 0 \qquad (3.2)$$

Gurson (1977) gets a macroscopic flow surface, which depends on the von Mises equivalent stress Σ_{eq}, the hydrostatic stress Σ_m, the yield stress of the matrix σ_o and the volume fraction of voids *f*. Thereafter, the Gurson model

has undergone many changes, including the replacement of the yield stress by the equivalent stress for a hardenable matrix, and the introduction of a critical porosity associated with void coalescence.

It should be noted that this criterion depends on both the stress hydrostatic Σ_m and the equivalent stress Σ_{eq}. However, it is not dependent on the third invariant stress Σ. Fig. 3.2 shows sections of this criterion for various values of the porosity f in the plane of stresses (Σ_m, Σ_{eq}). The Gurson criterion reduces to the von Mises yield surface when $f = 0$:

$$\Phi(\Sigma, f) = \frac{\Sigma_{eq}^2}{\sigma_o^2} - 1 = 0 \tag{3.3}$$

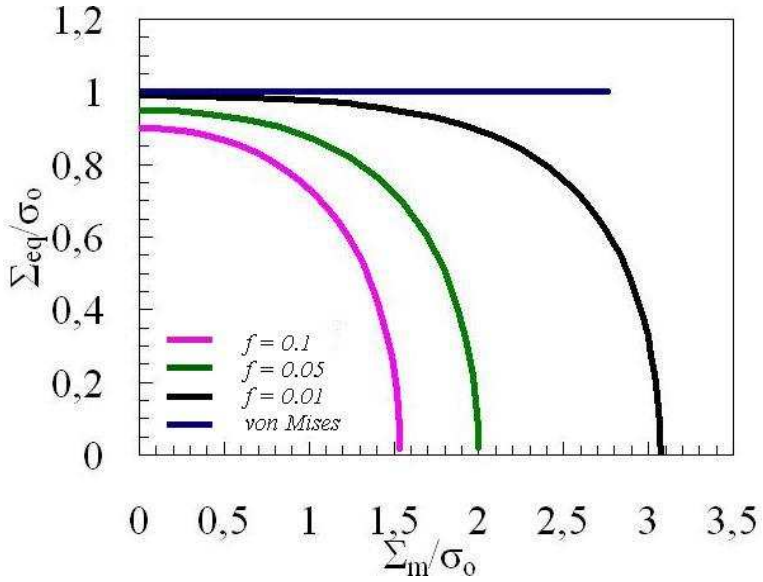

Fig. 3.2. Representation of the Gurson yield criterion for different porosities in the plane of stresses (Σ_m, Σ_{eq}).

Under purely hydrostatic stress (tension or compression) $\Sigma_{eq} \cong 0$, then according to the Gurson criterion the maximum value of hydrostatic stress can be obtained by:

$$\Sigma_m^{\max} = \frac{2}{3}\sigma_o \ln\left(\frac{1}{f}\right) \tag{3.4}$$

which represents the exact analytical solution to the pressurized hollow sphere problem. Under purely deviatoric stress $\Sigma_m \cong 0$, the criterion of Gurson leads to $\Sigma_{eq} = \sigma_o(1-f)$.

3.2.3. Gurson-Tvergaard (1981)

In what follows, various improvements which have been made by Tvergaard (1981) are presented. The Gurson criterion gives satisfactory approximations for high rates of stress triaxiality and overestimates the material response at low rates of stress triaxiality. To remedy this deficiency which was attributed to the interactions between cavities, Tvergaard (1981), on the basis of 2D numerical simulations, introduced three heuristic parameters q_1, q_2 and q_3 in the Gurson criterion. The yield surface as proposed by Tvergaard (1981) is:

$$\Phi(\Sigma, f) = \frac{\Sigma_{eq}^2}{\sigma_0^2} + 2q_1 f \cosh\left\{\frac{3}{2}q_2\frac{\Sigma_m}{\sigma_o}\right\} - 1 - q_3 f^2 = 0 \tag{3.5}$$

Tverggard (1981) obtained a good agreement with the values $q_2 = 1.0$ and $q_3 = q_1^2$, which are generally accepted in the literature. Nevertheless, the coefficient q_1 has been the subject of several proposals (see also Table 3.3): Tvergaard (1981) ($q_1 = 1.5$), Koplik and Needleman (1988) ($q_1 = 1.25$), Zhang et al. (1999) ($q_1 = 1.1$) and, Perrin and Leblond (1990) ($q_1 = 1.47$). Later, Faleskog et al. (1998) have shown that these heuristic parameters

depend on the plastic hardening exponent and on the ratio of the yield stress over the Young's modulus.

3.2.4. Rousselier (1987)

The model proposed by Rousselier (1987; 2001) is based on the thermodynamical framework proposed in Lemaitre and Chaboche (1990), and introduces a damage variable as a state variable. The damage variable is consequently identified as the porosity and the yield surface is expressed as:

$$\Phi(\Sigma, f) = \frac{\Sigma_{eq}}{(1-f)} + \sigma_1 f D \exp\left(\frac{\Sigma_m}{(1-f)\sigma_1}\right) - R = 0 \qquad (3.6)$$

where D and σ_1 are parameters that depend on the material, and $R = \sigma_o\left(\bar{\varepsilon}^p\right)$ with $\bar{\varepsilon}^p$ is the equivalent plastic deformation. The associated thermodynamical force and the yield surface must be such that the damage evolution law respects the mass conservation.

It is remarkable to outline some differences between the Gurson and Rousselier models. Under pure shear $\Sigma_m = 0$, damage is still generated in the case of the Rousselier model. Under pure hydrostatic stress states $\Sigma_{eq} = 0$, the Rousselier yield surface exhibits a vertex which implies that at high stress triaxiality ratios the plastic deformation tensor always keeps a nonzero shear component (Besson, 2010).

3.2.5. Sun-Wang (1989)

Sun and Wang (1989) first proposed a lower bound yield criterion for porous materials. However, they also employed the unit cell model in developing lower bound yield criterion. Considering the yield surface of a macroscopically porous material through the limit analysis of a basic cell identical to that used by Gurson, they obtained the following criterion:

$$\Phi(\Sigma, f) = \frac{\Sigma_{eq}^2}{\sigma_0^2} + \frac{f\left[\beta_1 \sinh\left(q\frac{\Sigma_m}{\sigma_o}\right) + \beta_2 \cosh\left(q\frac{\Sigma_m}{\sigma_o}\right)\right]}{\left[1+\beta_4 f^2 \sinh^2\left(q\frac{\Sigma_m}{\sigma_o}\right)\right]^{\frac{1}{2}}} - \beta_3 = 0 \qquad (3.7)$$

where q and β_i are determined by using finite element results.

3.2.6. Ponte Castañeda (1991)

By using non-linear homogenization methods, Ponte Castañeda (1991) improved both the Gurson criterion for low triaxialities and the non-linear Hashin-Shtrikman (HS) upper bound for spherical voids. The yield criterion takes the following form:

$$\Phi(\Sigma, f) = \left(1+\frac{2}{3}f\right)\frac{\Sigma_{eq}^2}{\sigma_0^2} + \frac{9}{4}f\frac{\Sigma_m^2}{\sigma_0^2} - (1-f)^2 = 0 \qquad (3.8)$$

3.2.7. Michel-Suquet (1992)

Following a non-linear homogenization scheme, Michel and Suquet (1992) derived the following equation:

$$\Phi(\Sigma, f) = \left(1+\frac{2}{3} f\right)\frac{\Sigma_{eq}^2}{\sigma_0^2} + \frac{9}{4}\left(\frac{1-f}{\ln f}\right)^2 \frac{\Sigma_m^2}{\sigma_0^2} - (1-f)^2 = 0 \tag{3.9}$$

3.2.8. Perrin-Leblond (1993)

According to the exploiting observation of Koplik and Needleman (1988), regarding the existence of a highly porous layer located between two rigid layers at the beginning of coalescence, Perrin (1992), Perrin and Leblond (1993) proposed to apply the theory of localization deformation of Rudnicki and Rice (1975). Later, they revisited this analysis to a porous core layer. This layer, which behavior obeys the Gurson model, is located between two layers described by the von Mises criterion. This criterion, which introduces the concept of multilayer RVE, is written in the following form:

$$\Phi(\Sigma, f) = \left\{\left[\frac{\Sigma_{eq}^{(p)}}{\sigma_o} - q_1 q_2 f^{(p)} \sinh\left(\frac{3}{2} q_2 \frac{\Sigma_m^{(p)}}{\sigma_o}\right)\right]^2 - \frac{3(1-\nu)\sigma_o}{E} q_1^2 q_2 \left(1-f^{(p)}\right) f^{(p)} \sinh\left(\frac{3}{2} q_2 \frac{\Sigma_m^{(p)}}{\sigma_o}\right)\left[\cosh\left(\frac{3}{2} q_2 \frac{\Sigma_m^{(p)}}{\sigma_o}\right) - q_1 f^{(p)}\right]\right\} = 0 \tag{3.10}$$

where the exponent p refers to a quantity in the porous layer, q_1 and q_2 are Tvergaard coefficients and f is the porosity of the porous layer.

3.2.9. Gologanu et al. (2001)

In the Gurson model, the void shape is not accounted for. Gologanu, et al. (Gologanu et al., 1993; 1994; 1997; 2001) proposed a comprehensive model taking into account the effect of void shape during loading. This

criterion, named GLD for Gologanu-Leblond-Devaux, is written as follows:

$$\Phi(\Sigma, f) = \left\{ \frac{C}{\sigma_0^2}\left(\Sigma_{zz} - \Sigma_{xx} + \eta\Sigma_h\right)^2 + 2(g+1)(g+f) \cosh\left(k\frac{\Sigma_h}{\sigma_0}\right) - (g+1)^2 - (g+f)^2 \right\} = 0 \tag{3.11}$$

$$\Sigma_h = 2\alpha_2\Sigma_{xx} + (1-2\alpha_2)\Sigma_{zz} \tag{3.12}$$

in which C, η, g, α_1, α_2 and k are quantities depending on the porosity f and the shape factor S.

A detailed description of the GLD model and its parameters is given by the references cited above. Recently, changes have been made on this model taking into account for example the anisotropy of the matrix (Croix et al., 2003; Benzerga et al., 2004) or matrix viscoplasticity (Flandi and Leblond, 2005a; 2005b). More recently following the limit analysis of Gurson criterion, an approximate expression of the macroscopic yield criterion, based on the Eshelby-like velocity fields, was proposed by Monchiet et al. (2006; 2007; 2011).

Many other models have been developed following the same idea of the Gurson model (Leblond et al., 1994; Zuo and Lou, 1996; Gãrãjeu and Suquet, 1997). Our purpose is now to achieve computations on RVE and to analyze the results through the framework of the Gurson-type models.

3.3. Computational homogenization

3.3.1. Porous microstructures

The porous media considered in the computations are made of perfectly-plastic matrix obeying to the commonly used isotropic von Mises yield criterion, the yield stress being constant and equal to 290 MPa. The plastic flow is assumed perfect in order to disregard hardening effects in the investigation and to compare the simulation results with the most common analytical models. The matrix material is sufficiently stiff in order to overcome any yield strain effects.

The porous media are represented by three-dimensional cubic cells containing a large number of pores, in order to assure that the studied material volume element is sufficiently large compared to porosities. The voids are randomly distributed and oriented in space in the cubic cell. Moreover, they are identical and non-overlapped. The question of the void content effects is examined in this work. The volume fraction of n spheroidal voids inside a cubic cell of volume V is given by:

$$f_{\text{spheroidal}} = \frac{4}{3}\frac{n\pi abc}{V} \tag{3.13}$$

where a is the polar radius along the *y* axis of the spheroidal void and, b and c are the equatorial radii along the *z* and *x* axis, respectively (see Fig. 3.3).

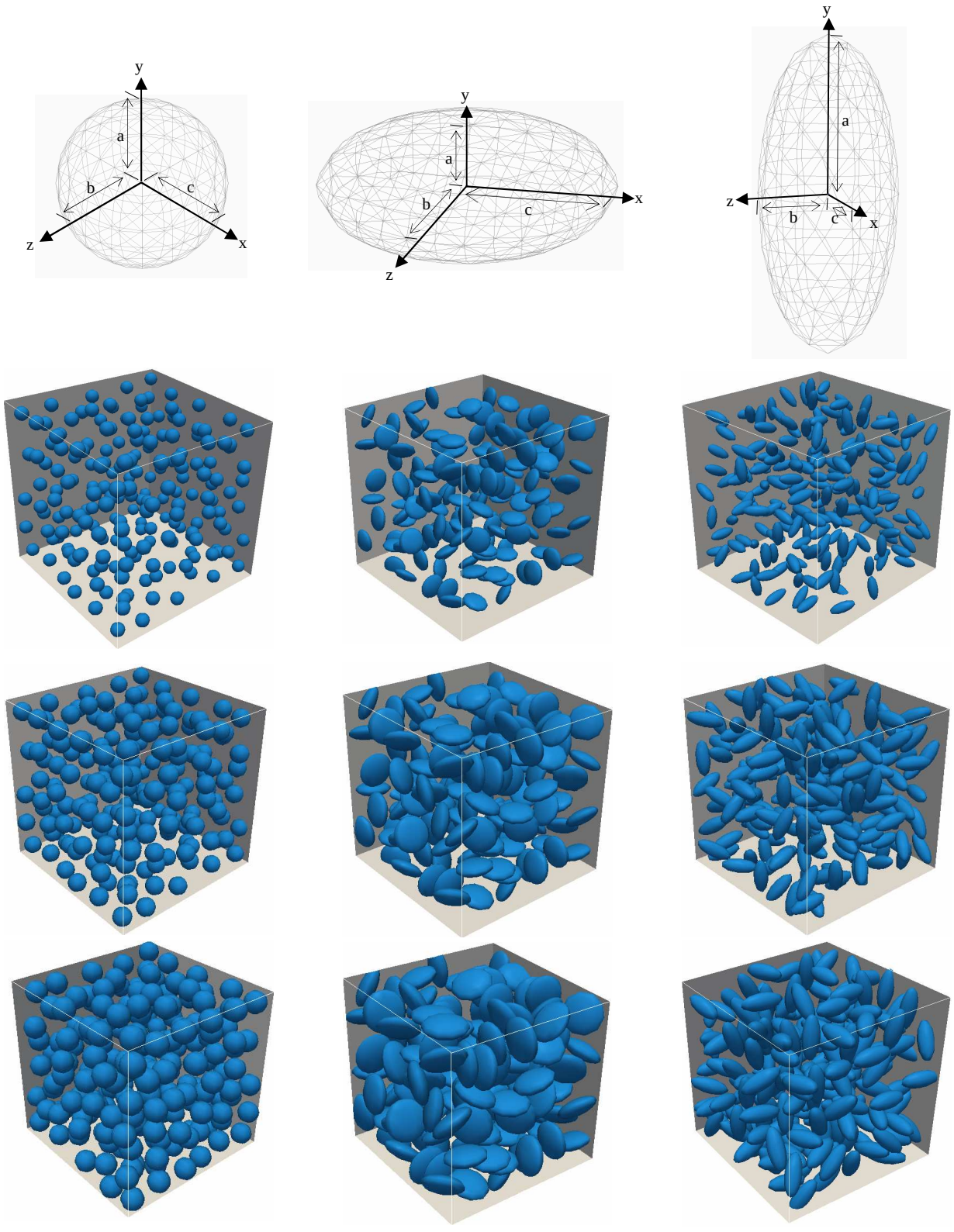

(a) (b) (c)

Fig. 3.3. Examined porous media at f = 0.05, 0.13 and 0.23: (a) spherical ($a = b = c$), (b) oblate ($b = c$ and b/a = 2.5) and (c) prolate ($b = c$ and a/b = 2.5) pores; $n \approx 200$ pores.

The void shape effects are examined in this work which constitutes a noteworthy difference with respect to existing literature (Bilger et al., 2005; 2007; Fritzen et al., 2012; 2013; Khdir et al., 2014). Fig. 3.3 presents the designed porous microstructures. The cases of spherical ($a = b = c$), oblate ($b = c$ and $b > a$) and prolate ($b = c$ and $a > b$) pores are examined. For each shape, three void volume fractions *f* are studied. The finite element method was chosen for the numerical computations using *Zebulon* software. A standard small-strain approximation was used for the simulations. The mesh size used was fine enough to represent accurately the geometry of the porosity and to ensure the overall response convergence.

3.3.2. Boundary conditions

The porous media being hydrostatic pressure-dependent, the boundary conditions imposed to the designed representative element should involve a wide range of stress trriaxiality ratios to be explored. The stress triaxiality parameter $T = \Sigma_m / \Sigma_{eq}$ is defined as the ratio of the overall hydrostatic stress Σ_m and the overall von Mises equivalent stress Σ_{eq}, respectively, given by:

$$\Sigma_m = \frac{1}{3} tr(\boldsymbol{\Sigma}) \text{ and } \Sigma_{eq} = \sqrt{\frac{3}{2}} (\boldsymbol{\Sigma}' : \boldsymbol{\Sigma}')^{1/2} \tag{3.14}$$

where $\boldsymbol{\Sigma}$ is the macroscopic (ensemble-volume average) stress tensor and $\boldsymbol{\Sigma}'$ denotes its deviatoric part.

Stress or strain-driven boundary conditions are usually employed in the literature. In this work, due to its computational robustness, the following mixed boundary conditions were imposed:

$$
\begin{aligned}
&E_{11}(t) = t\dot{\varepsilon}_0(\alpha+\beta)\\
&E_{22}(t) = t\dot{\varepsilon}_0(-\alpha+\beta)\\
&E_{33}(t) = t\dot{\varepsilon}_0\beta\\
&\Sigma_{12}(t) = \Sigma_{13}(t) = \Sigma_{23}(t) = 0
\end{aligned}
\qquad (3.15)
$$

in which the values assigned to shear components of the overall stress tensor are zero. The terms α and β, introduced to control the diagonal components of the overall strain tensor $\mathbf{E}$, are two loading parameters, $\dot{\varepsilon}_0 > 0$ is a prescribed deformation rate and t is the simulation time. The stress triaxiality is indirectly assigned by the two measures of stress, given by Eq. (3.14), which are defined implicitly by the mixed boundary conditions through the two loading parameters α and β. The different values of α and β used to obtain different stress triaxiality ratios are listed in Table 3.1.

ι	1	2	3	4	5	6	7	8	9
α	1.00	1.00	1.00	1.00	1.00	1.00	1.00	0.50	0.00
β	0.00	0.05	0.10	0.15	0.25	0.50	1.00	1.00	1.00

Table 3.1. Loading parameters used in the simulations.

3.4. Results and discussion

3.4.1. Asymptotic stress response

The asymptotic response of the ideally plastic porous microstructures was systematically examined by plotting the overall von Mises equivalent and hydrostatic stresses as a function of the overall von Mises equivalent strain. These two measures of stress are plotted in Fig. 2 in the case of a porosity value of 0.23 and for the three void shapes. This figure shows that the porous microstructures are subjected to a stationary response beyond a certain strain.

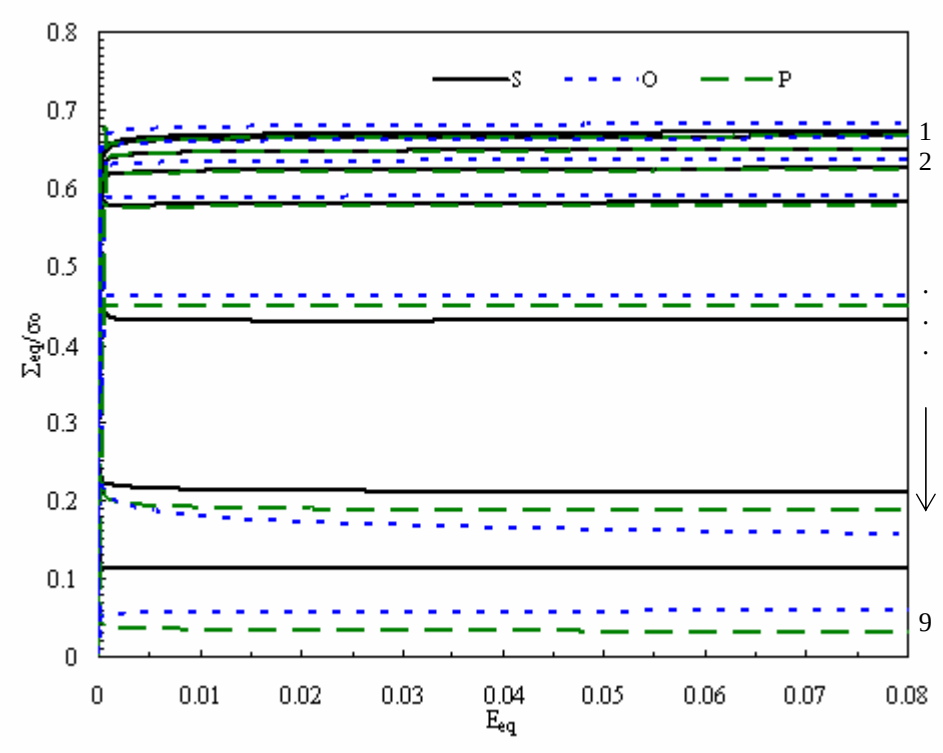

(a)

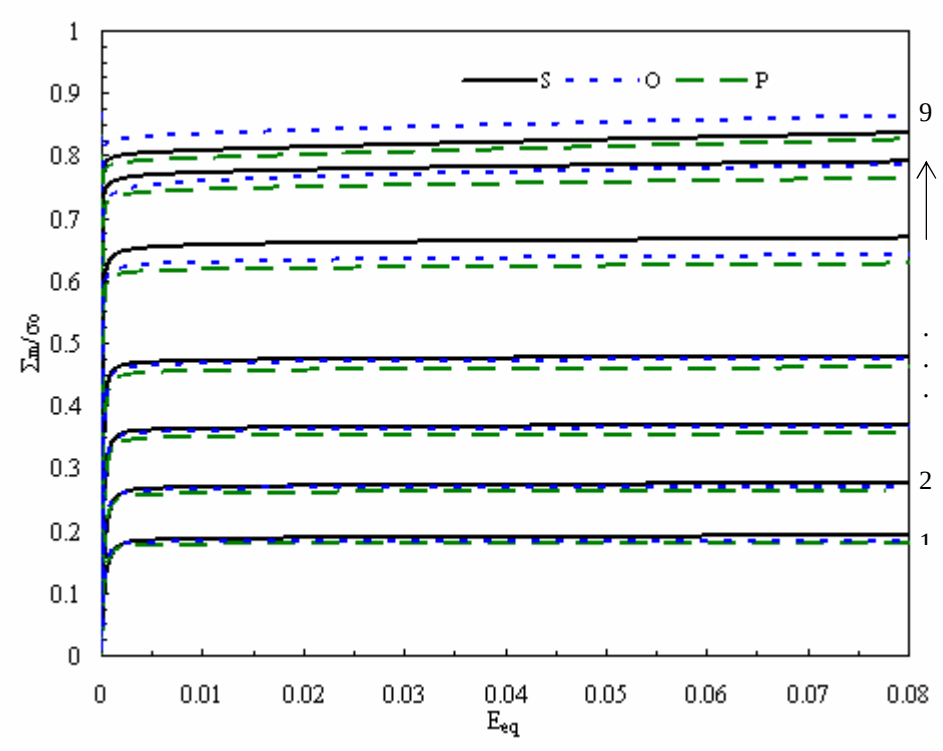

(b)

Fig. 3.4. Overall (a) von Mises equivalent and (b) hydrostatic stresses as a function of the overall von Mises equivalent strain for spherical (S), oblate (O) and prolate (P) pores at $f = 0.23$ and all the loading cases given in Table 3.1; $n \approx$ 200 pores.

Similar observations on large volume computations have been pointed out by Fritzen et al. (2012; 2013) and by Khdir et al. (2014). In order to define the numerical yield points, the overall stresses at the end of the simulation are considered. Except at very high mean stresses, it can be observed that the overall response is not affected by the void shape. This is particularly true at low hydrostatic pressure (or high equivalent stress) values. Note that the results obtained with the two other porosities (0.05 and 0.13) give similar trends.

3.4.2. Representativity

The size of the volume element is conditioned by the number of porosities which should be chosen large enough to ensure that the volume element is representative. This representativity was investigated in terms of the mechanical responses by Huet (1990), Drugan and Willis (1996) and Kanit et al. (2003). These authors have studied the effects of the volume element size on the elastic stiffness. More recently, Khdir et al. (2013) have investigated these effects on the elastic-plastic response. In the case of elastic-plastic composites, made of two phases with highly contrasted properties, Khdir et al. (2013) have shown that the minimum size of the volume element in the yield and post-yield region must be greater than the minimum size required in the elastic domain. This question which arises in three-dimensional computational homogenization has to be systematically accounted for. Several volume elements with different sizes (i.e. containing different number of pores) are simulated for a porosity of 0.23, and the mechanical representativity of the computational results are examined. The overall stationary stresses are plotted as a function of the number of pores in Fig. 3.5 for the three shapes.

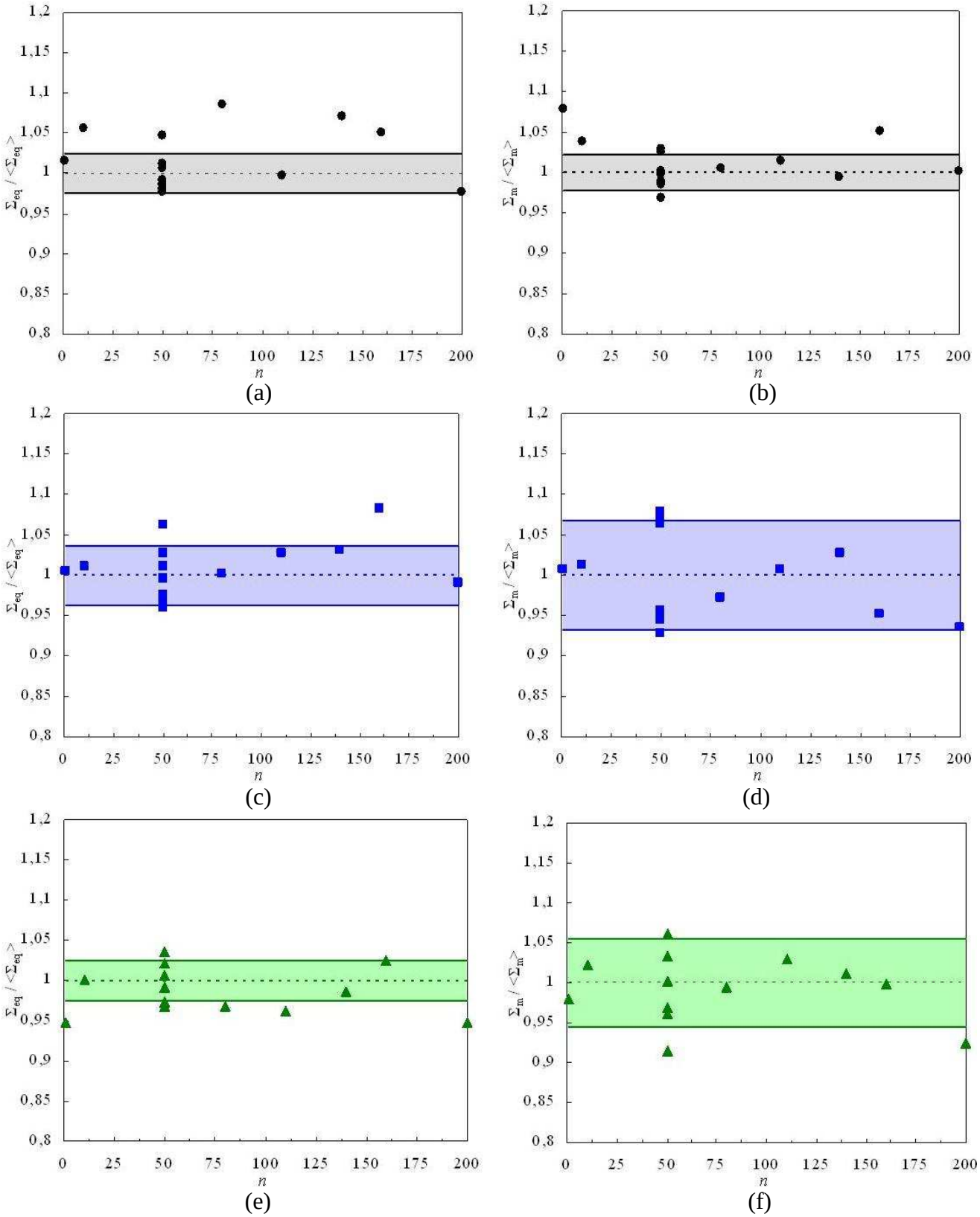

Fig. 3.5. Asymptotic overall von Mises equivalent stress and hydrostatic stresses as a function of the number of pores for spherical (a-b), oblate (c-d) and prolate (e-f) pores at $f = 0.23$ The average (dashed line) and the standard deviations (colored area) are calculated for $n = 50$.

Figs. 3.5a, c and e correspond to the loading path 1 in Table 1 characterized by ($\alpha = 1$, $\beta = 0$) for which the deviatoric component exhibits the highest stationary value, whereas Figs. 3.5b, d and f correspond to the loading path 9 in Table 1 characterized by ($\alpha = 0$, $\beta = 1$) for which the hydrostatic component takes its highest stationary value. The stationary stresses are normalized with respect to the average value of computational results of several realizations containing 50 pores. All computed data are found within or close to the colored area defined by the standard deviations. The stationary values for $n = 200$ are close to the averages of $n = 50$ pores (dashed line), the largest difference being about 7%.

The computations are performed using the largest cubic cells (containing $n = 200$ voids) in order to assure the mechanical representativity of the numerical yield surfaces. These cubic cells are successively stretched in the orthogonal directions and the results are reported in Fig. 3.6a for the three void shapes. It can be observed that identical overall mechanical responses are obtained which is, for isotropy, a necessary condition but not sufficient.

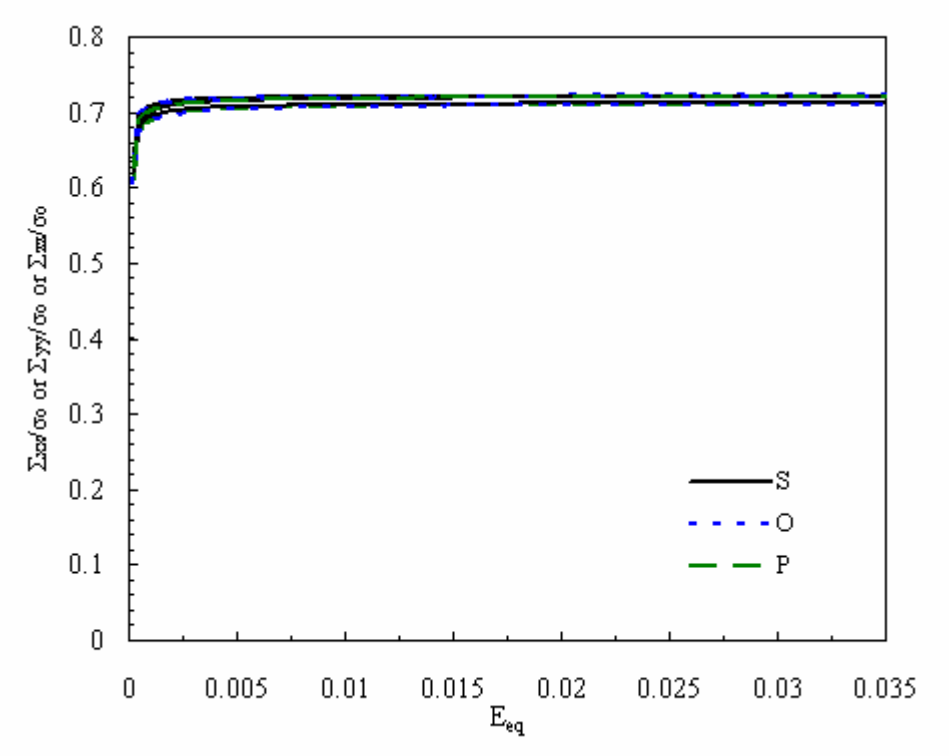

(a)

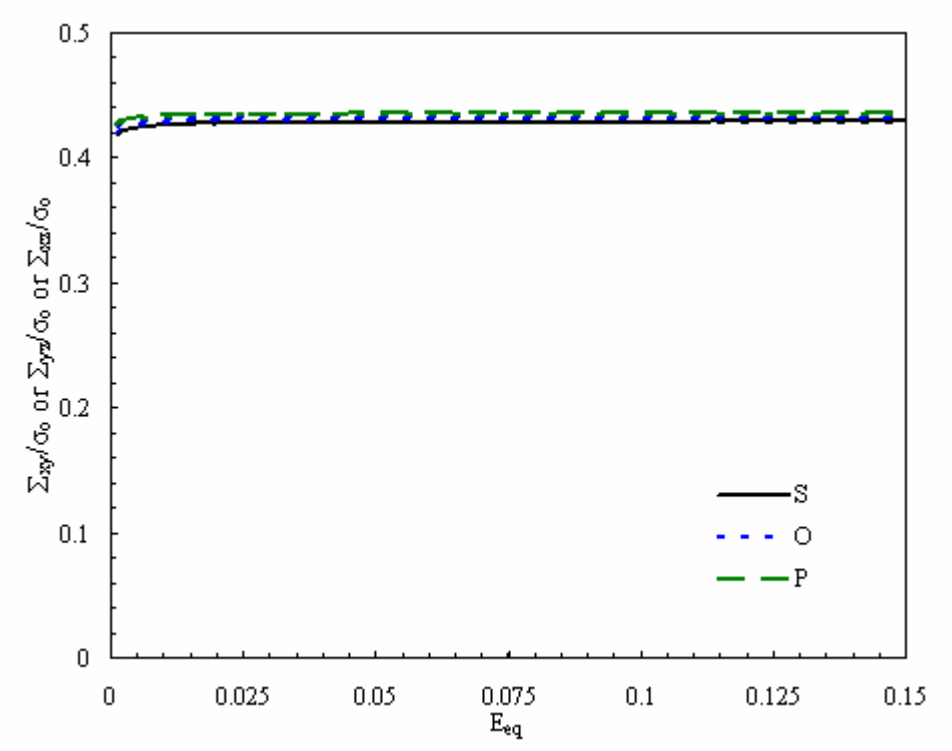

(b)

Fig. 3.6. RVE isotropy for spherical (S), oblate (O) and prolate (P) pores at $f = 0.23$: (a) overall tensile stress-strain responses in the three orthogonal directions and (b) overall shear stress-strain responses in three perpendicular planes; $n \approx 200$ pores.

To ensure this property the cubic cells must also be subjected to simple shear loading. The corresponding results presented in Fig. 3.6b show that the overall shear responses are the same in three perpendicular planes. Then, Fig. 3.6 shows that, when a sufficient number of pores are randomly distributed and oriented in the volume element, an isotropic response is obtained at the macroscopic scale. The found isotropy proves that this large volume element is representative enough of the random porous medium, whatever the void shape.

3.4.3. Local plastic strain fields

The local plastic strain fields can be observed in Figs. 3.7, 3.8 and 3.9 at different triaxiality ratios for the three void shapes. The porosity of 0.23 is chosen to illustrate this distribution because a more diffuse plastic strain is observed compared to the other void volume fractions. The observations are presented at the end of the prescribed loading. The pore-pore interactions and the triaxiality effects on the local fields are illustrated in the figures for three particular cases: The cases ($\alpha = 1$, $\beta = 0$) and ($\alpha = 0$, $\beta = 1$) correspond to the lowest and highest triaxiality ratios, respectively, and the case ($\alpha = 1$, $\beta = 0.25$) to an intermediate one.

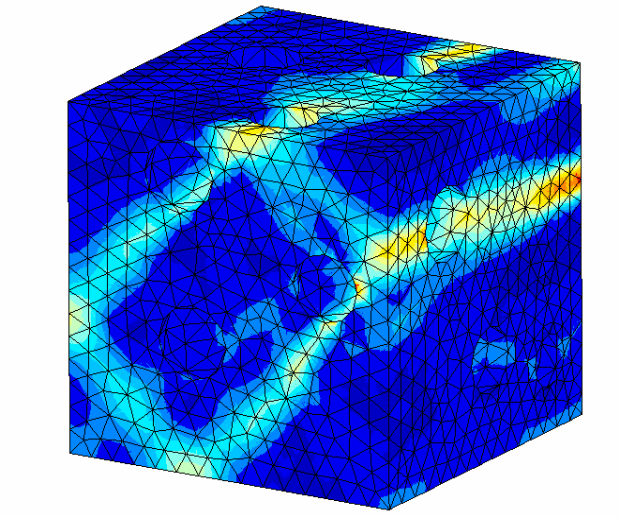

(a)

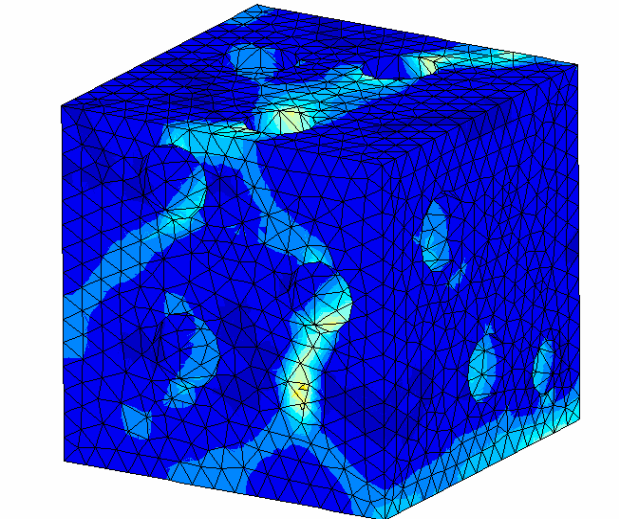

(b)

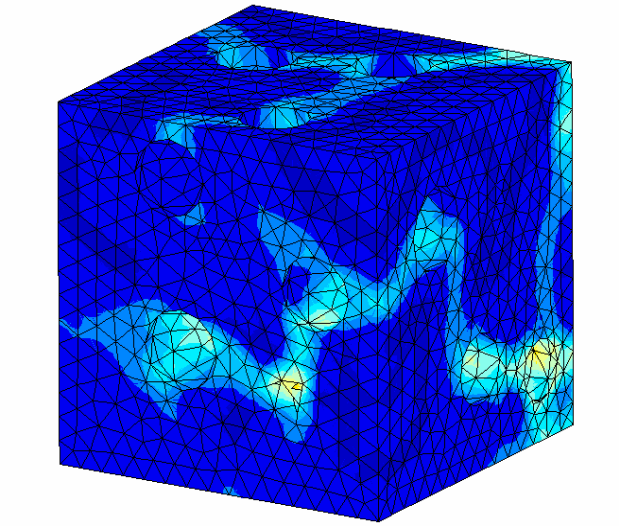

(c)

Fig. 3.7. Distribution of the accumulated plastic strain for spherical pores at f = 0.23 and three different loading cases:
(a) $\alpha = 1, \beta = 0$, (b) $\alpha = 1, \beta = 0.25$, (c) $\alpha = 0, \beta = 1$.

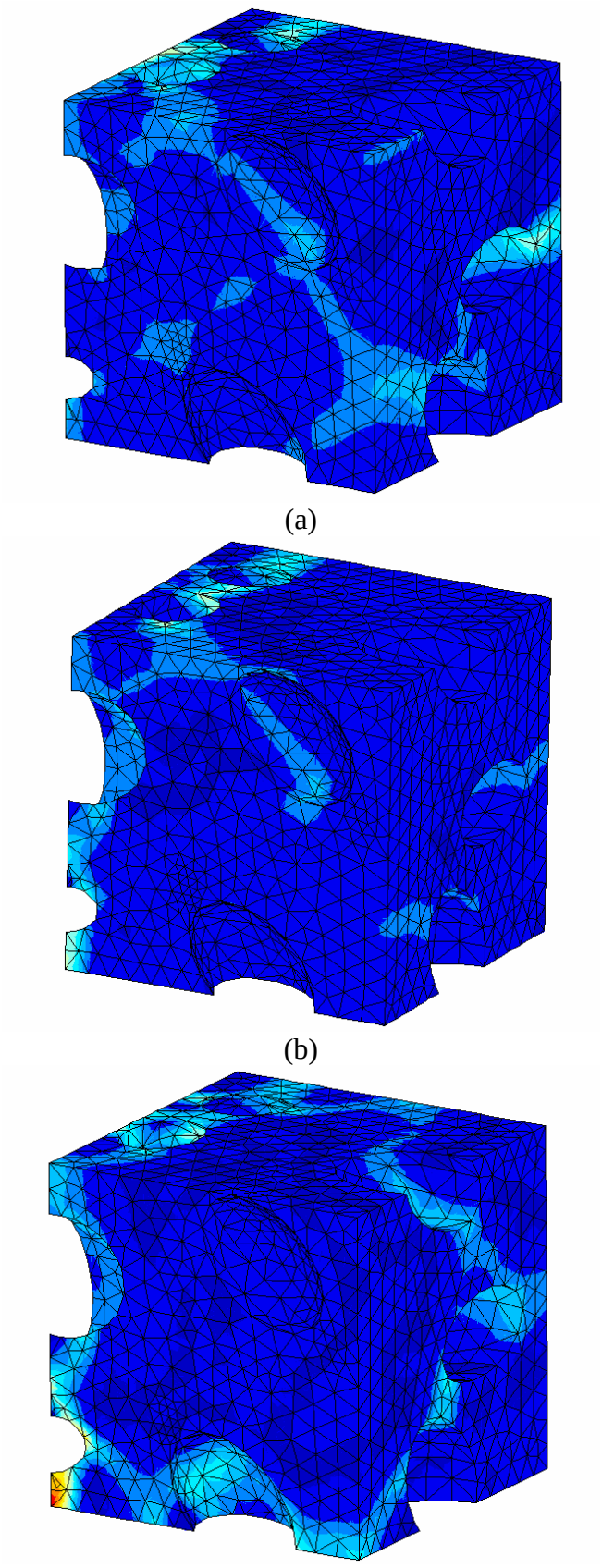

(a)

(b)

(c)

Fig. 3.8. Distribution of the accumulated plastic strain for oblate pores at $f = 0.23$ and three different loading cases:
(a) $\alpha = 1$, $\beta = 0$, (b) $\alpha = 1$, $\beta = 0.25$, (c) $\alpha = 0$, $\beta = 1$.

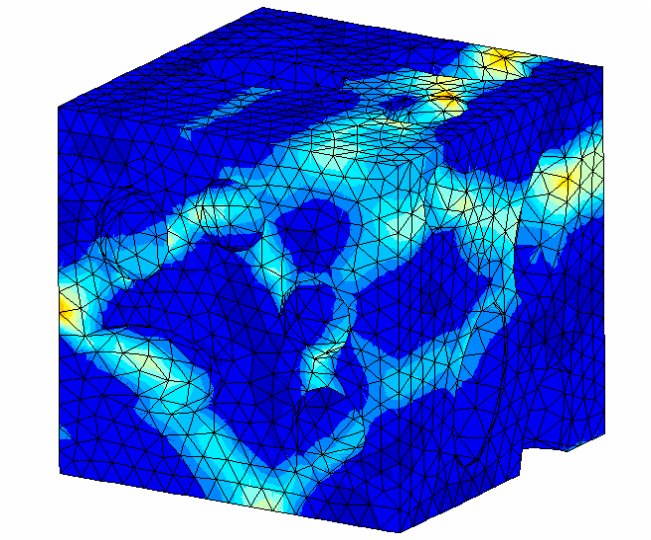

(a)

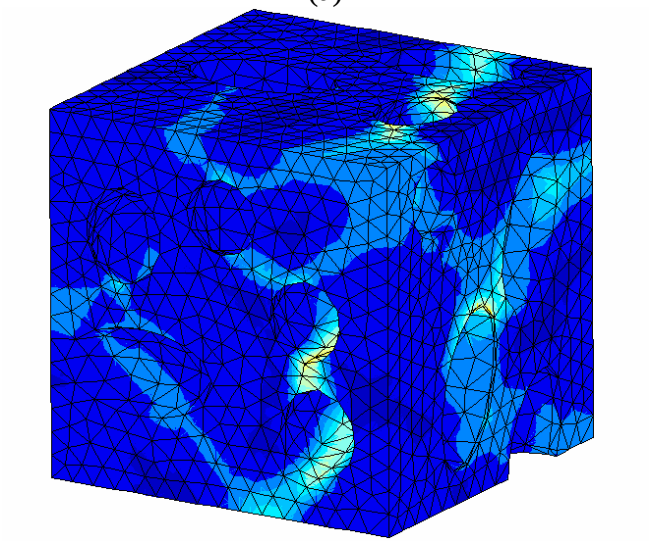

(b)

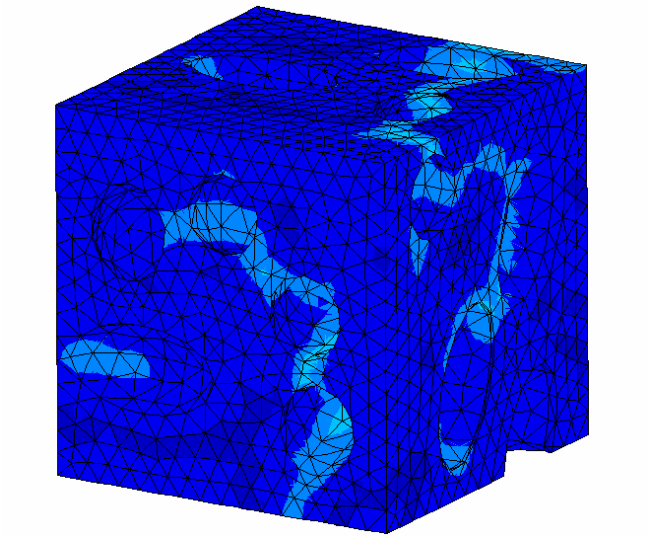

(c)

Fig. 3.9. Distribution of the accumulated plastic strain for prolate pores at f = 0.23 and three different loading cases:
(a) $\alpha = 1, \beta = 0$, (b) $\alpha = 1, \beta = 0.25$, (c) $\alpha = 0, \beta = 1$.

3.4.4. Comparison between numerical results and analytical criteria

In this subsection, only the case of spherical pores is analyzed. The common representation of the overall yield surface, plotting the overall von Mises equivalent stress as a function of the overall hydrostatic stress, is adopted to illustrate the computational data. Fig. 3.10 shows as an example the relationship between these two stresses for a given porosity value of 0.23. The normalization is performed with respect to the matrix yield stress σ_0. The hydrostatic pressure dependency of the macroscopic yield response of the porous material is clearly pointed out in the figure. The yield points, highlighted by filled circles in the figure, are obtained from the asymptotic stress response at the end of the simulations.

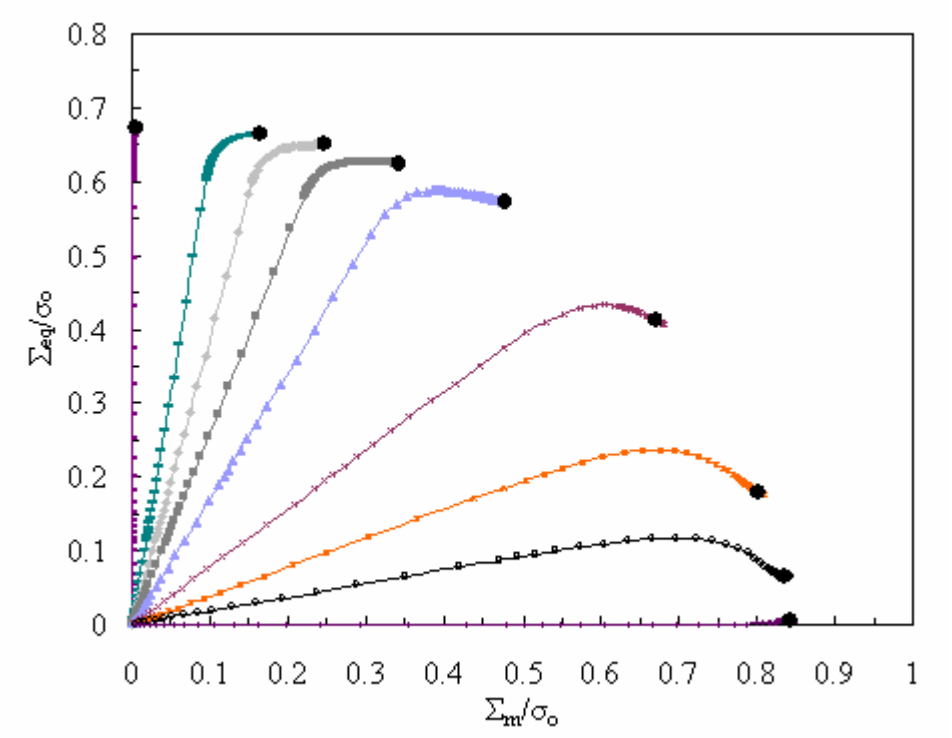

Fig. 3.10. Overall von Mises equivalent stress vs. overall hydrostatic stress for spherical pores at f = 0.23 and all the loading cases given in Table 3.1 ; $n \approx 200$ pores (The filled circles designate the numerical yield points).

The computed data are compared with some existing analytical models in Fig. 3.11 for the three considered void volume fractions.

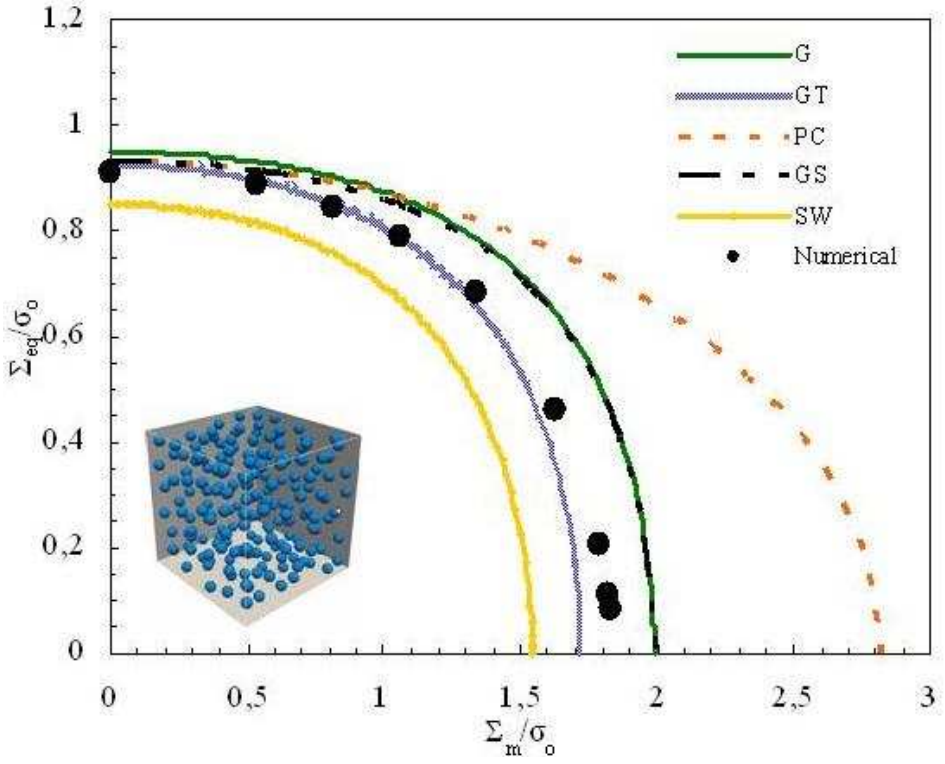

(a)

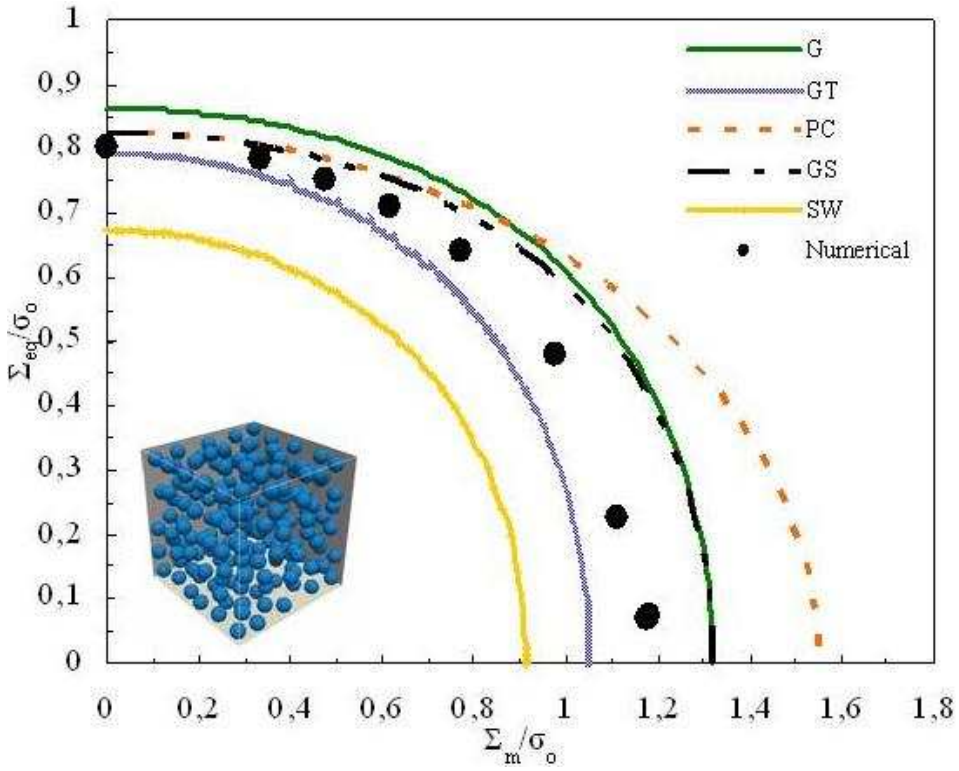

(b)

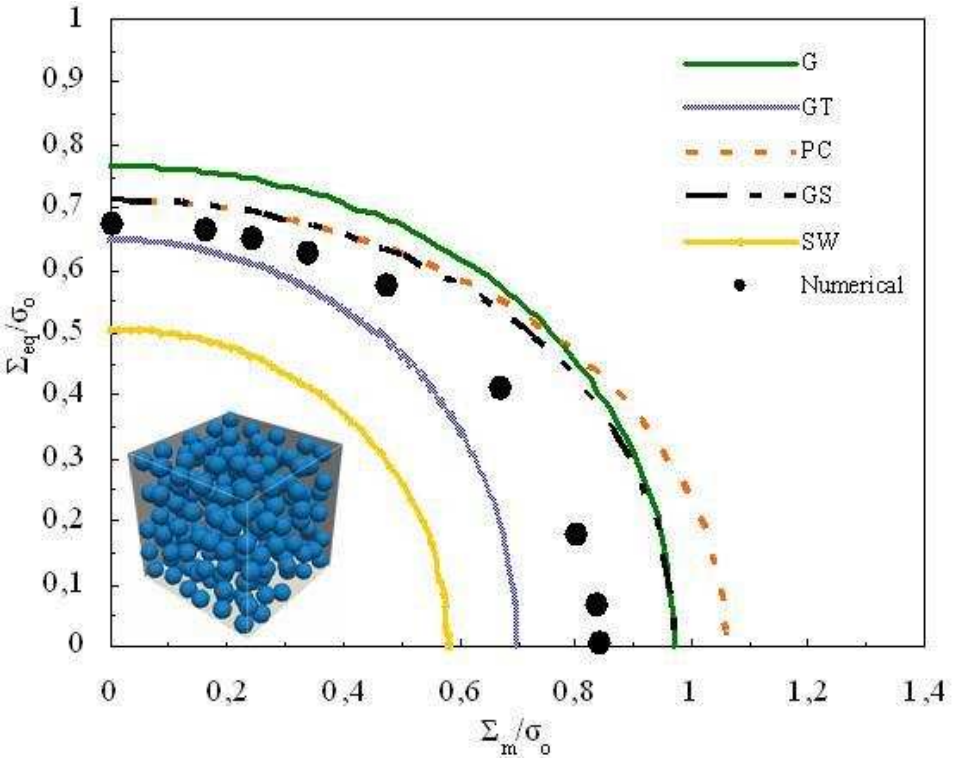

(c)

Fig. 3.11. Comparison between some existing analytical models and the simulation results for spherical pores at (a) $f = 0.05$, (b) $f = 0.13$, (c) $f = 0.23$; $n \approx$ 200 pores (G: Gurson, GT: Gurson-Tvergaard, PC: Ponte Castaneda, GS: Gărăjeu-Suquet, SW: Sun-Wang)..

Besides the commonly used Gurson model, other analytical models are selected. The mathematical expressions of some existing yield criteria for plastic porous materials are recalled in Table 3.2.

G yield criterion (Gurson, 1977)	$\Phi(\boldsymbol{\Sigma}, f) = \frac{\Sigma_{eq}^2}{\sigma_0^2} + 2f\cosh\left\{\frac{3}{2}\frac{\Sigma_m}{\sigma_0}\right\} - 1 - f^2 = 0$
GT yield criterion (Tvergaard, 1981)	$\Phi(\boldsymbol{\Sigma}, f) = \frac{\Sigma_{eq}^2}{\sigma_0^2} + 2q_1 f\cosh\left\{\frac{3}{2}q_2\frac{\Sigma_m}{\sigma_0}\right\} - 1 - q_3 f^2 = 0$
PC yield criterion (Ponte Castañeda, 1991)	$\Phi(\boldsymbol{\Sigma}, f) = \left(1 + \frac{2}{3}f\right)\frac{\Sigma_{eq}^2}{\sigma_0^2} + \frac{9}{4}f\frac{\Sigma_m^2}{\sigma_0^2} - (1-f)^2 = 0$
GS yield criterion (Gărăjeu and Suquet, 1997)	$\Phi(\boldsymbol{\Sigma}, f) = \left(1 + \frac{2}{3}f\right)\frac{\Sigma_{eq}^2}{\sigma_0^2} + 2f\cosh\left\{\frac{3}{2}\frac{\Sigma_m}{\sigma_0}\right\} - 1 - f^2 = 0$
SW yield criterion (Sun and Wang, 1989)	$\Phi(\boldsymbol{\Sigma}, f) = \frac{\Sigma_{eq}^2}{\sigma_0^2} + f\left(2 - \frac{1}{2}\ln f\right)\cosh\left\{\frac{3}{2}\frac{\Sigma_m}{\sigma_0}\right\} - 1 - f(1+\ln f) = 0$

Table 3.2. Gurson-type yield criteria used in Fig. 3.11.

It can be observed in Fig. 3.11 that the computed data satisfy the Gărăjeu and Suquet (1997) (denoted as GS) upper bound and the Sun and Wang (1995) (denoted as SW) lower bound. The GS model is identical to the Gurson model (denoted as G) around the normalized hydrostatic stress axis and to the Ponte Castaneda (1991) (denoted as PC) model around the normalized equivalent stress axis. Around the normalized hydrostatic stress axis, the GS model is identical to the Gurson model (denoted as G), but strongly deviates when decreasing the mean stress axis. It can be observed that the GS model overestimates the numerical data for high normalized hydrostatic stress, but becomes closer when decreasing the mean stress. All the computed data satisfy the SW lower bound but it is found that the SW model is close to the numerical data around the normalized equivalent stress axis at the lowest void content. The PC yield criterion provides too stiff predictions around the normalized hydrostatic stress axis. The divergences with the model decrease when the void content increases. The G criterion overestimates the numerical data, the difference between the two solutions increasing with the void content. The GT model using the calibrated parameters of Tvergaard (1982), see Table 3.3, underestimates the numerical yield surface. For the lowest void content, the GT model is

close to the numerical surface, especially around the normalized equivalent stress axis. For the highest void content, the GT model becomes a lower bound.

3.4.5. A GT model for random porous media

To improve its agreement with the computational results, the GT model can be calibrated using our computed data. The following expressions of the GT model parameters are found:

$$q_1(f) = 1.69 - f\ ,\ q_2 = 0.92\ ,\ q_3 = q_1(f)^2 \tag{3.16}$$

The model captures all the computed data in a very satisfactory manner as shown in Fig. 3.12. We obtain the same expressions as those found by Fritzen et al. (2012)

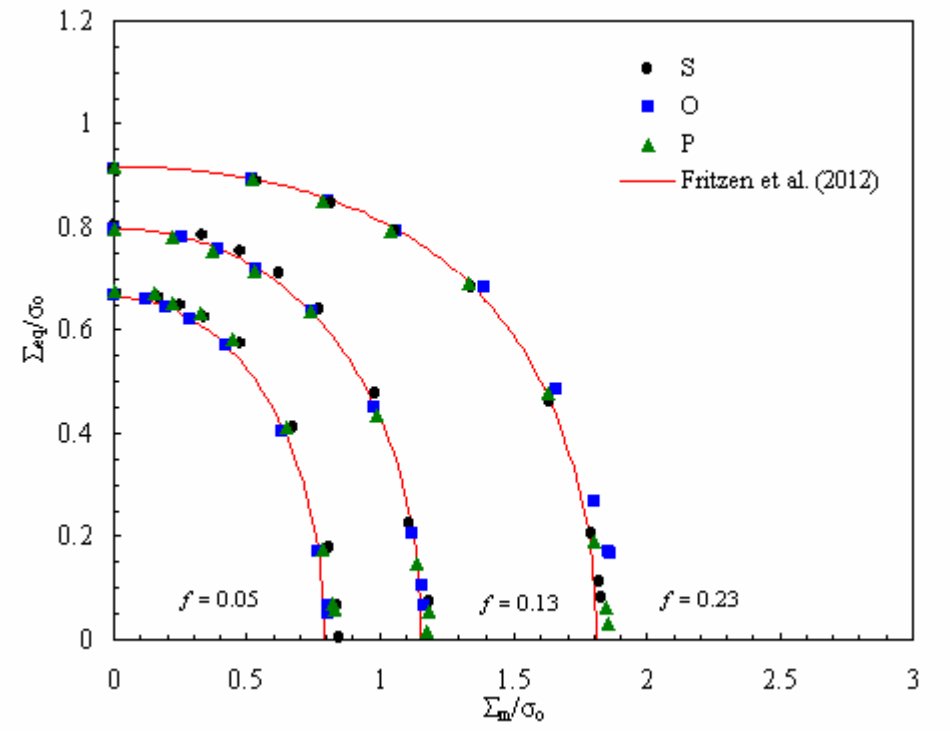

Fig. 3.12. Simulation results for spherical (S), oblate (O) and prolate (P) pores and, comparison with the Fritzen et al. (2012) model; $n \approx 200$ pores.

This calibration can be compared with the values (reported in Table 3.3) usually obtained by calibration on two-dimensional finite element simulation results using plane stress, plane strain or axisymmetric “periodic” unit cell models.

Various micromechanics-based analytical yield criteria including the effect of void shape were proposed by using unit cell representations (e.g. Gologanu et al., 1993; 1994; 1997; 2001; Monchiet et al., 2006; 2008; Madou and Leblond, 2012; Monchiet and Kondo, 2013). Because the unit cell is an elementary volume element containing a single void, periodicity is assumed in the material representation, and consequently void shape dependence of the overall response is expected. The overall response of a porous medium containing randomly oriented voids is then evaluated from that obtained with unidirectionally aligned voids averaged over all orientations, and consequently shape dependence is preserved in the micromechanics-based analytical models. The large volume computations performed in this contribution, show in the particular random media we have investigated, that there is no significant effect of the void shape on the volume average behavior. This could be a consequence of the cubic cell microstructure in which the pores are randomly distributed and oriented in space. However, this statement must be verified for a larger range of shape ratios.

References	q_1	q_2
Gurson (1977)	1.0	1.0
Tvergaard (1982)	1.5	1.0
Koplik and Needleman (1988)	1.25	1.0
Zuo et al. (1996)	1.4	1.0
Faleskog et al. (1998)	1.46	0.93
Ma and Kishimoto (1998)	1.35	0.95
Corigliano et al. (2000)	1.08	0.99
Zhang et al. (2000)	1.25	1.0
Negre et al. (2003)	1.5	1.2
Kim et al. (2004)	1.5856	0.909
McElwain et al. (2006)	1.31	1.16
Nielsen and Tvergaard (2009)	2.0	1.0
Vadillo and Fernandez-Saez (2009)	1.46	0.931
Dunand and Mohr (2011)	1.0	0.7
Fei et al. (2012)	1.8	1.0
Yan et al. (2013)	1.55	0.9

Table 3.3. Different values of GT model parameters ($q_3 = q_1^2$).

3.5. Concluding remarks

The overall yield surface of plastic porous media was investigated via computational micromechanics. The computational results were investigated in terms of representativity and were related to some existing Gurson-type yield criteria. The overall yield surfaces were found nearly the same for all investigated shapes of voids (spherical, oblate and prolate) provided that they are randomly distributed and oriented in a large volume element. Further computations are however required to confirm the independence of the overall yield surface vis-a-vis the void shape.

CHAPTER IV

COMPUTATIONAL HOMOGENIZATION OF POROUS MEDIA WITH TWO POPULATIONS OF VOIDS[5]

[5] This chapter is based on the following paper: Younis-Khalid Khdir, Toufik Kanit, Fahmi Zaïri, Moussa Naït-Abdelaziz, 2014. Computational homogenization of plastic porous media with two populations of voids. Materials Science and Engineering A 597, 324-330. Email: youniskhalid.khdir@gmail.com

4.1. Introduction

The mathematical description of the plastic behavior of porous media containing spherical voids has been widely investigated since the pioneering works of McClintock (1968) and, Rice and Tracey (1969). Green (1972) proposed a macroscopic yield function for porous media, and later, Gurson (1977) derived analytically an upper bound for the macroscopic yield surface of porous media. This yield function was found triaxiality-dependent although the matrix material obeys to the von Mises criterion, which assumes the material incompressible. The modeling, which considers an isotropic, incompressible, rigid and perfectly-plastic matrix, is based on the limit analysis approach, performed on a periodic unit cell. This cell consists in a hollow sphere or cylinder subjected to a uniform macroscopic strain rate at its external boundary.

To construct accurate macroscopic yield criteria for porous media, intense researches have been carried out to take into consideration the void shape or the matrix plastic anisotropy. The reader can refer to recent background papers on the subject (Benzerga and Leblond, 2010; Besson, 2010).

Several experimental works on metallic or polymeric materials have provided insights on the existence of two populations of voids with different sizes (Asserin-Lebert et al. 2005; Liu et al., 2011; Pawlak, 2013). To date, a limited number of theoretical or computational works have been devoted to this problem. Some investigations have been performed using FE calculations on a periodic unit cell containing one void embedded in a Gurson type matrix (Fabregue and Pardoen, 2008). Others have explicitly incorporated a second population of voids in the matrix surrounding the

primary void (Faleskog and Shih, 1997). To our knowledge, only Perrin and Leblond (2000), Vincent et al. (2008; 2009a; 2009b), Julien et al. (2011) and Shen et al. (2012) have developed analytical models devoted to a double population of voids. By considering the two populations existing at two different scales (microscopic and mesoscopic scales), the modeling is based on a two-step homogenization process, i.e. micro/meso and then meso/macro. After several approximations, the macroscopic yield functions are found to be similar to the Gurson form, but depend on the respective volume fraction of the two populations.

Recently, three-dimensional computational homogenization studies have been carried out on random porous materials containing multiple voids (Segurado and Llorca, 2002; Moraleda et al., 2007; Bilger et al., 2005; 2007; Fritzen et al., 2012; 2013). To our knowledge, there is no three-dimensional computational homogenization of double porous materials containing multiple voids and using sufficiently large volume elements.

The goal of the current chapter is to present a computational homogenization study of porous media containing two populations of spherical voids with different sizes. Computational homogenization is used to obtain the macroscopic yield surface for different stress triaxialities of material volume elements including a large number of randomly distributed voids. The computational data are compared with the macroscopic yield criteria found in the exhaustive literature for such porous materials. Modifications of the analytical criteria are proposed to overcome the discrepancies observed with the computational data. Based on the large volume computations, this part of the work brings two main results. First, the parameters involved in the modified analytical models are found

independent of the volume fraction and size of porosities. Secondly, it is found that a porous material with two populations of voids with different sizes can be replaced by a porous material including a single population of voids with an equivalent volume fraction of porosities.

The outline of the present chapter is as follows. Section 4.2 is devoted to a brief review of existing analytical yield criteria. The results of the computational homogenization are presented and discussed in Section 4.3. Concluding remarks are given in Section 4.4.

4.2. A brief survey of existing analytical models

In this section, a brief survey of macroscopic yield criteria for porous materials containing two populations of spherical voids in a von Mises matrix is presented. The two populations of voids cohabit at two different scales: microscopic and mesoscopic scales. As in any yield criteria for porous media, expressed at the macroscopic scale, the yield function relates the matrix yield stress σ_o, the macroscopic von Mises equivalent stress Σ_{eq} and the macroscopic hydrostatic stress Σ_m. The two macroscopic quantities are expressed as:

$$\Sigma_{eq} = \sqrt{\frac{3}{2}\boldsymbol{\Sigma}' : \boldsymbol{\Sigma}'} \text{ and } \Sigma_m = \frac{1}{3}\mathrm{tr}(\boldsymbol{\Sigma}) \tag{4.1}$$

where $\boldsymbol{\Sigma}$ is the applied macroscopic stress tensor and $\boldsymbol{\Sigma}'$ is its deviator. The double dot denotes the double contracted product.

Another essential quantity appearing in the yield function is the void volume fraction. Following the works of Vincent et al. (2008; 2009a;

2009b) and Shen et al. (2012) the volume fraction of smallest voids at the smallest (microscopic) scale, denoted f_b, and the volume fraction of largest voids at the upper (mesoscopic) scale, denoted f_e, are given by:

$$f_b = \frac{|\omega_b|}{|V - \omega_e|} \text{ and } f_e = \frac{|\omega_e|}{|V|} \tag{4.2}$$

where V denotes the volume of the RVE and, ω_b and ω_e denote the volumes occupied by the voids at the smallest and upper scales, respectively.

The mathematical derivation is based on the assumption of a separation between the two scales of the voids. The total volume fraction of voids f is therefore given by:

$$f = \frac{|\omega_b| + |\omega_e|}{|V|} = f_e + f_b(1 - f_e) \tag{4.3}$$

Shen et al. (2012) recently established two yield criteria for double porous materials by extending the Ponte Castañeda (1991) (PC) and Michel and Suquet (1992) (MS) models, originally developed for a single population of voids. The authors Shen et al. (2012) performed a two-step homogenization: in the first step, to achieve the transition from the smallest scale to the mesoscale, the PC and MS models were employed to represent the porous matrix at the mesoscale. In the second step, the transition to the macroscale is conducted by identifying the macroscopic yield criterion to a criterion of a porous medium consisting in a compressible Green (1972) matrix. At the smallest scale, the solid phase is homogeneous, isotropic and obeys to the pressure-independent von Mises criterion. The Vincent et al.

(2008; 2009a; 2009b) yield criterion for double porous materials was derived by considering for the micro/meso homogenization a Gurson-type matrix. A comparison between these analytical models can be found in Shen et al. (2012). Julien et al. (2011) extended the Vincent et al. (2008; 2009a; 2009b) yield criterion to include at the microscale a viscoplastic solid phase. In the present work, only the closed-form expressions of PC and MS yield criteria for double porous media, proposed by Shen et al. (2012), are retained for further comparisons with the computational results. The PC and MS yield criteria are respectively given by the following formula Shen et al. (2012):

$$\frac{1+\frac{2}{3}f_b}{\left(1-f_b\right)^2}\frac{\Sigma_{eq}^2}{\sigma_o^2}+\frac{9f_b}{4\left(1-f_b\right)^2}\frac{\Sigma_m^2}{\sigma_o^2}+2f_e\cosh\left(\frac{3}{2}\sqrt{\frac{1+\frac{2}{3}f_b}{\left(1-f_b\right)^2}}\frac{\Sigma_m}{\sigma_o}\right)-1-f_e^2=0 \tag{4.4}$$

$$\frac{1+\frac{2}{3}f_b}{\left(1-f_b\right)^2}\frac{\Sigma_{eq}^2}{\sigma_o^2}+\frac{9\left(\frac{1-f_b}{\ln f_b}\right)^2}{4\left(1-f_b\right)^2}\frac{\Sigma_m^2}{\sigma_o^2}+2f_e\cosh\left(\frac{3}{2}\sqrt{\frac{1+\frac{2}{3}f_b}{\left(1-f_b\right)^2}}\frac{\Sigma_m}{\sigma_o}\right)-1-f_e^2=0 \tag{4.5}$$

When considering the limit case of zero void content at the smallest scale, i.e. $f_b=0$ and $f_e=f$, both Eqs. (4.4) and (4.5) reduce to the original Gurson (1977) model:

$$\frac{\Sigma_{eq}^2}{\sigma_o^2}+2f\cosh\left(\frac{3}{2}\frac{\Sigma_m}{\sigma_o}\right)-1-f^2=0 \tag{4.6}$$

The von Mises solid phase at the microscopic scale appears for a zero void content.

4.3. Computational homogenization

Very few studies performed three-dimensional FE homogenization of porous media including numerous voids (Segurado and Llorca, 2002; Moraleda et al., 2007; Bilger et al., 2005; 2007; Fritzen et al., 2012; 2013). Generally, the random porous medium is considered as a volume of porous material which is periodically arranged. In this work, FE simulations on a RVE, taken sufficiently large compared to heterogeneities (Drugan and Willis, 1996; Kanit et al., 2003; Khdir et al., 2013), are achieved. The RVE includes a double population of voids randomly distributed in the matrix.

The *Zebulon* software was employed to achieve the FE simulations. The number of elements is chosen sufficiently large to accurately represent the void geometry and to ensure an accurate estimate of the yield surface.

4.3.1. Double porous microstructures

In Table 4.1 are reported the different configurations studied in this work.

#	f_e	f_b	n_e	n_b
1	0.05	0.05	30	234
2	0.05	0.1	30	468
3	0.1	0.05	60	234
4	0.1	0.0	200	0
5	0.15	0.0	200	0

Table 4.1. Volume fractions *f* and number of voids *n* in the investigated microstructures.

The volume fractions f_e and f_b correspond respectively to n_e and n_b voids inside the RVE. The notations used in Section 4.2 are used; the subscripts *e* and *b* denote the largest and smallest porosities, respectively.

Three porous microstructures containing two populations of voids are investigated: (1) f_e=0.05, f_b=0.05, (2) f_e=0.05, f_b=0.1 and (3) f_e=0.1, f_b=0.05. Examples of two-dimensional cross-sections, issued from the three-dimensional volume elements, are depicted in Fig. 4.1. In order to check the influence of a second population, two other porous microstructures containing only one void population are also examined. In this case, the total void volume fractions are: (4) $f_e = f$ =0.1 and (5) $f_e = f$ =0.15.

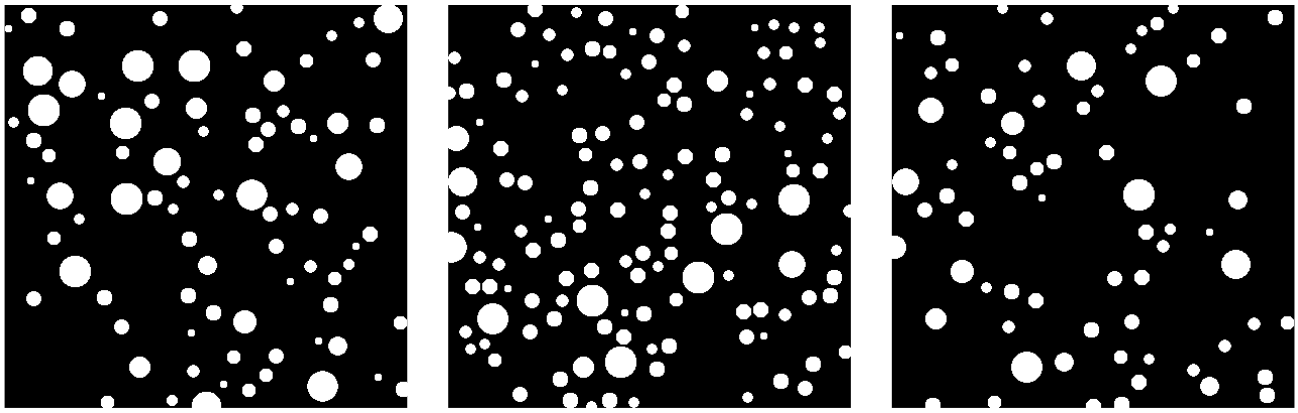

(a) (b) (c)

Fig. 4.1. Cross-sections of investigated double porous microstructures: (a) $f_e = 0.1$, $f_b = 0.05$, (b) $f_e = 0.05$, $f_b = 0.1$, (c) $f_e = 0.05$, $f_b = 0.05$.

Whatever the studied configuration, the voids are assumed spherical, randomly distributed, non-overlapped and exhibit a zero stiffness. Remind that the analytical models deal with porous medium the matrix of which is assumed rigid perfectly-plastic and governed by the von Mises yield criterion. To ensure these conditions, the Young's modulus value was taken sufficiently high and the hardening is disregarded in the numerical simulations. The Poisson's ratio and the initial yield stress of the matrix were 0.3 and 290 MPa, respectively. A standard small-strain approximation is used for the simulations.

4.3.2. Loading conditions

Mixed boundary conditions were used to control the triaxiality of the stress state during the loading. The shear components of the macroscopic stress tensor are cancelled and the diagonal components of the macroscopic strain tensor monotonically increase as a function of two loading parameters α and β:

$$\begin{aligned} E_{11}(t) &= t\dot{\varepsilon}_0(\alpha+\beta) \\ E_{22}(t) &= t\dot{\varepsilon}_0(-\alpha+\beta) \\ E_{33}(t) &= t\dot{\varepsilon}_0\beta \\ \Sigma_{12}(t) &= \Sigma_{13}(t) = \Sigma_{23}(t) = 0 \end{aligned} \tag{4.7}$$

where $\dot{\varepsilon}_0 > 0$ is a prescribed deformation rate and t is the loading time. Identical boundary conditions were already used in Fritzen et al. (2012; 2013). The values of α and β used in the present work are reported in Table 3.1.

4.3.3. Results and discussion

4.3.3.1. Stationary response

The asymptotic response is illustrated in Fig. 4.2 for a particular example (porosity of 0.15) and for the different loading cases given in Table 3.1.

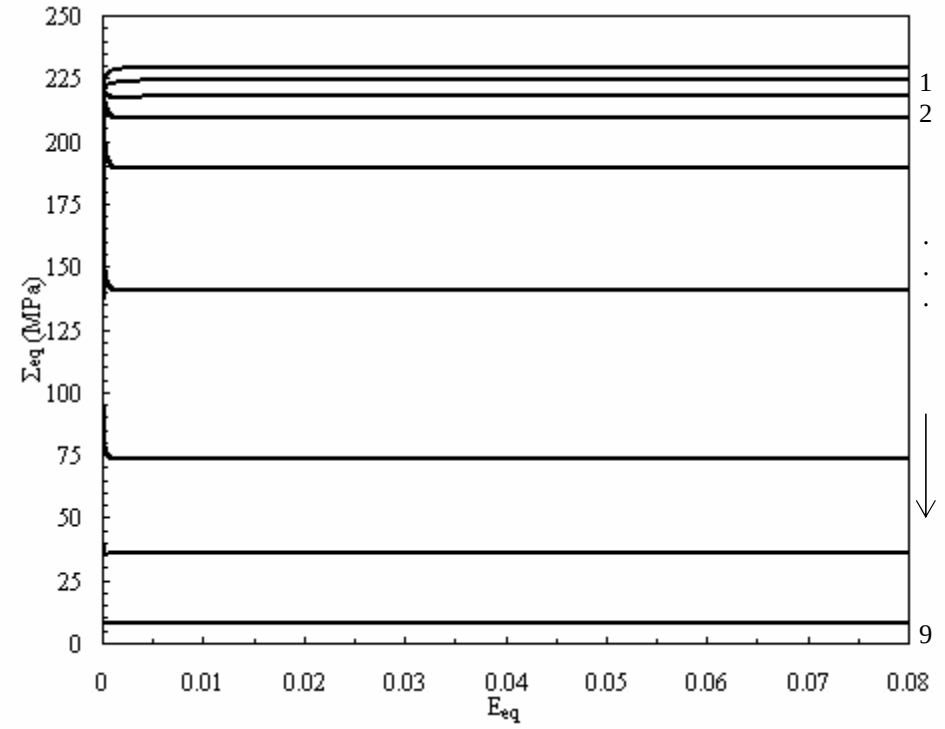

(a)

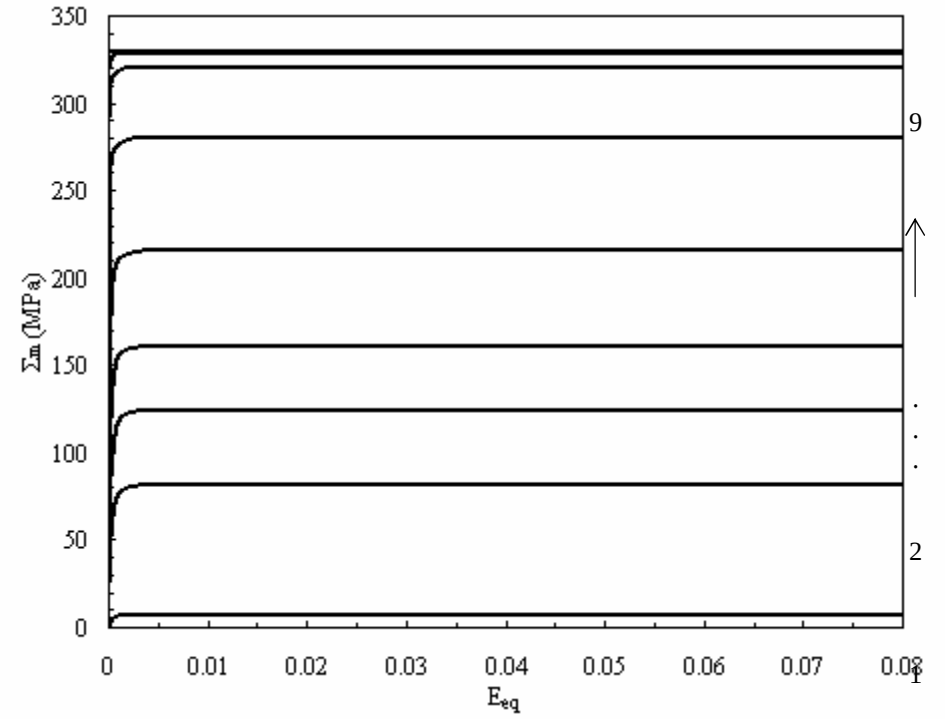

(b)

Fig. 4.2. Macroscopic von Mises equivalent stress (a) and macroscopic hydrostatic stress (b) as a function of the macroscopic von Mises equivalent strain at $f = 0.15$.

The macroscopic von Mises equivalent and hydrostatic stresses, both controlling directly the stress triaxiality ratio, are plotted in the figure as a function of the macroscopic von Mises equivalent strain. It can be observed that beyond a certain strain value the two measures of stress reach stationary values. All porous microstructures examined in this study exhibited an asymptotic behavior. In order to approximate the asymptotic response of the porous microstructures, and thus to define the numerical yield points, the macroscopic stresses at the end of the simulation are considered.

4.3.3.2. Representativity

The mechanical representativity of the computational results is examined for a porosity of 0.15 in Fig. 4.3. The asymptotic macroscopic von Mises equivalent and hydrostatic stresses are plotted for different number of pores in the figure. Different number of pores means different sizes of volume elements. Fig. 4.3a corresponds to the loading path 1 in Table 3.1 characterized by (α = 1, β = 0) for which the deviatoric component exhibits the highest stationary value, whereas Fig. 4.3b corresponds to the loading path 9 in Table 3.1 characterized by (α = 0, β = 1) for which the hydrostatic component takes its highest stationary value. Computational results of several realizations containing 50 pores are also reported in Fig. 4.3 with the corresponding average value and standard deviations. All computed data are found within or close to the grey area defined by the standard deviations. For this particular example, n = 200 gives stationary values close to the average. The largest cell sizes (see Table 3.1) are used to construct the FE yield surfaces in order to assure their mechanical representativity.

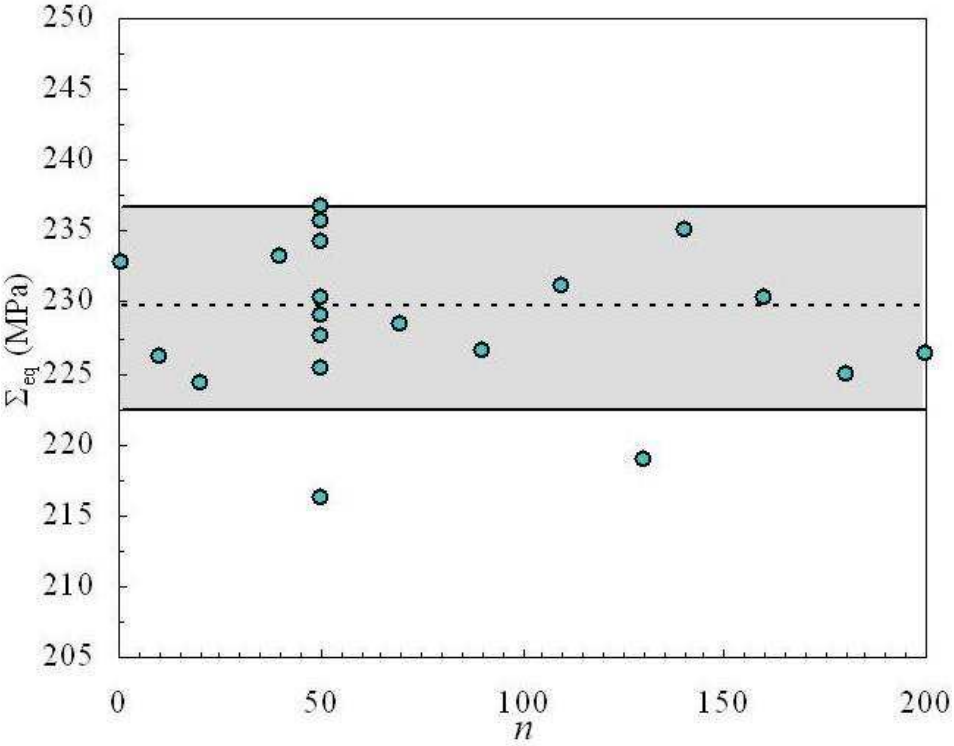

(a)

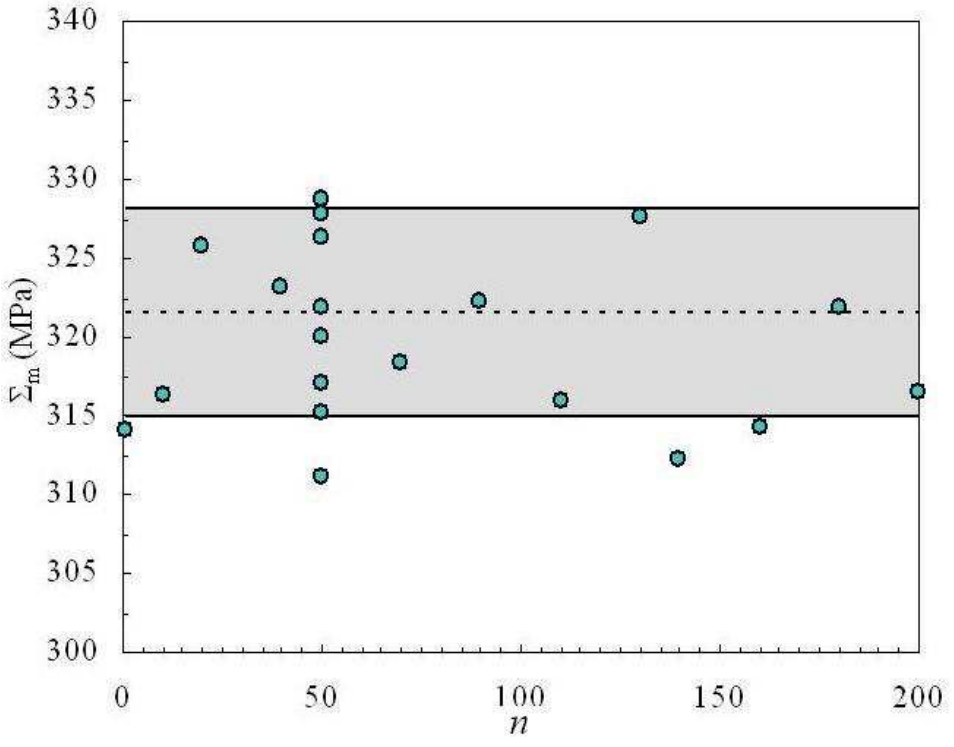

(b)

Fig. 4.3. Macroscopic von Mises equivalent stress (a) and macroscopic hydrostatic stress (b) for different number of pores at $f = 0.15$; the average (dashed line) and the standard deviations (grey area) are calculated for n = 50.

4.3.3.3. Local plastic strain fields

The local plastic yielding can be observed when the asymptotic response is reached. Figs. 4.4 and 4.5 present examples of the plastic strain fields for a single population of voids and for two populations of voids, respectively. These particular examples correspond to a total porosity of 0.15. The pore-pore interactions and the triaxiality effects on the plastic strain distribution are shown for three particular loading cases: The cases ($\alpha = 1$, $\beta = 0$) and ($\alpha = 0$, $\beta = 1$) correspond to the lowest and highest triaxiality ratios, respectively, and the case ($\alpha = 1$, $\beta = 0.25$) to an intermediate one. The main observation is a difference in the local fields between one and two populations of porosities at the same volume fraction. That may be due to smaller distances between neighboring pores when large and small porosities cohabit.

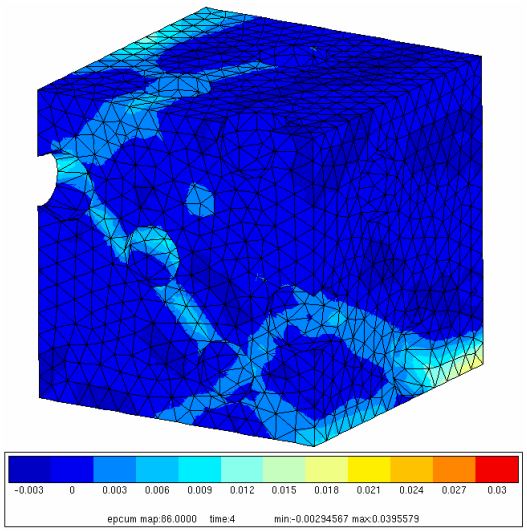

(a)

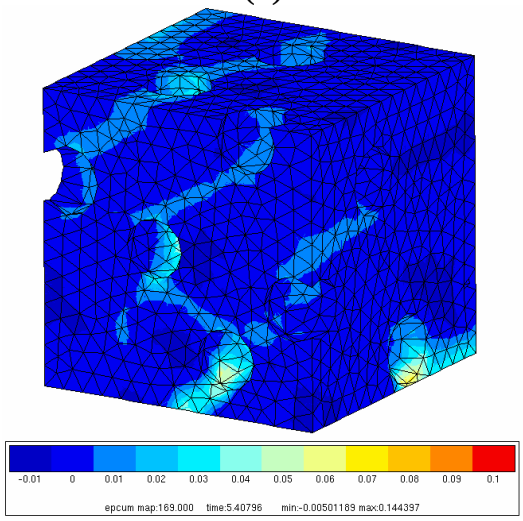

(b)

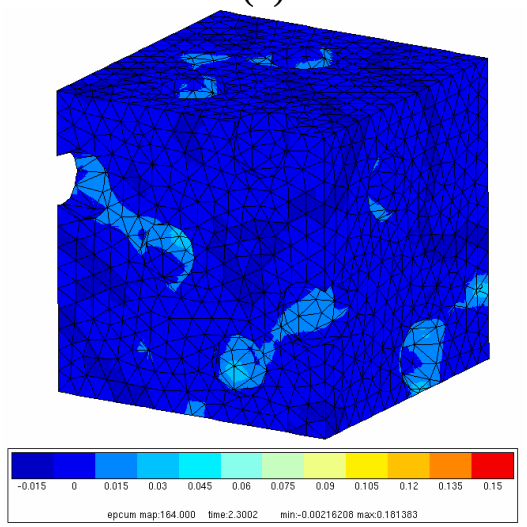

(c)

Fig. 4.4. Distribution of the accumulated plastic strain for a single population of voids at $f = 0.15$ and three different loading cases:
(a) $\alpha = 1$, $\beta = 0$, (b) $\alpha = 1$, $\beta = 0.25$, (c) $\alpha = 0$, $\beta = 1$.

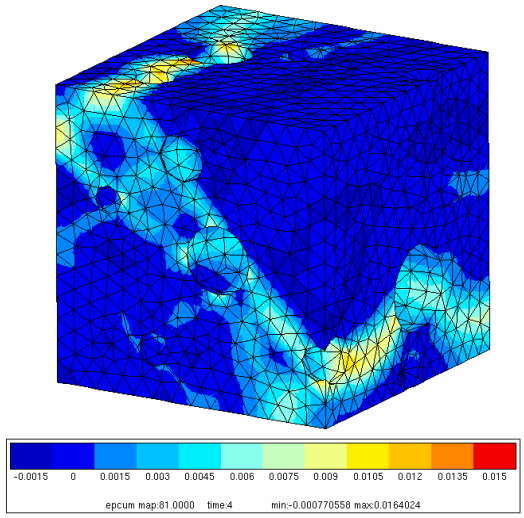

(a)

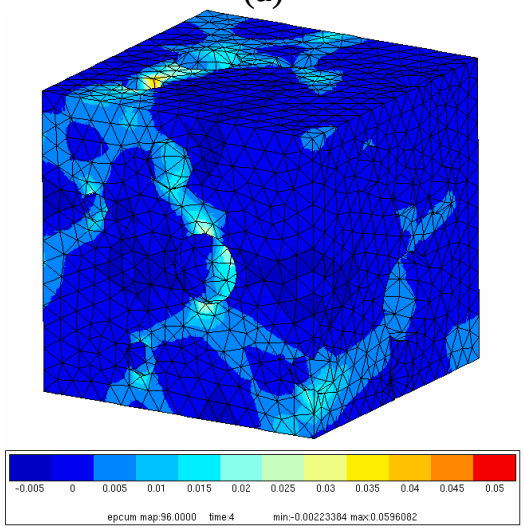

(b)

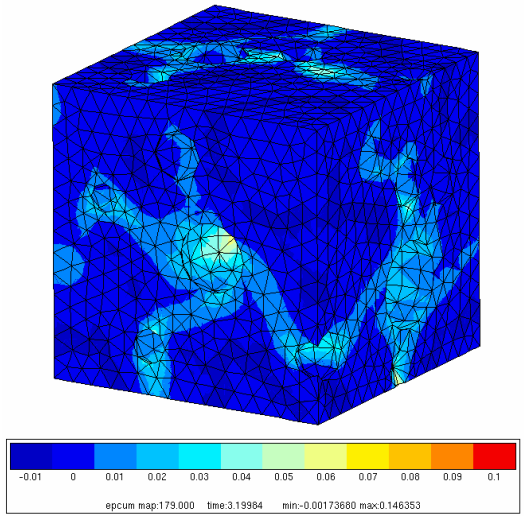

(c)

Fig. 4.5. Distribution of the accumulated plastic strain for two populations of voids at $f_e = 0.05$, $f_b = 0.1$ and three different loading cases: (a) $\alpha = 1$, $\beta = 0$, (b) $\alpha = 1$, $\beta = 0.25$, (c) $\alpha = 0$, $\beta = 1$.

4.3.3.4. Computational data vs. analytical estimates

The computational results are presented in the normalized macroscopic von Mises equivalent and hydrostatic stresses space in Fig. 4.6. The normalization is made with respect to the matrix yield stress. The generated FE yield points strongly highlight the convexity of the yield surface. The PC and MS analytical criteria are also depicted in Fig. 4.6. The FE data exhibit a yield surface which is inside that given by the analytical models, whatever the considered arrangement. Nevertheless, the responses of the analytical models are significantly different and the MS model estimates are found to be almost closer to our FE data.

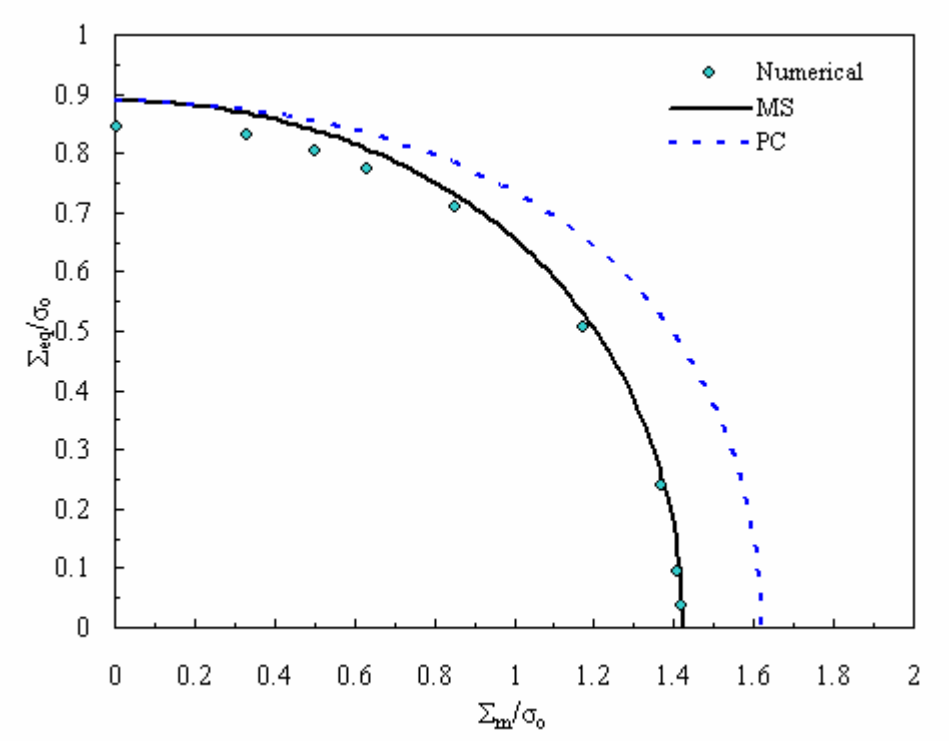

(a)

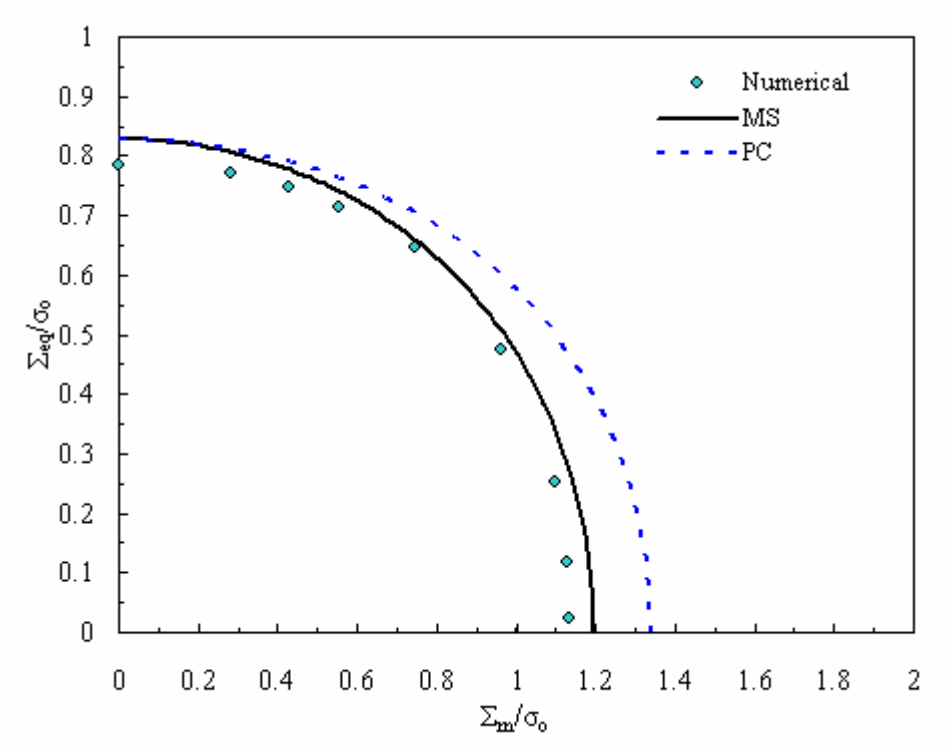

(b)

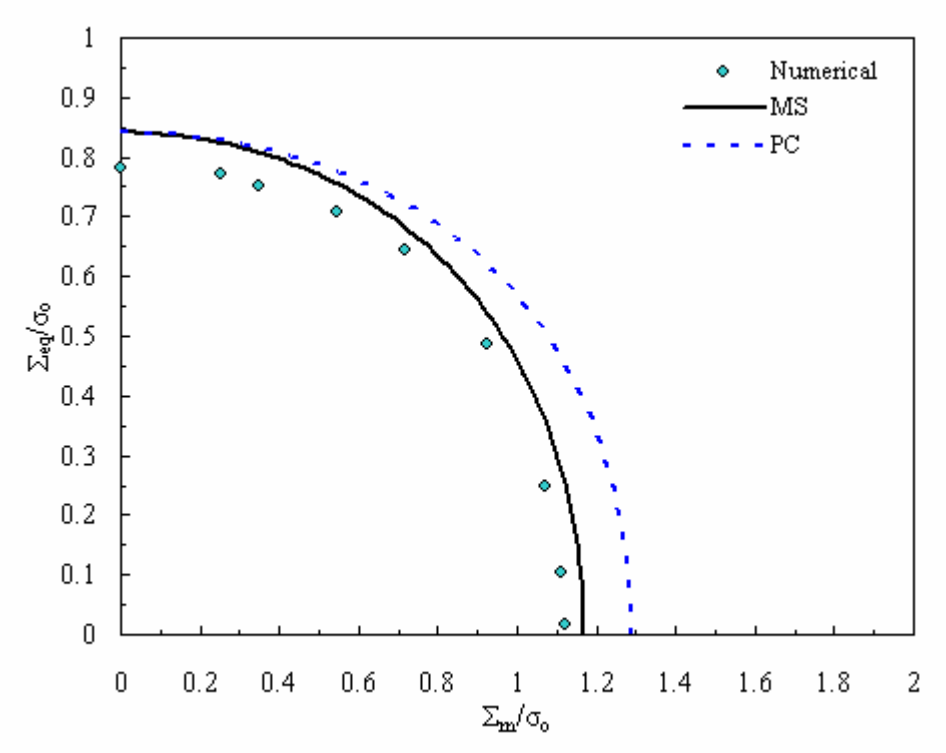

(c)

Fig. 4.6. Computational data compared to the MS and PC models:

(a) $f_e = 0.05$, $f_b = 0.05$, (b) $f_e = 0.05$, $f_b = 0.1$, (c) $f_e = 0.1$, $f_b = 0.05$.

4.3.3.5. Modification of the analytical models

In order to more closely match the PC and MS criteria with the FE results, one can slightly modify the analytical models by introducing adjusting parameters, q_1, q_2, $q_3 > 0$, as follows:

$$\frac{1+\frac{2}{3}f_b}{(1-f_b)^2}\frac{\Sigma_{eq}^2}{\sigma_o^2}+\frac{9f_b}{4(1-f_b)^2}\frac{\Sigma_m^2}{\sigma_o^2}+2q_1f_e\cosh\left(\frac{3}{2}q_2\sqrt{\frac{1+\frac{2}{3}f_b}{(1-f_b)^2}}\frac{\Sigma_m}{\sigma_o}\right)-1-q_3f_e^2=0 \qquad (4.8)$$

$$\frac{1+\frac{2}{3}f_b}{(1-f_b)^2}\frac{\Sigma_{eq}^2}{\sigma_o^2}+\frac{9\left(\frac{1-f_b}{\ln f_b}\right)^2}{4(1-f_b)^2}\frac{\Sigma_m^2}{\sigma_o^2}+2q_1f_e\cosh\left(\frac{3}{2}q_2\sqrt{\frac{1+\frac{2}{3}f_b}{(1-f_b)^2}}\frac{\Sigma_m}{\sigma_o}\right)-1-q_3f_e^2=0 \qquad (4.9)$$

These modifications are similar to that brought by Tvergaard (1982) to the original Gurson (1977) model which led to the famous Gurson-Tvergaard (GT) model for porous media with a single population of voids. That was achieved in order to improve agreement of the model with two-dimensional FE simulations on a periodic unit cell. The GT model is expressed as follows:

$$\frac{\Sigma_{eq}^2}{\sigma_o^2}+2fq_1\cosh\left(\frac{3}{2}q_2\frac{\Sigma_m}{\sigma_o}\right)-1-q_3f^2=0 \qquad (4.10)$$

Many numerical and experimental investigations use $q_3=q_1^2$ (Benzerga and Leblond, 2010; Besson, 2010) for the GT model.

The computational data obtained for the double population are compared to the predictions given by modified PC and MS criteria and given by Eqs. (4.8) and (4.9), respectively. In Table 4.2 are reported the values of the identified parameters we have introduced in these equations. As shown in Fig. 4.7, the two yield criteria are able to capture the whole FE yield surface in a satisfactory manner. Although a better agreement could be obtained by considering that these parameters are taken independent of the void content. More interestingly, the parameters are also found independent of the void size in the particular cases we have investigated.

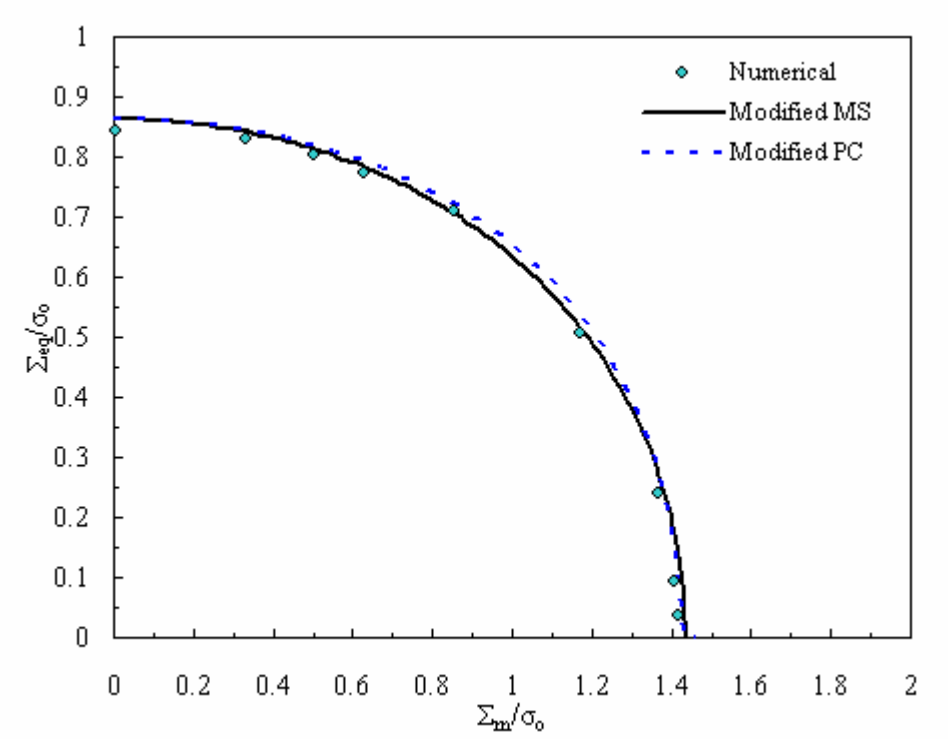

(a)

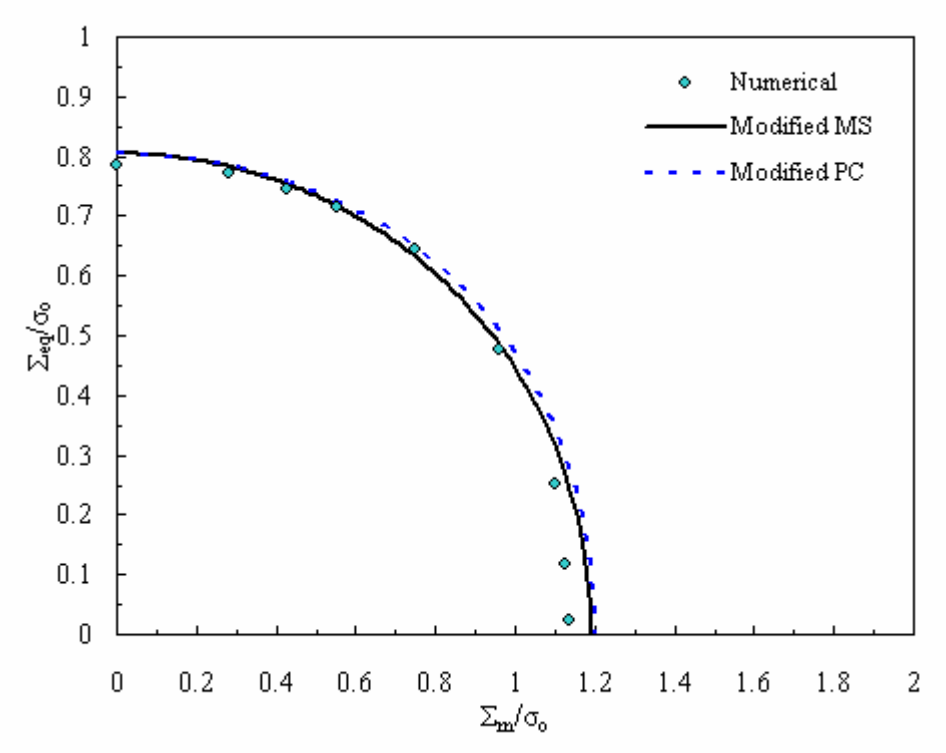

(b)

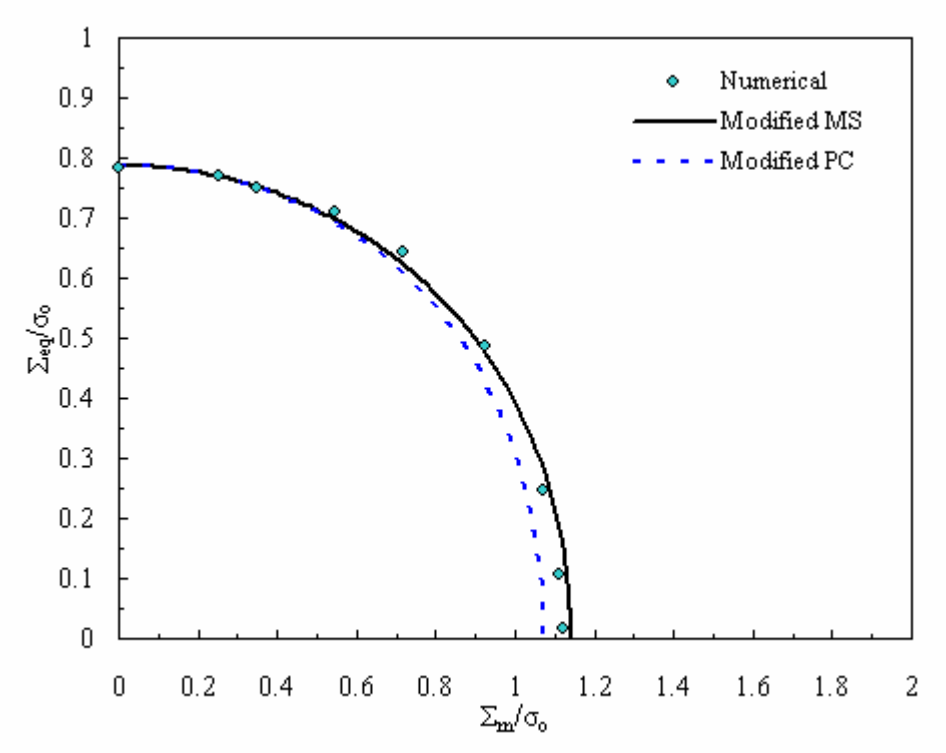

(c)

Fig. 4.7. Adjustment of the modified MS and PC models using the computational data: (a) $f_e = 0.05$, $f_b = 0.05$, (b) $f_e = 0.05$, $f_b = 0.1$, (c) $f_e = 0.1$, $f_b = 0.05$.

The corresponding *q*-parameters are listed in Table 4.2.

MS			PC		
q_1	q_2	q_3	q_1	q_2	q_3
1.5	0.8	q_1^2	1.5	1.0	q_1^2

Table 4.2. Parameters of the modified MS and PC models.

4.4. Concluding remarks

Since we have previously found that the parameters are independent of the void size, one could suggest that a porous medium containing a single population of voids could properly represent the same medium with two populations of voids. In order to address this issue, computations on porous materials containing only one population of voids with 0.1 and 0.15 void volume fractions were therefore performed (see Table 4.1). The obtained yield surfaces are plotted in Fig. 4.8 and compared with the previous data stored for double population.

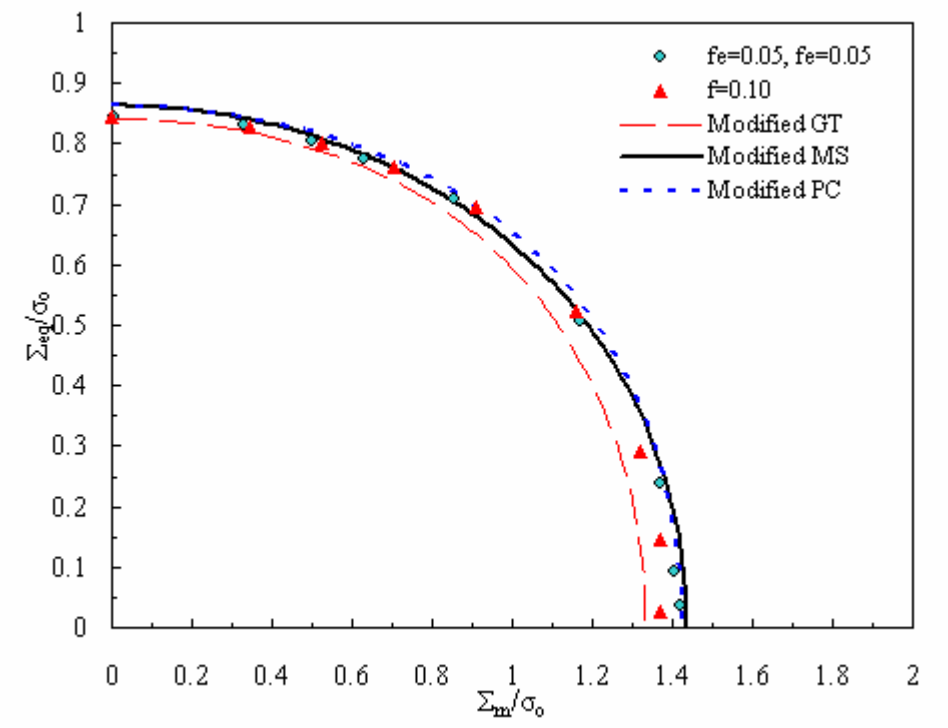

(a)

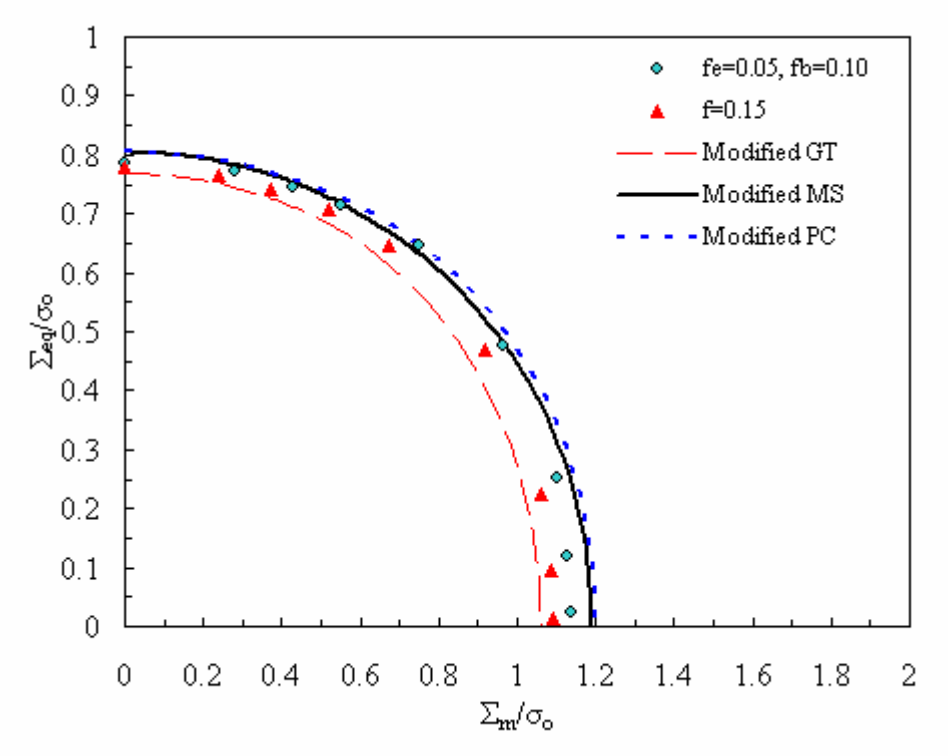

(b)

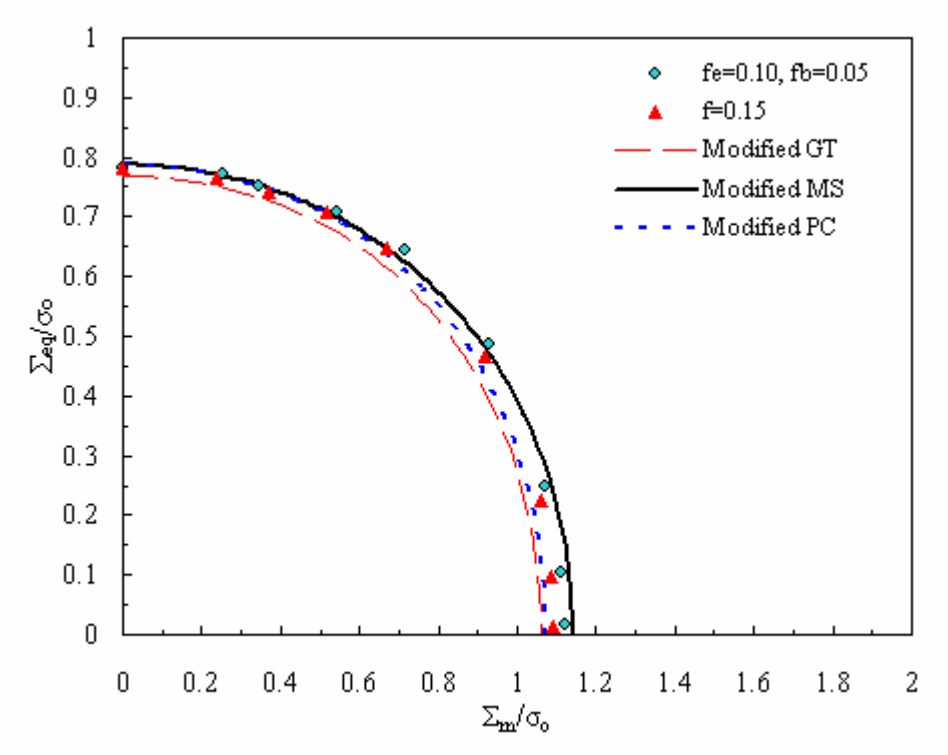

(c)

Fig. 4.8. Computational data of double and single porous media for the two total volume fractions of voids: (a) $f = 0.1$, (b) $f = 0.15$, (c) $f = 0.15$. The modified models are also depicted; The corresponding q-parameters are listed in Table 4.2 for MS and PC, and in Table 4.3 for GT.

As clearly highlighted the two sets of data are nearly superimposed, even a weak divergence is observed for low hydrostatic pressure values, which is more accentuated for the highest total void volume fraction. This result is particularly interesting since it implies that the yield surface of these porous media containing a double population of voids may be approximated by the GT function.

Recently, Fritzen et al. (2012) designed a model by fitting closely the GT model to their three-dimensional computational homogenization results of porous media containing a single population of voids with identical size. The modified GT model was constructed using a periodic assembly of multiple randomly distributed voids. Table 4.3 summarizes the parameters of the modified GT model, which is also depicted in Fig. 4.8. As expected, the modified GT model is close to the numerical yield envelopes.

GT		
q_1	q_2	q_3
$1.69 - f$	0.92	q_1^2

Table 4.3. Parameters of the modified GT model (Fritzen et al., 2012).

As a final point, we can recall that the recently developed analytical criteria for double porous media are based on the assumption of a large difference in size between the two populations of voids. The large volume computations performed in this work has pointed out that, in the particular cases we have investigated, a random porous material with two populations of voids with different sizes can be replaced by a random porous material with only one population of voids with an equivalent void volume fraction. Fig. 4.9 depicts this new insight.

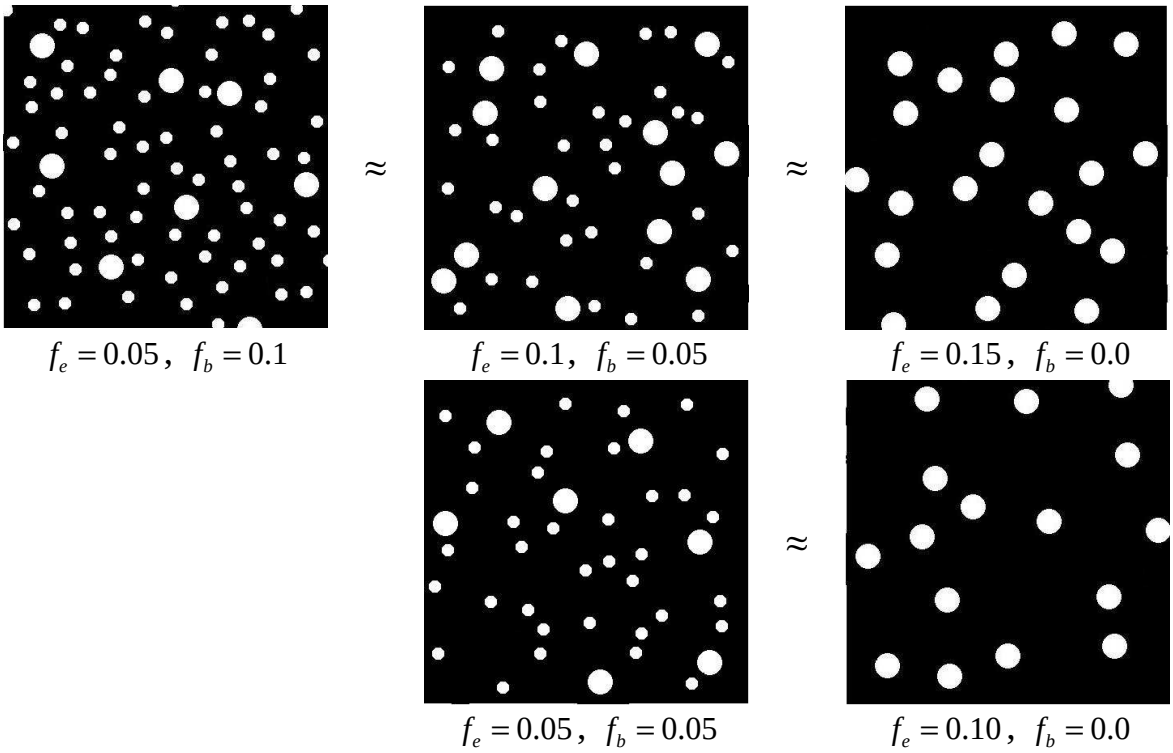

Fig. 4.9. Equivalence of double and single porous materials with equal total void volume fractions.

As a conclusion, in this study, large volume FE simulations on an RVE were used to obtain the macroscopic yield response of random porous materials containing two populations of randomly distributed spherical voids with different sizes. The FE results were compared to two existing analytical yield criteria. To overcome the observed discrepancies, extensions of the analytical models were proposed by introducing adjusting parameters. An independence of these GT-like parameters on the volume fraction and size of voids was highlighted. Moreover, for the particular cases investigated here, we have shown that a porous media containing a double population of voids could be replaced by one other with a single population. To confirm that finding, it is necessary to achieve FE simulations using much more volume fractions values, on the one hand, and the values for each population must be sufficiently remote from each other.

GENERAL CONCLUSION AND FUTURE WORKS

General conclusion and future works

This PhD dissertation is a contribution to the computation homogenization micromechanics of random media with elastic-plastic matrix. Both particulate composites and porous materials were investigated via this method.

In the first part of this work, a computational homogenization method was used to estimate the effective elastic-plastic response of particulate composites. The method was based on the computations of small limited volumes of fixed size extracted from a larger one and containing different realizations of the random microstructure. Both non-overlapping and overlapping partitions of the larger volume element into subvolumes were considered. If a small subvolume did not necessary exhibit an isotropic response (even if the microstructure is expected to be macroscopically isotropic) we showed that the average response of a sufficient number of different realizations is isotropic. A significant scatter in the plastic regime of the apparent stress-strain curves was observed for too small subvolumes. It was shown that the dispersion of the results decreases when the domain size increases. It was also found that for a given number of realizations the overlapping of subvolumes significantly decreases the dispersion. Finally, it was also shown that the elementary volume element (EVE) containing one centered inclusion, even widely used in the literature, represents a minor bound of the real mechanical response.

In the second part of this work, the overall yield surface of plastic porous media was investigated. The computational results were investigated in terms of representativity and were related to some existing Gurson-type yield criteria for single or double populations of voids. The

importance of the volume element size to estimate the overall yield surface was highlighted. The independence of the overall yield surface on the void shape permits to generalize the Fritzen et al. (2012) model to any void shape. Moreover, we have found that the Gurson-Tvergaard heuristic parameters are independent on the void size which could suggest that a porous medium containing a single population of voids could properly represent a same medium with two populations of voids.

It will be interesting in future investigations to examine the effects of the initial yield strain on the overall yield surface. Moreover, the evolution of the yield surface with deformation by including (isotropic and/or kinematic) hardening ought to be investigated.

References

Alabbasi, F., 2004. Micromechanical modeling of dual phase steels. PhD thesis, McGill University.

Alzebdeh, K., Al-Ostaz, A., Jasiuk, I., Ostoja-Starzewski, M., 1996. Fracture of random matrix-inclusion composites: scale effects and statistics. International Journal of Solids and Structures 35, 2537-2566.

Annapragada, S.R., Suresh, D.S., Garimella, V., 2007. Prediction of effective thermo-mechanical properties of particulate composites. Computational Materials Science 40, 255-266.

Anoukou, K., Zaïri, F., Naït-Abdelaziz, M., Zaoui, A., Messager, T., Gloaguen, J.M., 2011a. On the overall elastic moduli of polymer-clay nanocomposite materials using a self-consistent approach. Part I: Theory. Composites Science and Technology 71, 197-205.

Anoukou, K., Zaïri, F., Naït-Abdelaziz, M., Zaoui, A., Messager, T., Gloaguen, J.M., 2011b. On the overall elastic moduli of polymer-clay nanocomposite materials using a self-consistent approach. Part II: Experimental verification. Composites Science and Technology 71, 206-215.

Asserin-Lebert, A., Besson, J., Gourgues A.F., 2005. Fracture of 6056 aluminum sheet materials: effect of specimen thickness and hardening behavior on strain localization and toughness. Materials Science and Engineering A 395, 186-194.

Benzerga, A., Besson, J., Pineau. A., 2004. Anisotropic ductile fracture. Part II: theory. Acta Materialia 52, 4623-4638.

Benzerga, A., Leblond. J.B., 2010. Ductile fracture by void growth to coalescence. Advances in Applied Mechanics 44, 169-305.

Berger, H, Kari, S., Gabbert, U., Rodriguez-Ramos, R., Guinovart, R., Otero, J.A., Bravo-Castillero, J., 2005. An analytical and numerical approach for calculating effective material coefficients of piezoelectric fiber composites. International Journal of Solids and Structures 42, 5692-5714.

Berveiller, M., Zaoui, A., 1979. An extension of the self-consistent scheme to plastically-flowing polycrystals. Journal of the Mechanics and Physics of Solids 26, 325-344.

Besson, J., 2009. Damage of ductile materials deforming under multiple plastic or viscoplastic mechanisms. International Journal of Plasticity 25, 2204-2221.

Besson, J., 2010. Continuum models of ductile fracture: a review. International Journal of Damage Mechanics 19, 3-52.

Bilger, N., Auslender, F., Bornert, M., Michel, J.C., Moulinec, H., Suquet, P., Zaoui, A., 2005. Effect of a nonuniform distribution of voids on the plastic response of voided materials: a computational and statistical analysis. International Journal of Solids and Structures 42, 517-538.

Bilger, N., Auslender, F., Bornert, M., Moulinec, H., Zaoui, A., 2007. Bounds and estimates for the effective yield surface of porous media with a uniform or a nonuniform distribution of voids. European Journal of Mechanics A/Solids 26, 810-836.

Böhm, H.J., 2013. A short introduction to basic aspects of continuum micromechanics. Institute of lightweight design and structural biomechanics. ILSB Report 206.

Borberly, A., Biermann, H., Hartmanm, O., 2001. FE investigation of the effect of particle distribution on the uniaxial stress-strain behaviour of particulate reinforced metal-matrix composites. Materials Science and Engineering A 313, 34-45.

Brassart, L., Inglis, H.M., Delannay, L., Doghri, I., Geubelle P.H., 2009. An extended Mori-Tanaka homogenization scheme for finite strain modeling of debonding in particle-reinforced elastomers. Computational Materials Science 45, 611-616.

Brassart, L., Doghri, I., Delannay, L., 2010. Homogenization of elasto-plastic composites coupled with a non-linear finite element analysis of the equivalent inclusion problem. International Journal of Solids and Structures 47, 716-729.

Brassart, L., Stainier, L., Doghri, I., Delannay L., 2012. Homogenization of elasto-(visco) plastic composites based on an incremental variational principle. International Journal of Plasticity 36, 86-112.

Brockenbrough, J. R., Suresh, S. and Wienecke, H. A., 1991. Deformation of metal-matrix composites with continuous fibers: Geometrical effects of fiber distribution and shape. Acta Metallurgica et Materialia 39, 735-752.

Budiansky, B., 1965. On the elastic moduli of some heterogeneous materials. Journal of the Mechanics and Physics of Solids 13, 223-227.

Buryachenko, V.A., Pagano, N.J., Kim, R.Y., Spowart, J.E., 2003. Quantitative description and numerical simulation of random microstructures of composites and their effective elastic moduli. International Journal of Solids and Structures 40, 47-72.

Bystrom, J., 2003. Influence of the inclusions distribution on the effective properties of heterogeneous media. Composites: Part B 34, 587-592.

Charles, Y., Estevez, R., Bréchet, Y., Maire, E., 2010. Modelling the competition between interface debonding and particle fracture using a plastic strain dependent cohesive zone. Engineering Fracture Mechanics 77, 705-718.

Chawla, N., Chawla, K.K., 2006. Microstructure-based modeling of the deformation behavior of particle reinforced metal matrix composites. Journal of Materials Science 41, 913-925.

Chawla, N. Sidhu, R.S., Ganesh, V.V., 2006. Three-dimensional visualization and microstructure-based modeling of deformation in particle-reinforced composites. Acta Materialia 54, 1541-1548.

Corigliano, A., Mariani, S., Orsatti, B., 2000. Identification of Gurson-Tvergaard material model parameters via Kalman filtering technique. Part I: Theory. International Journal of Fracture 104, 349-373.

Croix, P., Lauro, F., Oudin, J., Christlein, J., 2003. Improvement of damage prediction by anisotropy of voids. Journal of Material Processing Technology 143-144, 202-208.

Danas, K., Aravas, N., 2012. Numerical modeling of elasto-plastic porous materials with void shape effects at finite deformations. Composites: Part B 43, 2544-2559.

Delannay, L., Doghri, I., Pierard O., 2007. Prediction of tension-compression cycles in multiphase steel using a modified incremental mean-field model. International Journal of Solids and Structures 44, 7291-7306.

Doghri, I., Leckie F.A., 1994. Elasto-plastic analysis of interface layers for fiber-reinforced metal-matrix composites. Composites Science and Technology 51, 63-74.

Doghri, I., Ouaar, A., 2003. Homogenization of two-phase elasto-plastic composite materials and structures: Study of tangent operators, cyclic plasticity and numerical algorithms. International Journal of Solids and Structures 40, 1681-1712.

Doghri, I., Friebel, C., 2005. Effective elasto-plastic properties of inclusion-reinforced composites. Study of shape, orientation and cyclic response. Mechanics of Materials 37, 45-68.

Doghri, I., Tinel, L., 2006. Micromechanics of inelastic composites with misaligned inclusions: Numerical treatment of orientation. Computer Methods in Applied Mechanics and Engineering 195, 1387-1406.

Doghri, I., Adam, L., Bilger, N., 2010. Mean-field homogenization of elasto-viscoplastic composites based on a general incrementally affine linearization method. International Journal of Plasticity 26, 219-238.

Drugan, W.J., Willis, J.R., 1996. A micromechanics-based nonlocal constitutive equation and estimates of representative volume element size for elastic composites. Journal of the Mechanics and Physics of Solids 44, 497-524.

Dunand, M., Mohr, D., 2011. On the predictive capabilities of the shear modified Gurson and the modified Mohr-Coulomb fracture models over a wide range of stress triaxialities and Lode angles. Journal of the Mechanics and Physics of Solids 59, 1374-1394.

El Ghezal, M.I., Maalej, Y., Doghri, I., 2013. Micromechanical models for porous and cellular materials in linear elasticity and viscoelasticity. Computational Materials Science 70, 51-70.

Eshelby, J.D., 1957. The determination of the elastic field of an ellipsoidal inclusion and related problems. Proceedings of the Royal Society of London Series A Mathematical Sciences 241, 376-396.

Evesque, P., 2000. Fluctuations, correlations and representative elementary volume (rev) in granular materials. Poudres & Grains 11, 6-17, ISSN 1257-3957.

Fabregue, D., Pardoen, T., 2008. A constitutive model for elastoplastic solids containing primary and secondary voids. International Journal of the Mechanics and Physics of Solids 56, 719-741.

Faleskog, J., Shih, C.F., 1997. Micromechanics of coalescence-I. Synergistic effects of elasticity, plastic yielding and multi-size-scale voids. Journal of the Mechanics and Physics of Solids 45, 21-50.

Faleskog, J., Gao, X., Shih, C.F., 1998. Cell model for non-linear fracture analysis - I. Micromechanics calibration. International Journal of Fracture 89, 355-373.

Fei, H., Yazzie, K., Chawla, N., Jiang, H., 2012. The effect of random voids in the modified gurson model. Journal of Electronic Materials 41, 177-183.

Flandi, L., Leblond, J.B., 2005a. A new model for porous non-linear viscous solids incorporating void shape effects I: Theory. European Journal of Mechanics A/Solids 24, 537-551.

Flandi, L., Leblond, J.B., 2005b. A new model for porous non-linear viscous solids incorporating void shape effects II: Numerical validation. European Journal of Mechanics A/Solids. 24, 552-571.

Friebel, C., Doghri, I., Legat V., 2006. General mean-field homogenization schemes for viscoelastic composites containing multiple phases of coated inclusions. International Journal of Solids and Structures 43, 2513-2541.

Fritzen, F., Forest, S., Böhlke, T., Kondo, D., Kanit, T., 2012. Computational homogenization of elasto-plastic porous metals. International Journal of Plasticity 29, 102-119.

Fritzen, F., Forest, S., Kondo, D., Böhlke, T., 2013. Computational homogenization of porous materials of Green type. Computational Mechanics 52, 121-134.

Galli, M., Botsis, J.3., Janczak-Rusch, J., 2008. An elastoplastic three-dimensional homogenization model for particle reinforced composites. Computational Materials Science 41, 312-321.

Galli, M., Cugnoni, J., Botsis J., 2012. Numerical and statistical estimates of the representative volume element of elastoplastic random composites. European Journal of Mechanics A/Solids 33, 31-38.

Gao, X., Zhang, T., Hayden, M., Roe, C., 2009. Effects of the stress state on plasticity and ductile failure of an aluminum 5083 alloy. International Journal of Plasticity 25, 2366-2382.

Gărăjeu, M., Suquet, P., 1997. Effective properties of porous ideally plastic or viscoplastic materials containing rigid particles. Journal of the Mechanics and Physics of Solids 45, 873-902.

Ghosh, S., Lee, K., Moorthy, S., 1996. Two scale analysis with asymptotic of heterogeneous elastic-plastic materials homogenization and Voronoi cell finite element model. Computer Methods in Applied Mechanics and Engineering 132, 63-116.

Ghosh, S., Lee, K., Raghavan, P., 2001. A multi-level computational model for multi-scale damage analysis in composite and porous materials. International Journal of Solids and Structures 38, 2335-2385.

Gitman, I.M., Askes, H., Sluys, L.J., 2007. Representative volume: Existence and Size determination. Engineering Fracture Mechanics 74, 2518-2534.

Gologanu, M., Leblond, J.B., Devaux, J., 1993. Approximate models for ductile metals containing non-spherical voids - case of axisymmetric prolate ellipsoidal cavities. Journal of the Mechanics and Physics of Solids 41, 1723-1754.

Gologanu, M., Leblond, J.B., Devaux, J., 1994. Approximate models for ductile metals containing non-spherical voids - case of axisymmetric oblate ellipsoidal cavities. Journal of Engineering Materials and Technology 116, 290-297.

Gologanu, M., Leblond, J.B., Perrin, G., Devaux, J., 1997. Recent extensions of Gurson's model for porous ductile metals. In: Suquet, P. Editor, Continuum Micromechanics. Berlin: Springer-Verlag pp. 61-130.

Gologanu, M., Leblond, J.B., Perrin, G., Devaux, J., 2001. Theoretical models for void coalescence in porous ductile solids. I. Coalescence “in Layers”. International Journal of Solids and Structures 38, 5581-5594.

Graham, L.L., Baxter, S.C., 2001. Simulation of local material properties based on moving-window GMC. Probabilistic Engineering Mechanics 16, 295-305.

Graham, S., Yang, N., 2003. Representative volumes of materials based on microstructural statistics. Scripta Materialia 48, 269-274.

Green, R.J., 1972. A plasticity theory for porous solids. International Journal of Mechanical Science 14, 215-224.

Grufman, C., Ellyin, F., 2007. Determining a representative volume element capturing the morphology of fibre reinforced polymer composites. Composites Science and Technology 67, 66-775.

Gurson, A.L., 1977. Continuum theory of ductile rupture by void nucleation and growth: Part I - Yield criteria and flow rules for porous ductile media. Journal of Engineering Materials and Technology 99, 2-15.

Gusev, A.A., 1997. Representative volume element size for elastic composites: a numerical study. Journal of the Mechanics and Physics of Solids 45, 1449-1459.

Hashin, Z., 1962. The elastic moduli of heterogeneous materials. Journal of Applied Mechanics 29, 143-150.

Hashin, Z., 1964. Theory of mechanical behavior of heterogeneous media. Applied Mechanics Reviews 17, 1-9.

Hashin, Z., 1983. Analysis of composite materials: A survey. Journal of Applied Mechanics 50, 481-505.

Hashin, Z., Shtrikman, S., 1963. A variational approach to the theory of the elastic behaviour of multiphase materials. Journal of the Mechanics and Physics of Solids 11, 127-140.

Hassani, B., Hinton, E., 1998, A review of homogenization and topology optimization; I- homogenization theory for media with periodic structure. Computers and Structures 69, 707-717.

Hazanov, S., Huet, C., 1994. Order relationships for boundary conditions effect in heterogeneous bodies smaller than the representative volume. Journal of the Mechanics and Physics of Solids 42, 1995-2011.

Hill, R., 1963. Elastic properties of reinforced solids: Some theoretical principles. Journal of the Mechanics and Physics of Solids 11, 357-372.

Hill, R., 1965a. A self-consistent mechanics of composite materials. Journal of the Mechanics and Physics of Solids 13, 213-222.

Hill, R., 1965b. Theory of mechanical properties of fibre-strengthened materials - III: self consistent model. Journal of the Mechanics and Physics of Solids 13, 189-198.

Hollister, S.J., Kikuchi, N., 1992. A comparison of homogenization and standard mechanics analysis for periodic porous composites. Computational Mechanics 10, 73-95.

Holm, E.A., Duxbury, F.M., 2006. Three-dimensional materials science. Scripta Materialia 54, 1035-1040.

Huet, C., 1990. Application of variational concepts to size effects in elastic heterogeneous bodies. Journal of the Mechanics and Physics of Solids 38, 813-841.

Hutchinson, J.W., 1970. Elastic-plastic behavior of polycrystalline metals and composites. Proceedings of the Royal Society of London A 319, 247-272.

Hutchinson, J.W., 1976. Bounds and self-consistent estimates for creep of polycrystalline materials. Proceedings of the Royal Society of London A 348, 101-127.

Ji-wei, D., Miao-lin, F., 2010. Asymptotic expansion homogenization for simulating progressive damage of 3D braided composites. Composite Structures 92, 873-882.

Ju, J.W., Sun, L.Z., 2001. Effective elastoplastic behavior of metal matrix composites containing randomly located aligned spheroidal inhomogeneities. Part I: Micromechanics-based formulation. International Journal of Solids and Structures 38, 183-201.

Julien, J., Gărăjeu, M., Michel, J.-C., 2011. A semi-analytical model for the behavior of saturated viscoplastic materials containing two populations of voids of different sizes. International Journal of Solids and Structures 48, 1485-1498.

Kalamkarov, A.L., Hassan, E.M., Georgiades, A.V., Savi, M.A., 2009. Asymptotic homogenization model for 3D grid-reinforced composite structures with generally orthotropic reinforcements. Composite Structures 89, 186-196.

Kalamkarov, A.L., Savi, M.A., 2012. Micromechanical modeling and effective properties of the smart grid reinforced composites. The Brazilian Society of Mechanical Sciences and Engineering 34, 343-351.

Kaminski, M., Kleiber, M., 2000. Perturbation based stochastic finite element method for homogenization of two-phase elastic composites. Computers and Structures 78,811-826.

Kaminski, M., Lauke, B., 2012. Probabilistic and stochastic analysis of the effective properties for the particle reinforced elastomers. Computational Materials Science 56, 147-160.

Kanit, T., Forest, S., Galliet, I., Mounoury, V., Jeulin, D., 2003. Determination of the size of the representative volume element for random composites: statistical and numerical approach. International Journal of Solids and Structures 40, 3647-3679.

Kanit, T., N'Guyen, F., Forest, S., Jeulin, D., Reed, M., Singleton, S., 2006. Apparent and effective physical properties of heterogeneous materials: representativity of samples of two materials from food industry. Computer Methods in Applied Mechanics and Engineering 195, 3960-3982.

Kari, S., Berger, H., Rodriguez-Ramos, R., Gabbert, U., 2007. Computational evaluation of effective material properties of composites reinforced by randomly distributed spherical particles. Composite Structures 77, 223-231.

Keralavarma, S.M., Benzerga, A.A., 2010. A constitutive model for plastically anisotropic solids with non-spherical voids. Journal of the Mechanics and Physics of Solids 58, 874-901.

Khdir, Y.-K., Kanit, T., Zaïri, F., Naït-Abdelaziz, M., 2013. Computational homogenization of elastic-plastic composites. International Journal of Solids and Structures 50, 2829-2835.

Khdir, Y.-K., Kanit, T., Zaïri, F., Naït-Abdelaziz, M., 2014. Computational homogenization of plastic porous media with two populations of voids. Materials Science and Engineering A 597, 324-330.

Khdir, Y.-K., Kanit, T., Zaïri, F., Naït-Abdelaziz, M., 2014. Computational homogenization of elastoplastic porous materials: effects of distribution and shape of voids. Submitted.

Khisaeva, Z.F., Ostoja-Starzewski, M., 2006. On the size of RVE in finite elasticity of random composites. Journal of Elasticity 85, 153-173.

Kim, J., Gao, X., Srivatsan, T.S., 2004. Modeling of void growth in ductile solids: effects of stress triaxiality and initial porosity. Engineering Fracture Mechanics 71, 379-400.

Kiris, A., Inan, E., 2006. Eshelby tensors for a spherical inclusion in microstretch elastic fields. International Journal of Solids and Structures 43, 4720-4738.

Knight, M.G., Wrobel, L.C., Henshall, J.L., 2003. Micromechanical response of fibre-reinforced materials using the boundary element technique. Composite Structures 62, 341-352.

Koplik, J., Needleman, A., 1988. Void growth and coalescence in porous plastic solids. International Journal of Solids and Structures 24, 835-853.

Koueznetsova, V., Brekelmans, W.A.M., Baaijens, F.P.T., 2001. An approach to micro-macro modeling of heterogeneous materials. Computational Mechanics 27, 37-48.

Laiarinandrasana, L., Besson, J., Lafarge, M., Hochstetter, G., 2009. Temperature dependent mechanical behaviour of PVDF: Experiments and numerical modeling. International Journal of Plasticity 25, 1301-1324.

Lemaitre, J. Chaboche, J.L., 1990. Mechanics of Solid Materials: Cambridge University Press.

Leblond, J.B., Perrin, G., Suquet, P., 1994. Exact results and approximate models for porous viscoplastic solids. International Journal of Plasticity 10, 213-235.

Lecarme, L., Tekoglu, C., Pardoen, T., 2011. Void growth and coalescence in ductile solids with stage III and stage IV strain hardening. International Journal of Plasticity 27, 1203-1223.

Lee, K., Ghosh, S., 1999. A microstructure based numerical method for constitutive modeling of composite and porous materials. Materials Science and Engineering, A272, 120-133.

Leroy, Y., Ponte Castañeda, P., 2001. Bounds on the self-consistent approximation for non-linear media and implications for the second-order method. Comptes Rendus Mécanique 329, 571-577.

Li, H., Fu, M.W., Lu, J., Yang, H., 2011. Ductile fracture: experiments and computations. International Journal of Plasticity 27, 147-180.

Li, W., Ostoja-Starzewski, M., 2006. Yield of random elastoplastic materials. Journal of Mechanics of Materials and Structures 1, 1055-1073.

Li, Y., Karr, D.G., 2009. Prediction of ductile fracture in tension by bifurcation, localization, and imperfection analyses. International Journal of Plasticity 25, 1128-1153.

Li, Z., Huang, M., 2005. Combined effects of void shape and void size - oblate spheroidal microvoid embedded in infinite non-linear solid. International Journal of Plasticity 21, 625-650.

Li, Z., Steinmann, P., 2006. RVE-based studies on the coupled effects of void size and void shape on yield behavior and void growth at micron scales. International Journal of Plasticity 22, 1195-1216.

Lieberman, S.I., Gokhalea, A.M., Tamirisakandala, S., 2006. Reconstruction of three-dimensional microstructures of TiB phase in a

powder metallurgy titanium alloy using montage serial sectioning. Scripta Materialia 55, 63-68.

Lin, J., Kanit, T., Monchiet, V., Shao, J.F., Kondo, D., 2010. Numerical implementation of a recent improved Gurson-type model and application to ductile fracture. Computational Materials Science 47, 901-906.

Liu, G., Scudino, S., Li, R., Kühn, U., Sun, J., Eckert J., 2011. Coupling effect of primary voids and secondary voids on the ductile fracture of heat-treatable aluminum alloys. Mechanics of Materials 43, 556-566.

Ma, F., Kishimoto, K., 1998. On yielding and deformation of porous plastic materials. Mechanics of Materials 30, 55-68.

Ma, J., Temizer, I., Wriggers, P., 2011. Random homogenization analysis in linear elasticity based on analytical bounds and estimates. International Journal of Solids and Structures 48, 280-291.

Madou, K., Leblond, J.B., 2012. A Gurson-type criterion for porous ductile solids containing arbitrary ellipsoidal voids. I: Limit-analysis of some representative cell. Journal of the Mechanics and Physics of Solids 60, 1020-1036.

McClintock, F.A., 1968. A criterion for ductile fracture by the growth of holes. Journal of Applied Mechanics 35, 363-371.

McElwain, D.L.S., Roberts, A.P., Wilkins, A.H., 2006. Yield criterion of porous materials subjected to complex stress states. Acta Materialia 54, 1995-2002.

Michailidis, N., Stergioudi, F., Omar, H., Tsipas, D.N., 2010. An image-based reconstruction of the 3D geometry of an Al open-cell foam and FEM modeling of the material response. Mechanics of Materials 42, 142-147.

Michel, J.C., Suquet, P., 1992. The constitutive law of non-linear viscous and porous materials. Journal of the Mechanics and Physics of Solids 40, 783-812.

Michel, J. C., Moulinec, H., Suquet, P., 1999. Effective properties of composite materials with periodic microstructure: a computational approach. Computer Methods in Applied Mechanics and Engineering 172, 109-143.

Miled, B., Doghri, I., Delannay L., 2011. Coupled viscoelastic-viscoplastic modeling of homogeneous and isotropic polymers: Numerical algorithm and analytical solutions. Computer Methods in Applied Mechanics and Engineering. 200, 3381-3394.

Miled, B., Doghri, I., Brassart, L., Delannay, L., 2013. Micromechanical modeling of coupled viscoelastic–viscoplastic composites based on an

incrementally affine formulation. International Journal of Solids and Structures 50, 1755-1769.

Monchiet, V., Gruescu, C., Charkaluk, E., Kondo, D., 2006. Approximate yield criteria for anisotropic metals with prolate or oblate voids. Comptes Rendus Mécanique 334, 431-439.

Monchiet, V., Charkaluk. E., Kondo. D., 2007. An improvement of Gurson-type models of porous materials by using Eshelby-like trial velocity fields. C.R. Mechanique 335, 32-41.

Monchiet, V., Cazacu, O., Charkaluk, E., Kondo, D., 2008. Macroscopic yield criteria for plastic anisotropic materials containing spheroidal voids. International Journal of Plasticity 24, 1158-1189.

Monchiet, V., Charkaluk, E., Kondo, D., 2011. A micromechanics-based modification of the Gurson criterion by using Eshelby-like velocity field. European Journal of Mechanics/A Solids 30, 940-949.

Monchiet, V., Kondo, D., 2013. Combined voids size and shape effects on the macroscopic criterion of ductile nanoporous materials. International Journal of Plasticity 43, 20-41.

Moraleda, J., Segurado, J., Llorcayz, J., 2007. Finite deformation of porous elastomers: a computational micromechanics approach. Philosophical Magazine 87, 5607-5627.

Morais, A.B., 2000. Transverse moduli of continuus-fibre-reinforced polymers. Composites Science and Technology 60, 997-1002.

Mori, T., Tanaka, K., 1973. Average stress in matrix and average elastic energy of materials with misfitting inclusions. Acta Metallurgica 21, 571-574.

Mortazavi, B., Bardon, J., Sarno Bomfim, J.A., Ahzi, S., 2012. A statistical approach for the evaluation of mechanical properties of silica/epoxy nanocomposite: Verification by experiments. Computational Materials Science 59, 108

Mortazavi, B., Hassounaa, F., Laachachi, A., Rajabpour, A., Ahzi, S., Chapron, D., Toniazzo, V., Ruch, D., 2013a. Experimental and multiscale modeling of thermal conductivity and elastic properties of PLA/expanded graphite polymer nanocomposites. Thermochimica Acta 552, 106-113.

Mortazavi, B., Baniassadi, M., Bardon, J., Ahzi, S., 2013b. Modeling of two-phase random composite materials by finite element, Mori-Tanaka and strong contrast methods. Composites: Part B 45, 1117-1125.

Mortazavi, B., Bardon, J., Ahzi, S., 2013c. Interphase effect on the elastic and thermal conductivity response of polymer nanocomposite materials: 3D finite element study. Computational Materials Science 69, 100-106.

Moulinec, H., Suquet, P., 1994. A fast numerical method for computing for computing the linear and non-linear properties of composites. Comptes Rendus Mécanique 318, 1471-1423.

Moulinec, H., Suquet, P., 1998. A numerical method for computing the overall response of non-linear composites with complex microstructure. Computer Methods in Applied Mechanics and Engineering 157, 69-94.

Mroginski, J.L., Etse, G., Vrech, S.M., 2011. A thermodynamical gradient theory for deformation and strain localization of porous media. International Journal of Plasticity 27, 620-634.

Nakamura T., Suresh S., 1993. Effects of thermal residual stresses and fiber packing on deformation of metal-matrix composites. Acta metallurgica et materialia 41, 1665-1681.

Negre, P., Steglich, D., Brocks, W., Koçak, M., 2003. Numerical simulation of crack extension in aluminum welds. Computational Materials Science 28, 723-731.

Nemat-Nasser, S., Hori, M., 1993. Micromechanics: overall properties of heterogeneous materials. New York: North-Holland.

Neto, M.A., Yu, W., Tang, T., leal, R., 2010. Analysis and optimization of heterogeneous materials using the variational asymptotic method for unit cell homogenization. Composite Structures 92, 2946-2954.

Nicoletto, G., 2004. Micromechanical modeling of the elsto-plastic behavior of heterogeneous nodular cast iron. PhD thesis, Degli Studi di Parma.

Nielsen, K.L., Tvergaard, V., 2009. Effect of a shear modified Gurson model on damage development in a FSW tensile specimen. International Journal of Solids and Structures 46, 587-601.

Orlik, J., 2010. Asymptotic homogenization algorithm for reinforced metal-matrix elasto-plastic composites. Composite Structures 92, 1581-1590.

Ostoja-Starzewski, M., 1993. Micromechanically as a basis of stochastic finite elements and differences: An overview. Applied Mechanics Reviews 46, 136-147.

Ostoja-Starzewski, M., Alzebdeh, K., 1996. Micromechanically based stochastic finite elements: length scales and anisotropy. Probablilitic Engineering Mechanics 11, 205-214.

Ostoja-Starzewski, M., Sheng, P.Y., Jasiuk, I., 1997. Damage patterns and constitutive response of random matrix-inclusion composites. Engineering Fracture Mechanics 58, 581-606.

Ostoja-Starzewski, M., 1998. Random field models of heterogeneous materials. International Journal of Solids and Structures 35, 2429-2455.

Ostoja-Starzewski, M., 2002. Microstructural randomness versus representative volume element in thermomechanics. Journal of Applied Mechanics 69, 25-35.

Pardoen, T., Hutchinson, J. W., 2000. An extended model for void growth and coalescence. Journal of the Mechanics and Physics of Solids 48, 2467-2512.

Pawlak, A., 2013. Cavitation during tensile deformation of isothermally crystallized polypropylene and high-density polyethylene. Colloid and Polymer Science 291, 773-787.

Pelissou, C., Baccou, J., Monerie, Y., Perales, F., 2009. Determination of the size of the representative volume element for random quasi-brittle composites. International Journal of Solids and Structures 46, 2842-2855.

Pellegrini, Y.-P., BarthHelHemy, M., Perrin, G., 2000. Functional methods and effective potentials for non-linear composites. J. Mech. Phys. Solids 48, 429–460.

Pierard, O., Friebel, C., Doghri I., 2004. Mean-field homogenization of multi-phase thermo-elastic composites: a general framework and its validation. Composites Science and Technology 64, 1587-1603.

Pierard, O., Doghri, I., 2006. An enhanced affine formulation and the corresponding numerical algorithms for the mean-field homogenization of elasto-viscoplastic composites. International Journal of Plasticity 22,131-157.

Pierard, O, LLorca, J., Segurado, J., Doghri, I., 2007a. Micromechanics of particle-reinforced elasto-viscoplastic composites: Finite element simulations versus affine homogenization. International Journal of Plasticity 23, 1041-1060.

Pierard, O., Gonzalez, C., Segurado, J., LLorca, J., Doghri, I., 2007b. Micromechanics of elasto-plastic materials reinforced with ellipsoidal inclusions. International Journal of Solids and Structures 44, 6945-6962.

Perrin G., Leblond J.B., 1990. Analytical study of a hollow sphere made of plastic porous material and subjected to hydrostatic tension-application to some problems in ductile fracture of metals. International Journal of Plasticity 6, 677-699.

Perrin, G., 1992. Contribution à l'étude théorique et numérique de la rupture ductile des métaux. PhD thesis, École Polytechnique.

Perrin, G., Leblond, J.B., 1993. Rudnicki and rice's analysis of strain localization revisited. Journal of Applied Mechanics 60, 842-846.

Perrin, G., Leblond J.B., 2000. Accelerated void growth in porous ductile solids containing two populations of cavities. International Journal of Plasticity 16, 91-120.

Ponte Castañeda, P., 1991. The effective mechanical properties of non-linear isotropic composites. Journal of the Mechanics and Physics of Solids 1, 45-71.

Ponte Castañeda, P., 1992. New variational principle in plasticity and their application to composite materials. Journal of the Mechanics and Physics of Solids 40, 1757-1788.

Ponte Castañeda, P., 1996. Exact second-order estimates for the effective mechanical properties of non-linear composite materials. Journal of the Mechanics and Physics of Solids 44, 827-862.

Ponte Castañeda, P., Suquet, P., 1998. Non-linear composites. Advances in Applied Mechanics 34, 171-302.

Ponte Castañeda, P., Willis, J.R., 1999. Variational second-order estimates for non-linear composites. Proceedings of the Royal Society of London A 455, 1799-1811.

Ponte Castañeda, P., Tiberio, E., 2000. A second-order homogenization method in finite elasticity and applications to black-filled elastomers. Journal of the Mechanics and Physics of Solids 48, 1389-1411.

Ponte Castañeda, P., Suquet, P., 2002. Non-linear composites and microstructure evolution. Mechanics for a New Mellennium, pp 253-274.

Ponte Castañeda, P., 2002a. Second-order homogenization estimates for non-linear composites incorporating field fluctuations: I-theory. Journal of the Mechanics and Physics of Solids 50, 737-757.

Ponte Castañeda, P., 2002b. Second-order homogenization estimates for non-linear composites incorporating field fluctuations: II-Applications. Journal of the Mechanics and Physics of Solids 50, 759-782.

Ponte Castañeda, P., 2012. Bounds for non-linear composites via iterated homogenization. Journal of the Mechanics and Physics of Solids 60, 1583-1604.

Qiu, Y., Weng, G.J., 1992. A theory of plasticity for porous and particle-reinforced composites. Journal of Applied Mechanics 59, 261-268.

Rice, J.R., Tracey, D.M., 1969. On the ductile enlargement of voids in triaxial stress fields. Journal of the Mechanics and Physics of Solids 17, 201-217.

Riku, I., Mimura, K., Tomita, Y., 2008. Effect of size-dependent cavitation on micro- to macroscopic mechanical behavior of rubber-blended polymer. Journal of Engineering Materials and Technology 130, 1-9.

Ristinmaa, M., 1997. Void growth in cyclic loaded porous plastic solids. International Journal of Plasticity 11, 163-181.

Rousselier, G., 1987. Ductile fracture models and their potential in local approach of fracture. Nuclear Engineering and Design 105, 97-111.

Rousselier, G., 2001. Dissipation in porous metal plasticity and ductile fracture. Journal of the Mechanics and Physics of Solids 49, 1727-1746.

Rudnicki, J.W., Rice, J.R., 1975. Conditions for the localization of deformation in pressure-sensitive dilatant materials. Journal of the Mechanics and Physics of Solids 23, 371-394.

Sab, K., Nedjar, B., 2005. Periodization of random media and representative volume element size for linear composites. Comptes Rendus Mécanique 333, 187-195.

Scheyvaerts, F., Onck, P.R., Tekoglu, C., Pardoen, T., 2011. The growth and coalescence of ellipsoidal voids in plane strain under combined shear and tension. Journal of the Mechanics and Physics of Solids 59, 373-397.

Schmidt, F., Kuhbacher, M., Gross, U., Kyriakopoulos, K., Schubert, H., Zehbe, R., 2011. From 2D slices to 3D volumes: Image based reconstruction and morphological Characterization of hippocampal cells on charged and uncharged surfaces using FIB/SEM serial sectioning. Ultra microscopy 111, 259-266.

Segurado, J., LLorca, J., 2002. A numerical approximation to the elastic properties of sphere-reinforced composites. Journal of the Mechanics and Physics of Solids 50, 2107-2121.

Selmi, A., Friebel, C., Doghri, I., Hassis H., 2007. Prediction of the elastic properties of single walled carbon nanotube reinforced polymers: A comparative study of several micromechanical models. Composites Science and Technology 67, 2071-2084.

Shen, W., Shao, J.F., Dormieux, L., Kondo, D., 2012. Approximate criteria for ductile porous materials having a green type matrix: application to double porous media. Computational Materials Science 62, 189-194.

Siruguet, K., Leblond, J.B., 2004. Effect of void locking by inclusions upon the plastic behavior of porous ductile solids - I: theoretical modeling and numerical study of void growth. International Journal of Plasticity 20, 225-254.

Socrate, S., Boyce, M.C., 2000. Micromechanics of toughened polycarbonate. Journal of the Mechanics and Physics of Solids 48, 233-273.

Son, H.S., Kim, Y.S., 2003. Prediction of forming limits for anisotropic sheets containing prolate ellipsoidal voids. International Journal of Mechanical Sciences 45, 1625-1643.

Steenbrink, A.C., van der Giessen, E., Wu, P.D., 1997. Void growth in glassy polymers. Journal of the Mechanics and Physics of Solids 45, 405-437.

Stroeven, M., Askes, H., Sluys, L.J., 2004. Numerical determination of representative volumes for granular materials. Computational Methods in Applied Mechanics and Engineering 193, 3221-3238.

Sun, C.T., Vaidya, R.S., 1996. Prediction of composite properties from a representative volume element. Composites Science and Technology 56, 171-179.

Sun, Y., Wang, D., 1989. A lower bound approach to the yield loci of porous materials. Acta Mechanica 5, 237-243.

Sun, Y., Wang, D., 1995. Analysis of shear localization in porous materials based on a lower bound approach. International Journal of Fracture 71, 71–83.

Suquet, P., 1987. Elements of homogenization: theory for inelastic solid mechanics, Springer-Verlag, Berline-Heidelberg-New York, 194–275.

Suquet, P., 1993. Overall potentials and extremal surfaces of power law or ideally plastic composites. Journal of the Mechanics and Physics of Solids 41, 981-1002.

Suquet, P., Ponte Castañeda, P., 1993. Small-contrast perturbation expansions for the effective properties of non-linear composites, Comptes Rendus Mécanique 317, 1515-1522.

Suquet, P., 1995. Overall properties of non-linear composites: a modified secant moduli theory and its link with Ponte Castañeda's non-linear variational procedure. Comptes Rendus Mécanique 320, 563-571.

Talbot, D.R.S., Willis, J.R., 1985. Variational principles for inhomogeneous non-linear media. Journal of Applied Mathematics 35, 39-54.

Talbot, D.R.S., Willis J.R., 1992. Some simple explicit bounds for the overall behaviour of non-linear composites. International Journal of Solids and Structures 29, 1981-1987.

Talbot, D.R.S., Willis, J.R., 1997. Bounds of third order for the overall response of non-linear composites. Journal of the Mechanics and Physics of Solids 45, 87-111.

Tandon, G.P., Weng, G.J., 1988. A theory of particle-reinforced plasticity. Journal of Applied Mechanics 55, 126-135.

Terada, K., Hori, M., Kyoya, T., Kikuchi, N., 2000. Simulation of the multi-scale convergence in computational homogenization approaches. International Journal of Solids and Structures 37, 2285-2311.

Torquato, S., 1997. Effective stiffness tensor of composite media-I. Exact series expansions. Journal of the Mechanics and Physics of Solids 45, 1421-1448.

Trias, D., Costa, J., Turon, A., Hurtado J.E., 2006. Determination of the critical size of a statistical representative volume element (SRVE) for carbon reinforced polymers. Acta Materialia 54, 3471-3484.

Tsukamoto, H., 2010. A mean-field micromechanical formulation of a non-linear constitutive equation of a two-phase composite. Computational Materials Science 50, 560-570.

Tvergaard. V., 1981. Influence of voids on shear band instabilities under plane strain conditions. International Journal of Fracture 17, 389-407.

Tvergaard, V., 1982. On localization in ductile materials containing spherical voids. International Journal of Fracture 18, 237-252.

Vadillo, G., Fernandez-Saez, J., 2009. An analysis of Gurson model with parameters dependent on triaxiality based on unitary cells. European Journal of Mechanics A/Solids 28, 417-427.

Vincent, P.-G., Monerie, Y., Suquet, P., 2008. Ductile damage of porous materials with two populations of voids. Comptes Rendus Mechanics 336, 245-259.

Vincent, P.-G., Monerie, Y., Suquet, P., 2009a. Porous materials with two populations of voids under internal pressure: I. Instantaneous constitutive relations. International Journal of Solids and Structures 46, 480-506.

Vincent, P.-G., Monerie, Y., Suquet, P., 2009b. Porous materials with two populations of voids under internal pressure: II. Growth and Coalescence of Voids. International Journal of Solids and Structures. 46, 507-526.

Wen, J., Huang, Y., Hwang, K.C., Liu, C., Li, M., 2005. The modified Gurson model accounting for the void size effect. International Journal of Plasticity 21, 381-395.

Willoughby, N., Parnell, W.J., Hazel, A.L., Abrahams, I.D., 2012. Homogenization methods to approximate the effective response of

random fibre-reinforced composites. International Journal of Solids and Structures 49, 1421-1433.

Wongsto, A., Li, S., 2005. Micromechanical FE analysis of UD fibre-reinforced composites with fibres distributed at random over the transverse cross-section. Composites Part A: Applied Science and Manufacturing 36, 1246-1266.

Wu, L., Noels, L., Adam, L., Doghri, I., 2012. A multiscale mean-field homogenization method for fiber- reinforced composites with gradient-enhanced damage models. Computer Methods in Applied Mechanics and Engineering 233-236, 164-179.

Xu, X.F., 2011. On the third-order bounds of the effective shear modulus of two-phase composites. Mechanics of Materials 43, 269-275.

Xu, X.F., Jie, Y., 2014. Third-order bound of non-linear composites and porous media under hydrostatic deformation. Mechanics of Materials 68, 137-146.

Yan, C., 2003. On homogenization and de-homogenization of composite materials. PhD thesis, Drexel University.

Yan, Y., Sun, Q., Chen, J., Pan, H., 2013. The initiation and propagation of edge cracks of silicon steel during tandem cold rolling process based on the Gurson-Tvergaard-Needleman damage model. Journal of Materials Processing Technology 213, 598-605.

Yang, Y., Ma, F.Y., Lei, C.H., Liu, Y.Y., Li, J.Y., 2013. Non-linear asymptotic homogenization and the effective behavior of layered thermoelectric composites. Journal of the Mechanics and Physics of Solids 61, 768-1783.

Yee, K.C., Mear, M.E., 1996. Effect of void shape on the macroscopic response of non-linear porous solids. International Journal of Plasticity 12, 45-68.

Ye, Z., 2013. Enhance variational asymptotic method for unit cell homogenization (VAMUCH) for real engineering structures and materials. PhD thesis, Utah State University.

Yu, W., Tang, T., 2007. Variational asymptotic method for unit cell homogenization of periodically heterogeneous materials International Journal of Solids and Structures 44, 3738-3755.

Yuan, F.G., Pagano, N.J., Cai, X., 1997. Elastic moduli of brittle matrix composites with interfacial debonding. International Journal of Solids and Structures 34, 177-201.

Zadpoor, A.A., Sinke, J., Benedictus, R., 2009. Formability prediction of high strength aluminum sheets. International Journal of Plasticity 25, 2269-2297.

Zaïri, F., Naït-Abdelaziz, M., Woznica, K., Gloaguen, J.M., 2005. Constitutive equations for the viscoplastic-damage behaviour of a rubber-modified polymer. European Journal of Mechanics A/Solids 24, 169-182.

Zaïri, F., Naït-Abdelaziz, M., Gloaguen, J.M., Lefebvre, J.M., 2008. Modelling of the elasto-viscoplastic damage behaviour of glassy polymers. International Journal of Plasticity 24, 945-965.

Zaïri, F., Gloaguen, J.M., Naït-Abdelaziz, M., Mesbah, A., Lefebvre, J.M., 2011a. Study of the effect of size and clay structural parameters on the yield and post-yield response of polymer/clay nanocomposites via a multiscale micromechanical modelling. Acta Materialia 59, 3851-3863.

Zaïri, F., Naït-Abdelaziz, M., Gloaguen, J.M., Lefebvre, J.M., 2011b. A physically-based constitutive model for anisotropic damage in rubber-toughened glassy polymers during finite deformation. International Journal of Plasticity 27, 25-51.

Zangenberg, J., Brondsted, P., 2013. Determination of the minimum size of a statistical representative volume element from a fibre-reinforced composite based on point pattern statistics. Scripta Materialia 68, 503-505.

Zhang, K.S., Bai, J.B., François, D., 1999. Ductile fracture of materials with high void volume fraction. International Journal of Solids and Structures 25, 2396-2314.

Zhang, Z.L., Thaulow, C., Odegard, O., 2000. A complete Gurson model approach for ductile fracture. Engineering Fracture Mechanics 67, 155-168.

Zheng, Q.S., Du, D.X., 2001. An explicit and universally applicable estimate for the effective properties of multiphase composites which accounts for inclusion distribution. Journal of the Mechanics and Physics of Solids 49, 2765-2788.

Zou, W., He, Q., Huang, M., Zheng, Q., 2010. Eshelby's problem of non-elliptical inclusions. Journal of the Mechanics and Physics of Solids 58, 346-372.

Zuo, J.Z., Lou, Z.W., Kuang, Z.B., 1996. A yield function for porous ductile materials. Engineering Fracture Mechanics 53, 557-559.